ISSN 1070-3284, Russian Journal of Coordination Chemistry, 2021, Vol. 47, No. 12, pp. 791–860. © Pleiades Publishing, Ltd., 2021.
Russian Text © The Author(s), 2021, published in Koordinatsionnaya Khimiya, 2021, Vol. 47, No. 12, pp. 719–788.

Organic Compounds of Bismuth: Synthesis, Structure, and Applications

V. V. Sharutin[a], *, A. I. Poddel'sky[b], **, and O. K. Sharutina[a]

[a] *Southern Ural State University (National Research University), Chelyabinsk, Russia*

[b] *G.A. Razuvaev Institute of Organometallic Chemistry, Russian Academy of Sciences, Nizhny Novgorod, Russia*

**e-mail: vvsharutin@rambler.ru*

***e-mail: aip@iomc.ras.ru*

Received February 16, 2021; revised April 21, 2021; accepted April 24, 2021

Abstract—The present review, describing the modern achievements in the area of synthetic methods, investigation of specific structural features, and possibilities of practical use of the organic compounds of bismuth, is based on an analysis of the scientific literature published from 2010 to 2020. Some earlier works are also reviewed due to their significance. The bibliography consists of 190 references.

Keywords: bismuth, organic compounds of bismuth, synthesis, structure

DOI: 10.1134/S1070328421120022

CONTENTS

INTRODUCTION

Since the discovery in 1975 of the possibility of using organic compounds of bismuth in fine organic synthesis [1], the number of publications devoted to the development of the synthesis methods and studying the reactivity and structural features of the organic bismuth derivatives has significantly been increased. The bismuth atom in the organic compounds can directly be bound to one, two, three, four, five, or six organic radicals. In addition, many types of bismuth derivatives are known in which one or several organic substituents are replaced by halogen atoms or other electronegative groups. The variety of types of organobismuth compounds resulted in a considerable extension of studies in this field [2], which is observed in the recent years. Direct causes for this were unceasing attempts to find possibilities for a broader use of the organobismuth compounds in chemistry and medicine. The key position in the chemistry of organic derivatives of bismuth is occupied by compounds R_3Bi among which the aryl derivatives are predominant. Numerous bismuth compounds of the nonsymmetrical structure ($RBiX_2$ and R_2BiX) and pentavalent bismuth derivatives can be synthesized from the aryl derivatives.

TRIORGANYLBISMUTH COMPOUNDS

Triorganyl derivatives of bismuth R_3Bi are synthesized, as a rule, from organomagnesium or organolithium compounds in high yields. For example, the benzyl derivatives of bismuth were synthesized by the reaction of arylbismuth dichloride $Ar'BiCl_2$ (Ar' = 2,6-$(Me_2NCH_2)_2C_6H_3$) with benzylmagnesium chloride in tetrahydrofuran (THF) giving $Ar'Bi(\eta^1\text{-}CH_2Ph)_2$ in high yields (Scheme 1) [3].

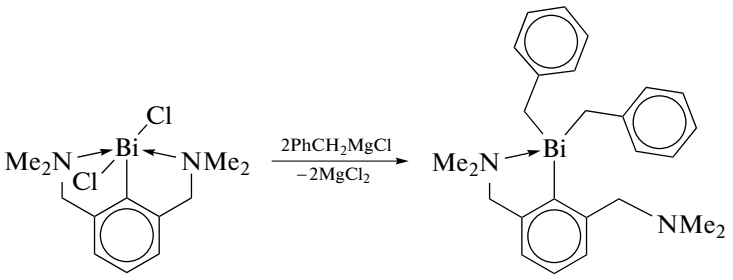

$Ar'BiCl_2$ $Ar' = 2,6\text{-}(Me_2NCH_2)_2C_6H_3$ $Ar'Bi(\eta^1\text{-}CH_2Ph)_2$

Scheme 1.

Tribenzylbismuth $Bi(\eta^1\text{-}CH_2Ph)_3$ was synthesized similarly. The X-ray crystallographic and spectroscopic studies confirm that the benzyl ligands in these compounds are bonded via the η^1 mode. The first compound, $Ar'Bi(\eta^1\text{-}CH_2Ph)_2$, contains only one short Bi···N contact (3.058(4) Å), and the $Bi-C_{Alk}$ distances (2.299(4) and 2.340(4) Å) are longer than those in $Bi(\eta^1\text{-}CH_2Ph)_3$ (2.289(4), 2.291(4), and 2.295(4) Å) and trimethylbismuth (2.23(2), 2.26(2), and 2.288(16) Å) [4]. Note a specific feature of the structure of the latter: the molecules in the crystal are associated into dimers (Bi···Bi distance 3.899(1) Å).

Triallylbismuth All_3Bi synthesized from allylmagnesium bromide and bismuth trichloride was proposed as an initiator of controlled radical styrene polymerization [5]. The protonolysis of All_3Bi by a sufficiently strong Brönsted acid $[PhNMe_2H]^+[B(C_6H_3Cl_2)_4]^-$ allowed the bismuth complex $[All_2Bi(THF)_2]^+[B(C_6H_3Cl_2)_4]^-$ to be isolated as a yellow solid (Scheme 2). The bismuth atom in the cation has the bis(phenoidal) coordination geometry with the apically arranged THF molecules.

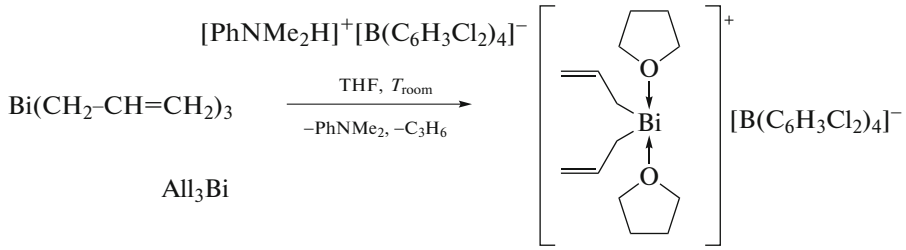

$[All_2Bi(THF)_2]^+[B(C_6H_3Cl_2)_4]^-$

Scheme 2.

Tris(methylallyl)bismuth produced from the Grignard reagent and bismuth trichloride was also structurally characterized. According to the X-ray diffraction (XRD) data, the allyl ligands in this compound coordinate to the bismuth atom via the η^1 mode, and the average length of the Bi–C bond (2.32(2) Å) is close to an analogous bond for another characterized bismuth compound containing the allyl ligand: $\{2,6\text{-}(Me_2NCH_2)_2C_6H_3\}_2(\eta^1\text{-All})Bi$ [6]. Complex $[All_2Bi(THF)_2]^+[B(C_6H_3Cl_2)_4]^-$ quantitatively reacts with two equivalents of aldehyde in THF at ambient temperature to form the carbometallation product $[(AllCH(Ar)O)_2Bi(THF)_2]^+[B(C_6H_3Cl_2)_4]^-$ in the yield up to 99% (Scheme 3).

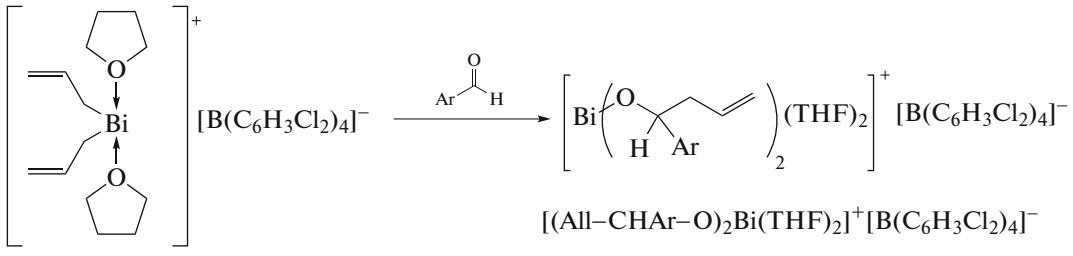

$[All_2Bi(THF)_2]^+[B(C_6H_3Cl_2)_4]^-$

$[(All\text{–}CHAr\text{–}O)_2Bi(THF)_2]^+[B(C_6H_3Cl_2)_4]^-$

Scheme 3.

Triorganylbismuth $Bi(CH_2C_6H_4Cl\text{-}2)_3$ synthesized from bismuth trichloride and alkylmagnesium bromide was characterized by XRD, which revealed the formation of a two-dimensional network due to the coordination π interactions bismuth–arene with distances of 3.659 Å (bismuth–arenocentroid) and 3.869 Å (arene centroids), respectively (Scheme 4) [7].

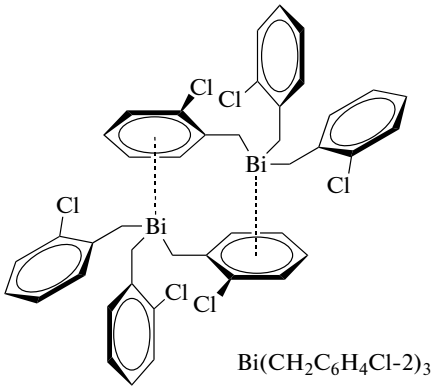

$Bi(CH_2C_6H_4Cl\text{-}2)_3$

Scheme 4.

The nonsymmetric bismuth compounds Ar_2BiR containing the N,C,N-ligands 2,6-$(Me_2NCH_2)_2C_6H_3$ were synthesized and structurally characterized [6] in order to compare their properties with the coordination chemistry of lanthanides. In particular, the addition of a solution of allylmagnesium chloride in THF to diarylbismuth chloride in THF afforded the allylbismuth complex $(2,6\text{-}(Me_2NCH_2)_2C_6H_3)_2Bi(All)$ in which the allyl ligand is linked to the metal atom via the η^1 mode, where one N,C,N-ligand is tridentate and the second ligand forms only one coordination bond Bi···N (Scheme 5).

$(2,6\text{-}(Me_2NCH_2)_2C_6H_3)_2BiCl \xrightarrow{AllMgCl}$

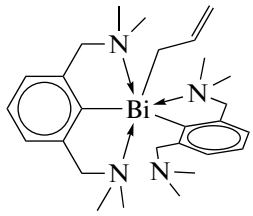

$(2,6\text{-}(Me_2NCH_2)_2C_6H_3)_2Bi(All)$

Scheme 5.

Tris(pentafluoroethyl)bismuth $Bi(CF_2{-}CF_3)_3$ was synthesized from pentafluoroethyllithium and bismuth trichloride in ether at reduced temperature (Scheme 6). In this compound, the Bi–C bond lengths (2.331(5), 2.338(5), and 2.351(5) Å) [8] are maximal in the series of the R_3Bi derivatives due to an increase in the electronegativity of the alkyl substituents at the bismuth atom.

$$3F_3C{-}CF_2H \xrightarrow[-3n\text{-BuH}]{\substack{3n\text{-BuLi}\\ Et_2O/n\text{-hexane}\\ -80^\circ C}} 3F_3C{-}CF_2Li \xrightarrow[-3LiCl]{\substack{BiCl_3\\ Et_2O\\ -65^\circ C}} Bi(CF_2{-}CF_3)_3$$

Scheme 6.

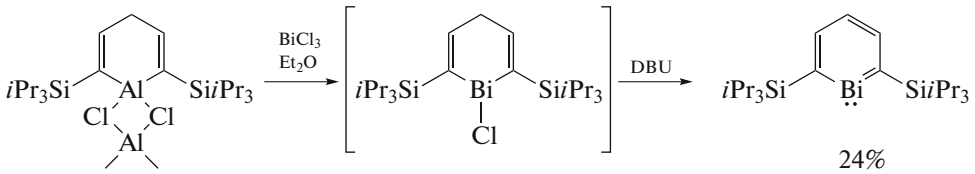

DBU = 1,8-diazabicyclo[3.4.0]undecene-7

Scheme 7.

Stable bismabenzene was synthesized from the organoaluminum derivative (Scheme 7) [9].

The assumed aromaticity of this heavy benzene including the sixth period element was studied by XRD, NMR method, UV spectroscopy, and theoretical calculations. The XRD study of the synthesized bismabenzene revealed the planar ring containing unsaturated Bi–C and C–C bonds. The reaction of bismabenzene with dimethylacetylenedicarboxylate (Scheme 8) leading to bisma[2.2.2]bicyclooctadiene, which was characterized by XRD, was also studied.

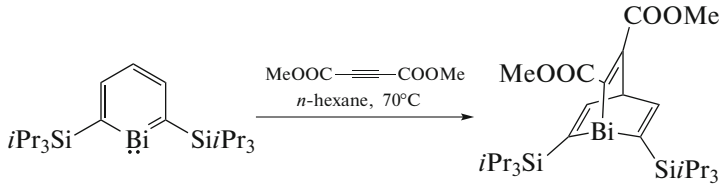

Scheme 8.

The organobismuth derivative of propeller-like *ortho*-substituted fluorotriphenylsilane (bismasilatriptycene) was synthesized from bismuth chloride and tris(2-lithiumphenyl)fluorosilane, which was prepared by the lithiation of tris(2-bromophenyl)fluorosilane or tris(2-iodophenyl)fluorosilane with butyllithium in hexane (Scheme 9) [10].

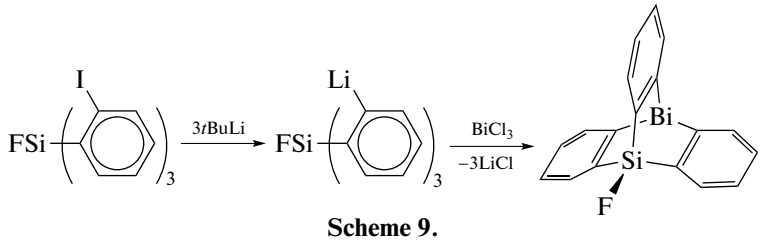

Scheme 9.

It follows from the XRD data that no interactions between the silicon and bismuth atoms were observed in spite of their large sizes.

The organobismuth compounds with the N,C-aryl ligand LBi(Ph)Cl and $LMPh_2$ were synthesized in high yields from aryllithium dichloride $LBiCl_2$ (L = *o*-(CH=N-Dipp)C_6H_4) and phenyllithium in a ratio of 1 : 1 or 1 : 2 (Scheme 10) [11].

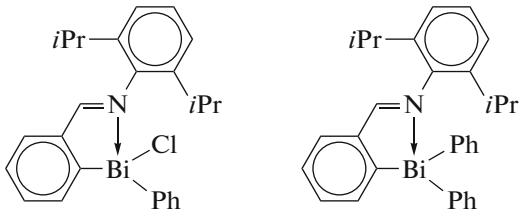

LBi(Ph)Cl LBiPh_2

L = *o*-(CH=N-Dipp)C_6H_4
Dipp = 2,6-*i*$Pr_2C_6H_3$

Scheme 10.

Nonsymmetric compounds $(C_6F_5)_2BiR$ and $[2,4,6\text{-}(C_6F_5)_3C_6H_2]_2BiR$, where R = 2-$(Me_2NCH_2)$-$C_6H_4$, were synthesized by the reactions of $RBiBr_2$ with C_6F_5MgBr and 2,4,6-$(C_6F_5)_3C_6H_2Li$, respectively, at the 1 : 2 molar ratio [12]. Bromides $R(C_6F_5)BiBr$, R(Mes)BiBr, and R(Ph)BiBr were synthesized from the equimolar amounts of $RBiBr_2$ and C_6F_5MgBr, MesMgBr, or PhMgBr or from $PhBiBr_2$ and RLi in the 1 : 1 molar ratio. All compounds bearing the dimethylaminomethyl group in the aryl ligand contain the very strong coordination Bi···N bond (2.511(9)–3.334(16) Å).

Triarylbismuth $(2\text{-}(Et_2NCH_2)C_6H_4)_3Bi$ is the product of the reaction of RLi (R = 2-$(Et_2NCH_2)C_6H_4$ with $BiCl_3$ in the 3 : 1 molar ratio (Scheme 11) [13].

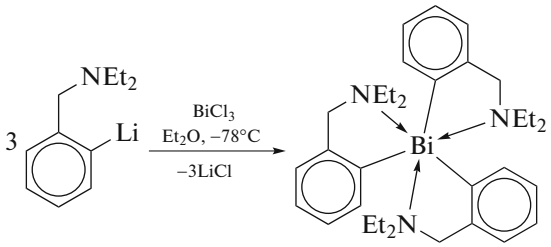

$(2\text{-}(Et_2NCH_2)C_6H_4)_3Bi$

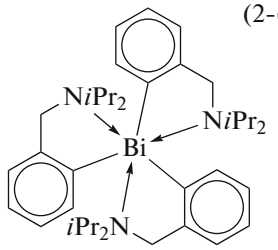

$(2\text{-}(i\text{Pr}_2NCH_2)C_6H_4)_3Bi$

Scheme 11.

The use of an analogous scheme gave (2-$i\text{Pr}_2NCH_2{-}C_6H_4)_3Bi$ in which the coordination polyhedron of the central atom is a distorted octahedron (Bi–C 2.272(3), 2.276(3), and 2.279(3) Å, and tight contacts Bi···N 3.052(3), 3.021(3), and 3.074(2) Å) (Scheme 11) [14].

The $(i\text{Pr}_2P{-}Ace)_3Bi$ and $(i\text{Pr}_2P{-}Ace)_2BiPh$ derivatives (Ace is acenaphthene-5,6-diyl) were synthesized from bismuth chloride and aryllithium [15] via the following scheme (Scheme 12).

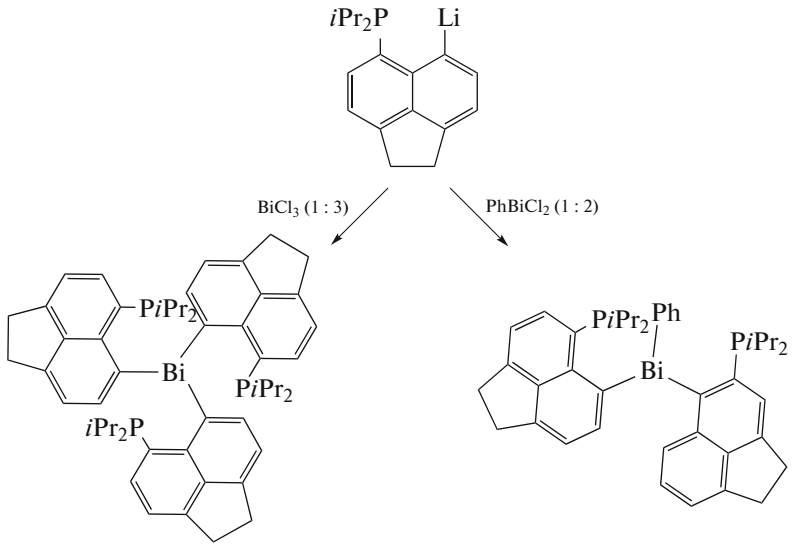

$(i\text{Pr}_2P{-}Ace)_3Bi$ $(i\text{Pr}_2P{-}Ace)_2BiPh$

Scheme 12.

The synthesis of the neutral Bi-containing tris-2-pyridyl ligand (6-Me-2-Py)$_3$Bi, which transforms into the copper complex {[(6-Me-2-Py)$_3$Bi]Cu(MeCN)}$^+$[PF$_6$]$^-$ upon the treatment with [Cu(MeCN)$_4$]$^+$[PF$_6$]$^-$ in an acetonitrile solution (Scheme 13), was described in [16].

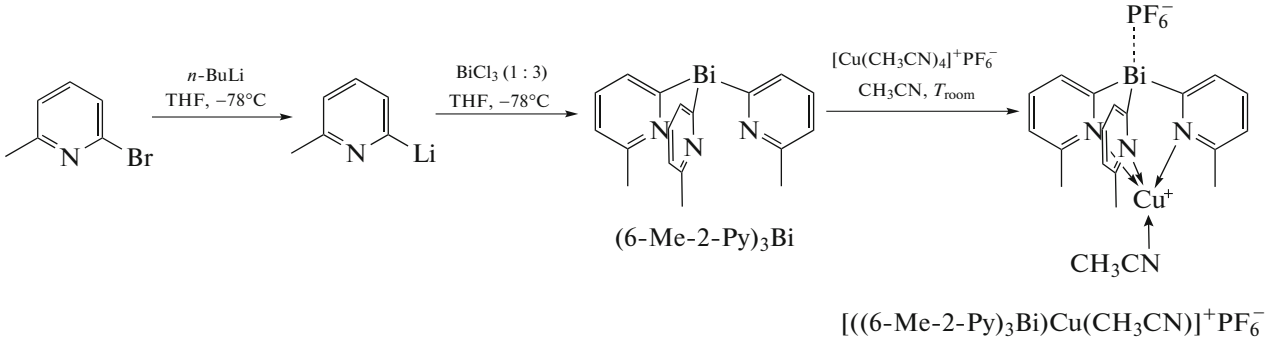

Scheme 13.

The addition of tetrabutylammonium chloride to [((6-Me-2-Py)$_3$Bi)Cu(MeCN)]$^+$[PF$_6$]$^-$ results in the quantitative formation of the dimeric complex [(6-Me-2-Py)Bi(6-Me-2-Py)$_2$CuCl]$_2$ (Scheme 14).

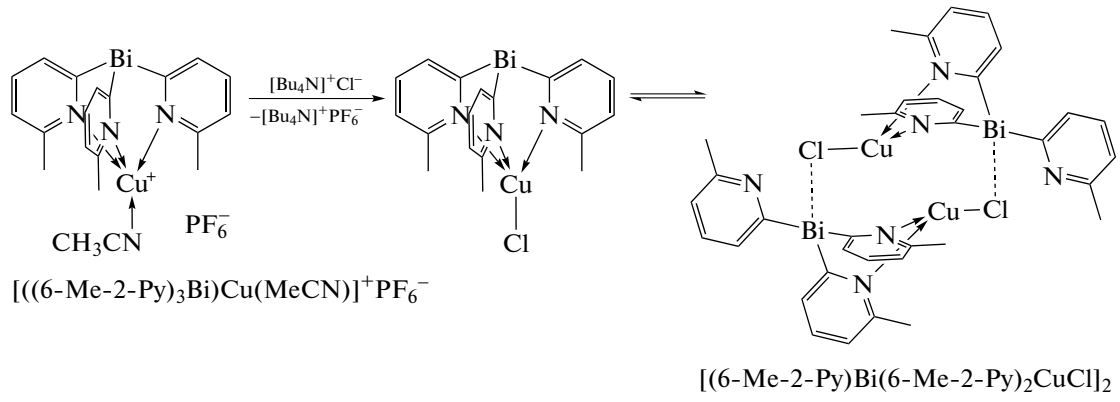

Scheme 14.

The reaction of dimesityl-1,8-naphthalenediyllithium borate with diphenylbismuth chloride afforded 1-(diphenylbismuth)-8-(dimesitylboron)naphthalenediyl Mes$_2$B(1,8-Napht)BiPh$_2$ (Scheme 15) [17].

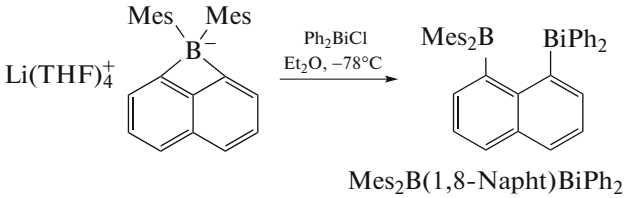

Scheme 15.

It follows from the XRD data that the 1,8-naphthalenediyl cage provides short Bi → B distances (3.330 Å). The stability of the complex increases by 6.32 kcal/mol due to the p(Bi) → p(B) interaction.

The bismuth compounds (o-PPh$_2$–C$_6$H$_4$)$_2$BiX (X = Me, C$_6$F$_5$) were synthesized from diarylbismuth chloride and organyllithium (Scheme 16) [18].

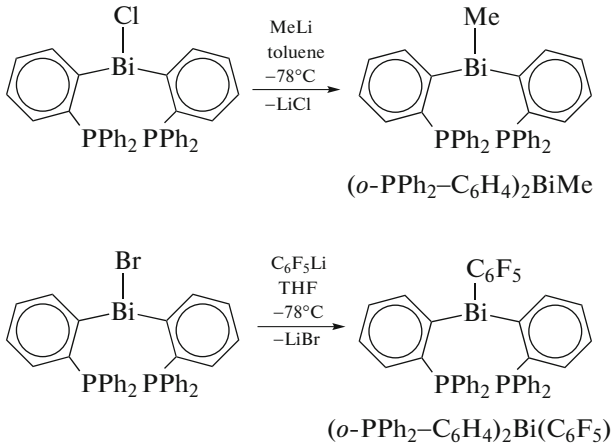

Scheme 16.

The P,Bi-containing xanthene ligand Xan(PPh$_2$)(BiPh$_2$) was synthesized [19] from diphenylphosphorus and diphenylbismuth chlorides (Scheme 17).

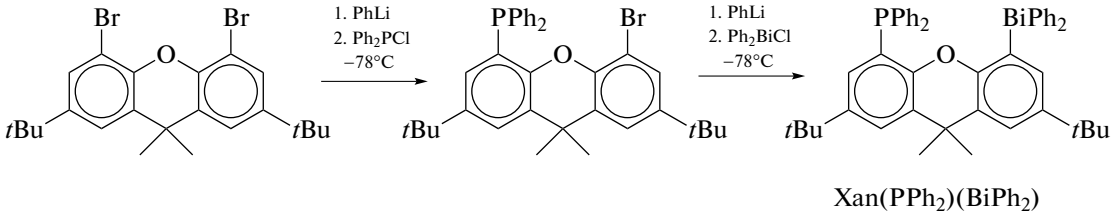

Scheme 17.

The phosphorus and bismuth atoms in $Xan(PPh_2)(BiPh_2)$ have the tetrahedral environment, but the distance between them (4.2096(15) Å) is insignificantly shorter than the sum of their van der Waals radii (4.3 Å) [20].

The new bismuth compound $(p\text{-Tol})_2BiR$ (Scheme 18) containing the amide fragment was synthesized and structurally characterized [21].

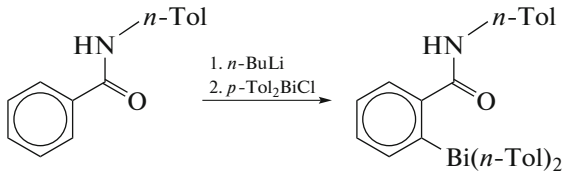

Scheme 18.

The XRD data show intramolecular interactions between bismuth and the carbonyl oxygen atom. The central atom has the pseudotrigonal bipyramidal coordination. The compound manifested a strong antiproliferative activity in all tested cell lines. In particular, the complex was more sensitive than the analogous antimony compound.

The complex with the N,C,N-pincer ligand, [2-(dimethylaminomethyl)phenyl]bis(4-methylphenyl)-bismuth $(2\text{-}Me_2NCH_2C_6H_4)Bi(p\text{-Tol})_2$, was synthesized from bis(*para*-tolyl)bismuth chloride and *o*-lithium-*N*-dimethylbenzylamine [22]. The Bi···N intramolecular contacts (2.902(4) Å) are observed in the molecules of the compound.

The bismuth compounds $[2\text{-}\{E(CH_2CH_2)_2NCH_2\}C_6H_4]_3Bi$, where E = O or MeN, were synthesized by the reaction of the corresponding *ortho*-lithium derivative with bismuth trichloride in the 3 : 1 molar ratio [23]. For R_3Bi, the N···Bi intramolecular interactions of the medium strength (3.170(7) Å for $[2\text{-}\{O(CH_2CH_2)_2NCH_2\}C_6H_4]_3Bi$ and 3.211(5) Å for $[2\text{-}\{MeN(CH_2CH_2)_2NCH_2\}C_6H_4]_3Bi$) lead to the distortion of the octahedral $(C,N)_3Bi$ core. The six-membered rings of morpholine and piperazine in these complexes adopt the chair conformation that prevents the intramolecular coordination of the oxygen or nitrogen atoms.

The reaction of substituted ferrocenyllithium and diphenylbismuth chloride afforded $Ph_2Bi(2\text{-}Me_2NCH_2\text{–}Fc')$, where $2\text{-}Me_2NCH_2\text{–}Fc'$ is the ferrocenyl substituent $(2\text{-}Me_2NCH_2\text{–}C_5H_3)FeCp$ containing the additional functional group Me_2NCH_2 in the second position of the ferrocenyl ring bound to the bismuth atom. The quaternization of the latter by methyl iodide yielded ferrocenylbismuthine-containing ammonium salt $[Ph_2Bi(2\text{-}Me_3N^+CH_2\text{–}Fc')][I]^-$ (Scheme 19) [24].

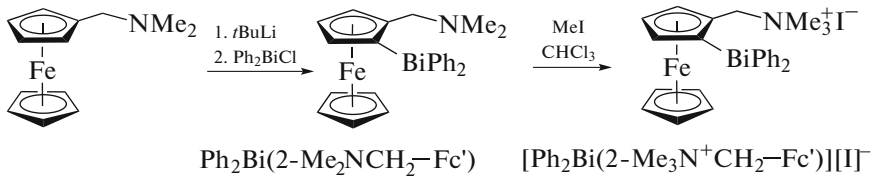

Scheme 19.

The molecular structures of bismuthines $Ph_2Bi(2\text{-}Me_2NCH_2\text{–}Fc')$ and $[Ph_2Bi(2\text{-}Me_3N^+CH_2\text{–}Fc')][I]^-$ in the crystalline state were determined by X-ray crystallography. No hypervalent Bi···N interaction was observed in the $Ph_2Bi(2\text{-}Me_2NCH_2\text{–}Fc')$ compound.

The reactions of the lithium derivatives and bismuth trichloride gave N,C,N-chelated bismuth(III) chlorides $LBiCl_2$, where L = 2,6-(*t*Bu-N=CH)$_2C_6H_3$ and 2,6-(2',6'-$Me_2C_6H_3$–N=CH)$_2C_6H_3$) (Scheme 20) [25]. The treatment of the obtained arylbismuth dichlorides $LBiCl_2$ with alkyl- or phenyllithium (Scheme 20) results in the formation of triorganylbismuth compounds $LBiR'_2$ in which no intramolecular Bi···N contacts are observed.

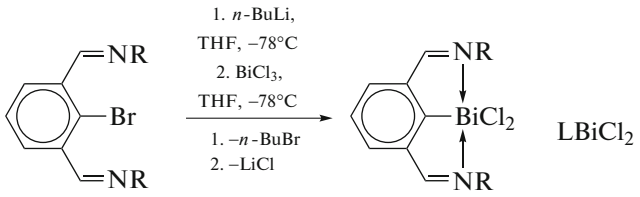

R = *t*Bu L = 2,6-(*t*Bu-N=CH)$_2$C$_6$H$_3$

R = 2,6-Me$_2$C$_6$H$_3$ L = 2,6-(2',6'-Me$_2$C$_6$H$_3$–N=CH)$_2$C$_6$H$_3$

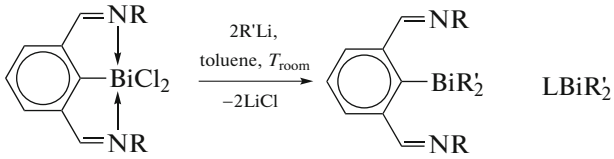

R = *t*Bu, R' = Me

R = *t*Bu, R' = Ph

R = 2,6-Me$_2$C$_6$H$_3$, R = Me

Scheme 20.

The problems of the synthesis of triorganylbismuth compounds are directly related to the search for their possible use in fine organic synthesis [26]. For this purpose, the reactivity of a series of sterically hindered triarylbismuth compounds Ar_3Bi (Ar_3Bi = (2-MeOC$_6$H$_4$)$_3$Bi, (2-MeC$_6$H$_4$)$_3$Bi, Mes$_3$Bi, (2,6-Me$_2$C$_6$H$_3$)$_3$Bi, (1-Napht)$_3$Bi, and [2,4-(MeO)$_2$-C$_6$H$_3$]$_3$Bi) was studied in the cross-coupling with aryl iodides or aryl bromides in the presence of the Pd/Cu-containing compounds (Scheme 21).

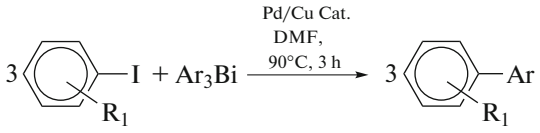

Scheme 21.

It is expected that this study would provide prospects for the further application of the bismuth reagents in fine organic synthesis. A similar use of the functionalized triarylbismuth derivatives in the C-, N-, and O-arylation catalyzed by the palladium and copper compounds (Scheme 22) was reported [27].

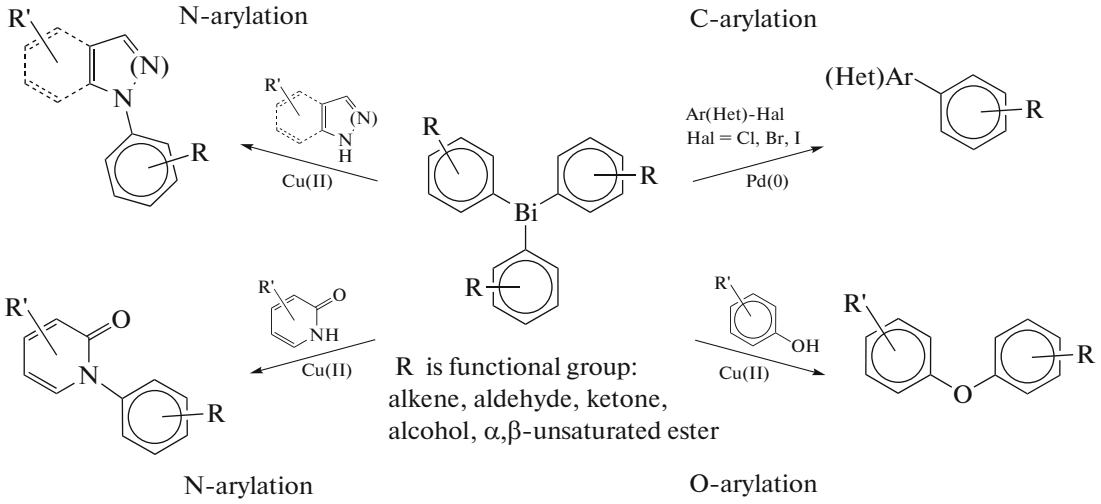

Scheme 22.

The cross-coupling reactions of triphenylbismuth or functionalized triarylbismuth with halogen-substituted pyridines, pyrazines, and pyridazines bearing reactive fragments catalyzed by the palladium compounds are reported (e.g., Scheme 23) [28].

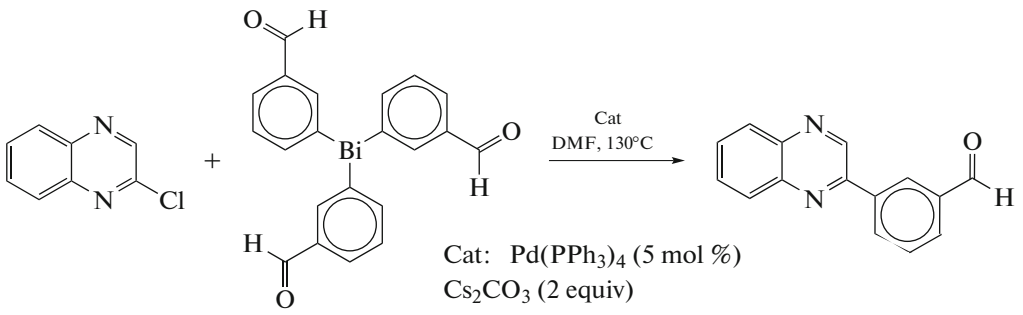

Scheme 23.

The reactions occur under mild conditions with excellent yields of the target products.

The chemioselective copper catalyst was developed for the O-arylation of (1R,2R)-N-BOC-2-amino-1-(4-nitrophenyl)-1,3-propanediols using triarylbismuth, where BOC is *tert*-butoxycarbonyl group (Scheme 24). The method makes it possible to transfer *ortho*-, *meta*-, and *para*-substituted aryl groups, is highly tolerant to functional groups, and leads to the arylation of primary alcohols [29].

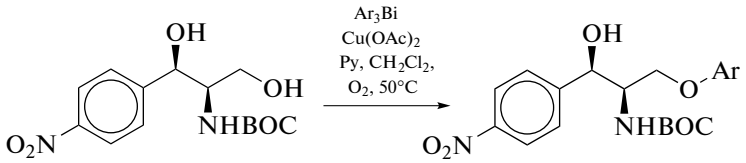

Scheme 24.

In addition to the triarylbismuth derivatives with nitrogen atoms in the aryl substituents, the synthesis of similar complexes with other potential coordinating centers, such as the oxygen atom of the methoxy groups, was described. For instance, tris(2-bromo-5-methoxyphenyl)bismuth was synthesized from bismuth trichloride and 5-bromo-2-methoxyphenyllithium prepared by the metallation of *para*-bromoanisole with phenyllithium in ether [30, 31].

Other triorganylbismuth compounds (Scheme 25) in which two bismuth atoms are linked to each other by bridging oxygen-containing ligands, such as $O\{(CH_2)_2BiPh_2\}_2$, $MeN(CH_2{-}2\text{-}C_6H_4BiR_2)_2$, and $S(CH_2{-}2\text{-}C_6H_4BiR_2)_2$ (R = Me, Ph), were synthesized and characterized by XRD [32].

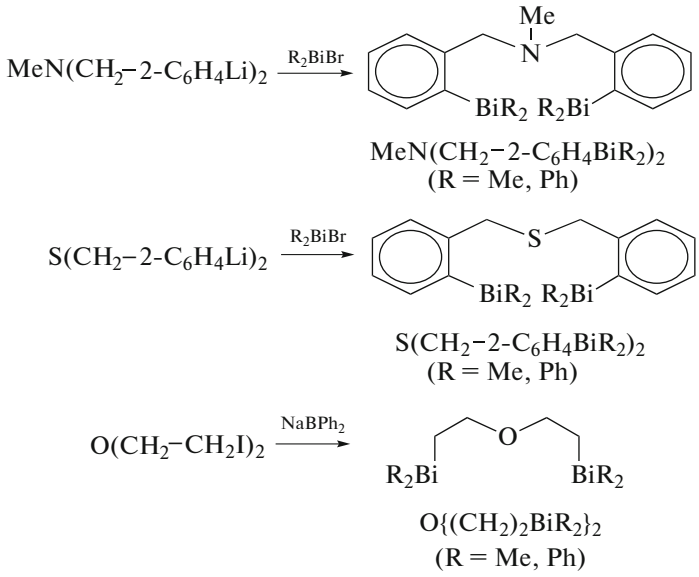

Scheme 25.

Hypervalent interactions between the O or S atoms and bismuth atoms are observed in the structures of $O\{(CH_2)_2BiPh_2\}_2$ and $S(CH_2{-}2\text{-}C_6H_4BiPh_2)_2$ (Bi···O 3.203(3), 3.126(3) Å at the sum of the van der Waals radii of bismuth and oxygen equal to 3.52 Å and Bi···S 3.3254(12), 3.3013(12) Å at the sum of the van der Waals radii of bismuth and sulfur equal to 3.8 Å) [20].

The new photosensitizer $[L^+BiR][PF_6]^-$ based on substituted triarylbismuth LBiPh (Scheme 26) was synthesized from phenylbismuth dichloride and lithium derivative of bis(4-dimethylamino-2-bromophenyl)-2-tolylmethane by its lithiation with *sec*-BuLi followed by the oxidation of the formed LBiPh with *p*-chloranil (Scheme 26). The target compound was obtained as hexafluorophosphate salt $[L^+BiR][PF_6]^-$ in a 4% yield from LBiPh [33].

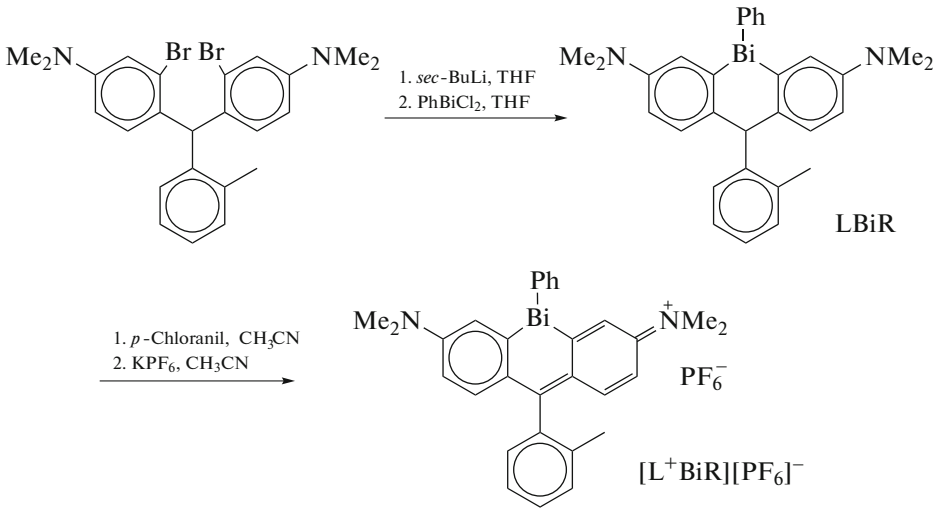

Scheme 26.

A number of new phosphorescent materials (bismuth compounds with heterocyclic ligands) was obtained from β,β-dilithiobithiophenes and phenylbismuth dihalide (Scheme 27) [34].

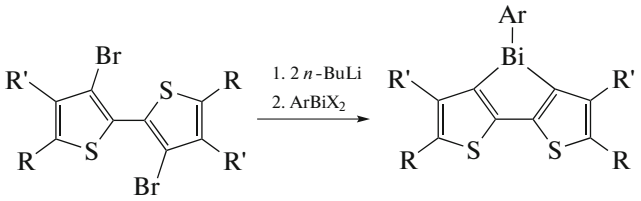

Ar = *p*-Tol, R = H, R' = H
Ar = Ph, R = $SiMe_3$, R' = H
Ar = Ph, R = $SiMe_3$, R' = Me
Ar = Ph, RR' =

Scheme 27.

The new bismuth compound, [(2-di-*p*-tolylbismuthanophenyl)diazenyl]pyrrolidine (Scheme 28), was synthesized from di(*p*-tolyl)bismuth chloride and corresponding lithium compound, which was prepared by the lithiation of 1-[(2-iodophenyl)diazenyl]pyrrolidine with butyllithium in THF. The new compound was tested to biological activity against human cancer cell lines [35].

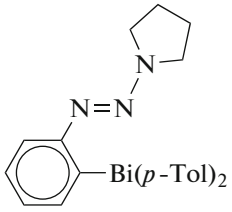

Scheme 28.

The compound was shown to exert a strong antiproliferative effect.

A new method was proposed for the synthesis of the triorganylbismuth compounds $Bi(2\text{-}C_4H_2X\text{-}5\text{-}R)_3$ from silanols and bismuth alkoxides or amides (Scheme 29) [36, 37].

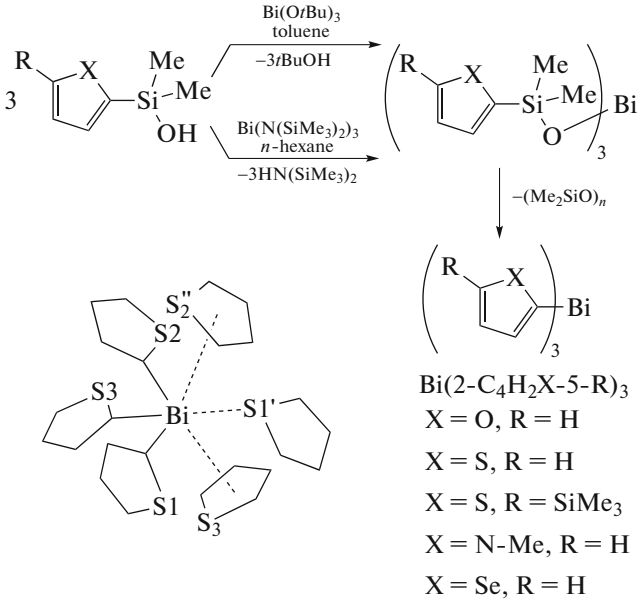

Scheme 29.

According to the XRD data, the obtained compounds $Bi(2\text{-}C_4H_2X\text{-}5\text{-}R)_3$ (X = O, R = H; X = S, R = H; X = S, R = $SiMe_3$; X = NMe, R = H; X = Se, R = H) and $Bi(3\text{-}C_4H_3S)_3$ contain intermolecular Bi···π heteroarene interactions, for example, as those shown in Scheme 29.

The triarylbismuth derivatives $[2\text{-}(ArS)\text{-}C_6H_4]_nBiAr_{3-n}$ with the *ortho*-thioaryl substituent can conveniently be synthesized by the insertion of benzene into the bond of bismuth with sulfur in $(ArS)_nBiAr_{3-n}$ (n = 1, 2) (Scheme 30) [38].

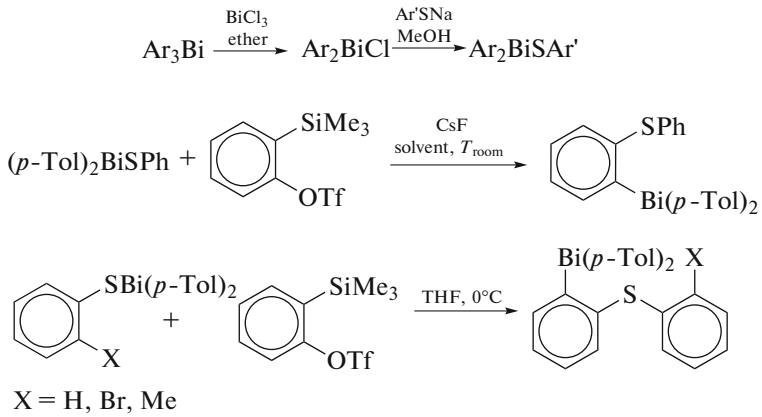

Scheme 30.

The Bi–C bond in $[2\text{-}(2\text{-}BrC_6H_4S)C_6H_4]_nBiAr_{3-n}$ is cleaved in the presence of the Pd catalyst to form dibenzothiophene in a high yield. The XRD study of $2\text{-}(2\text{-}BrC_6H_4S)C_6H_4Bi(p\text{-}Tol)_2$ shows the presence of the S···Bi intramolecular contact (3.397(2) Å), which is considerably shorter than the sum of van der Waals radii of these elements (4.2 Å [20]). Dihydrobenzene can insert in two Bi–S bonds simultaneously resulting in the formation of the functionalized triarylbismuth compounds, the synthesis of which by other methods is rather complicated (Scheme 31).

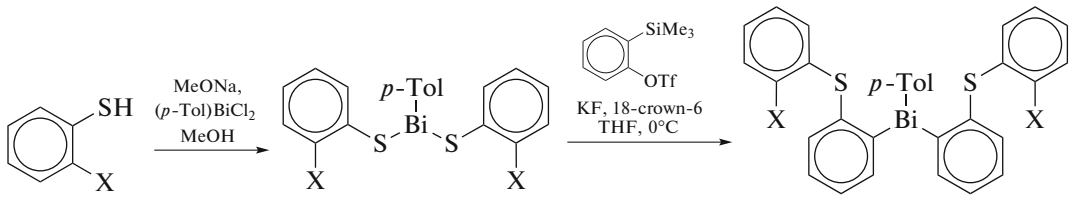

X = H, Br, Me

Scheme 31.

Several heterocyclic compounds of bismuth, C_4R_4BiAr (R = Et, Ph; Ar = Ph, Mes) and $L(Thi)_2$-BiMes, were synthesized using an efficient transfer of the metallocycle involving easily available zirconocycles, and their luminescence properties were studied (Scheme 32) [39].

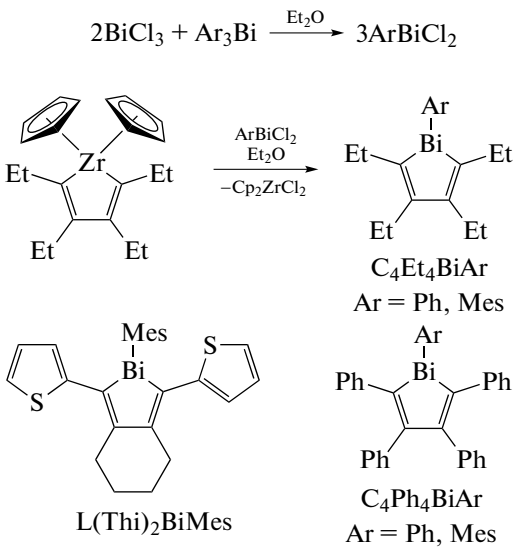

Scheme 32.

Azide–alkyne cycloaddition catalyzed by the copper(I) compound is presently widely used as a reliable method for covalent binding of diverse building blocks [40]. The application of organobismuth acetylenide $R^1-C\equiv C-BiAr_2$ eliminates undesirable protodehalogenation reactions, and the target product $N_3C_2(R^1R^2)-BiAr_2$ is isolated from the reaction mixture in the yield up to 99% (Scheme 33). The syntheses of various functionalized N-heterocyclic derivatives based on this method were described (Scheme 34).

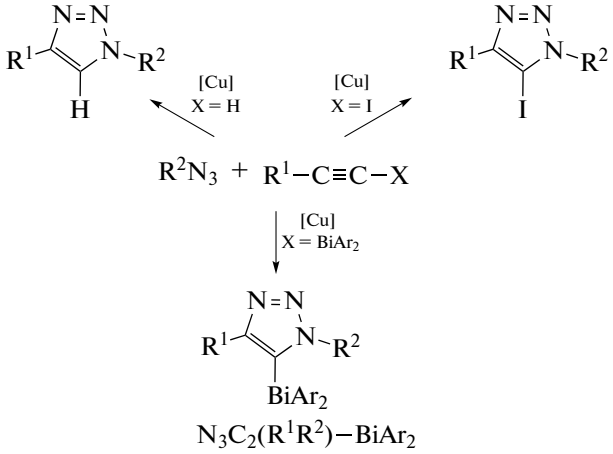

Scheme 33.

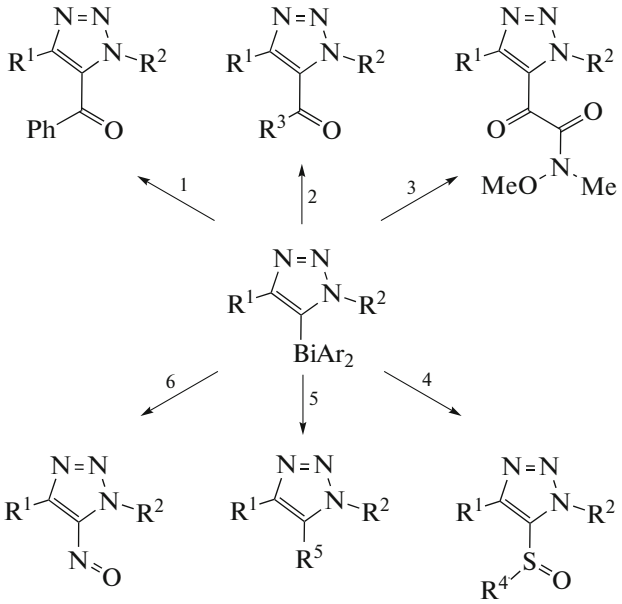

1. $PhC(O)Cl$, Me_2N–Py, Et_3N (4 : 1 : 4)
2. Diphosgene, Me_2N–Py, Et_3N, NucH (2 : 1 : 4 : 20) $R^3 = NEt_2$, OM
3. Oxalyl chloride, iPr_2NEt, NucH (2 : 3 : 20)
4. $SOCl_2$, iPr_2NEt, NucH (2 : 2 : 20) $R^4 = NEt_2$, OMe
5. $SOCl_2$, Et_3N (2 : 2) or Br_2 (1.2 equiv.) $R^5 = Cl$, Br
6. $NO^+[BF_4]^-$ (2 equiv.)

Scheme 34.

The preparation of a series of phosphorescent bismuth-containing polymers and block copolymers with arylated norbornenes (Scheme 35) was reported [41].

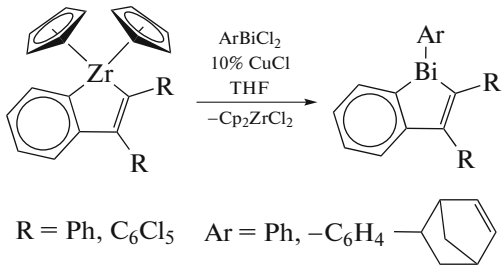

R = Ph, C_6Cl_5 Ar = Ph, $-C_6H_4$

Scheme 35.

The produced polymers with a high molecular weight contain benzobismuth resins in the carbon cage formed due to metathesis with ring opening (Scheme 36).

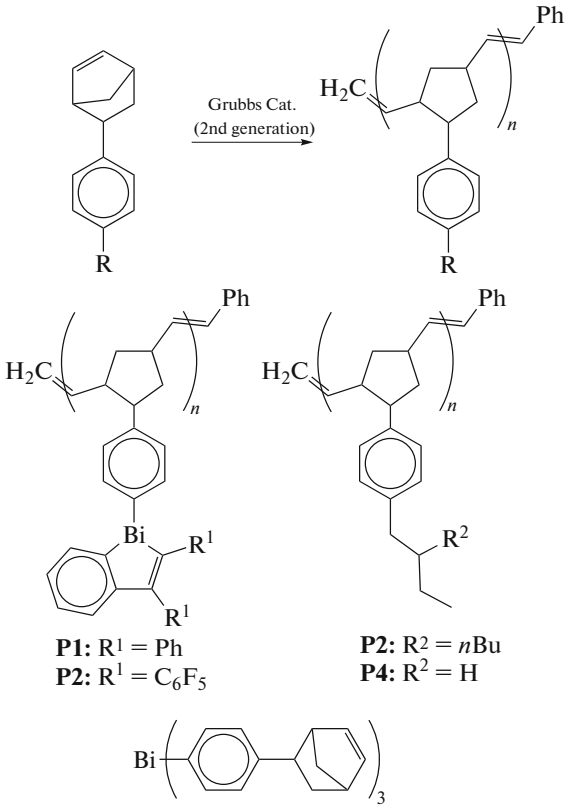

Scheme 36.

Dipyridinobismol DPyBi was synthesized by the reaction of the dilithium derivative of 2,2'-dibromo-4,4'-bipyridyl with diiodophenylbismuth (Scheme 37). The cyclic voltammogram of this compound in acetonitrile indicates an enhanced electron affinity compared to bipyridyl without a bridge. This compound and related antimony derivative (DPySb) possess a weak fluorescence at room temperature and an appreciable phosphorescence at 77 K with the emission maxima at λ_{max} = 453 and 454 nm and the lifetimes τ = 1.03 and 0.26 ms for DPySb and DPyBi, respectively. Solid-phase phosphorescence was also observed for these dipyridinoheterols at 77 K. The reaction of DPyBi with $Cu_2I_2(PPh_3)_3$ affords the corresponding copper complex $[(PPh_3)CuI(DPyBi)CuI(PPh_3)]_2$, which demonstrates red phosphorescence in the solid state at room temperature [42].

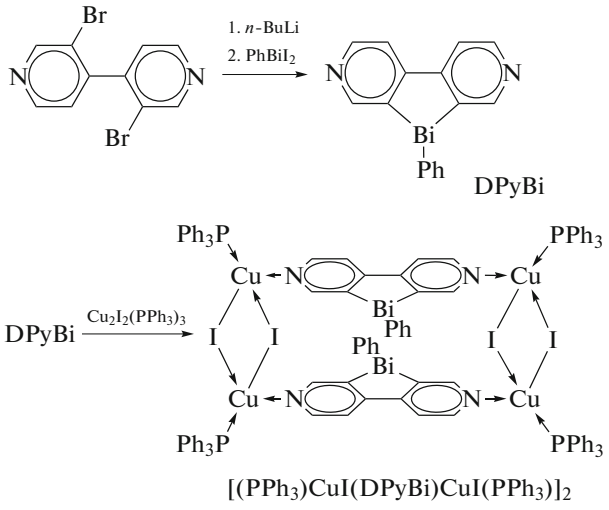

Scheme 37.

BISMUTH DERIVATIVES OF GENERAL FORMULAS $RBiX_2$ AND R_2BiX

Trivalent bismuth derivatives bearing one or two organic groups at the metal atom are prepared using several methods. The elimination of organic compounds from triorganylbismuth by the compounds containing the active hydrogen atom is the simplest and rather efficient method. Other methods are less efficient for the synthesis of these compounds and are based on substitution, addition, and insertion reactions.

Reactions of elimination of organic substituents from triorganylbismuth. A series of works devoted to the dephenylation of triphenylbismuth by carboxylic acids, the products of which are aryl- or diarylbismuth carboxylates, was published. A distinctive feature of diarylbismuth carboxylates is their polymeric structure caused by the bidentate properties of the carboxylate ligand. However, similar coordination polymers are presented by single examples. For instant, the synthesis of diphenylbismuth 2-phenylcarboranyl carboxylate via substitution between triphenylbismuth and 2-phenylcarboranylcarboxylic acid in benzene (Scheme 38) was described, and its structural features were determined by XRD [43].

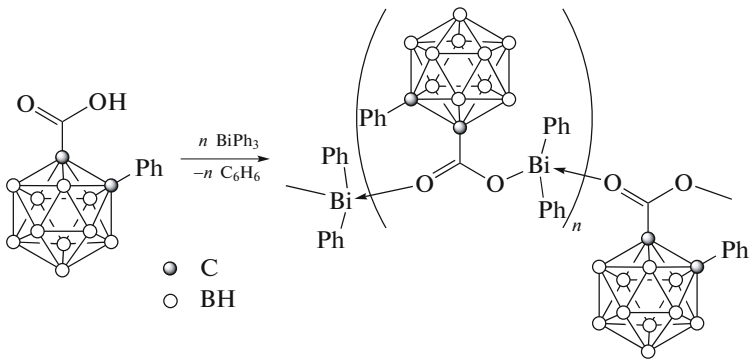

Scheme 38.

According to the XRD data, diphenylbismuth 2-phenylcarboranyl carboxylate represents a coordination polymer crystallized as a solvate with benzene. The bismuth atoms have the bis(phenoid) coordination with the apically arranged oxygen atoms of the 2-phenylcarboranylcarboxylate substituents. The equatorial plane contains two phenyl ligands and a lone electron pair.

The reactions of triphenylbismuth with 4-nitrophenylacetic and 2-nitrobenzoic acids in toluene at 90°C was studied [44]. Phenylbismuth bis(4-nitrophenylacetate) and phenylbismuth bis(2-nitrobenzoate) were shown to be formed at the equimolar ratio of the reactants in 49 and 46% yields, respectively. The minor reaction products are diphenylbismuth 4-nitrophenylacetate and diphenylbismuth 2-nitrobenzoate (27 and 16% yields, respective).

In order to study the influence of the solvent and nature of carboxylic acid on the formation of bismuth carboxylates, triphenylbismuth was treated with salicylic, 5-bromosalicylic, 3-methoxysalicylic, 5-nitrososalicylic, 3-methylanthranilic, 5-chloroanthranilic, and *N*-acetylanthranilic acids at the 1 : 2 molar ratio of the starting reactants under various conditions (Scheme 39) [45].

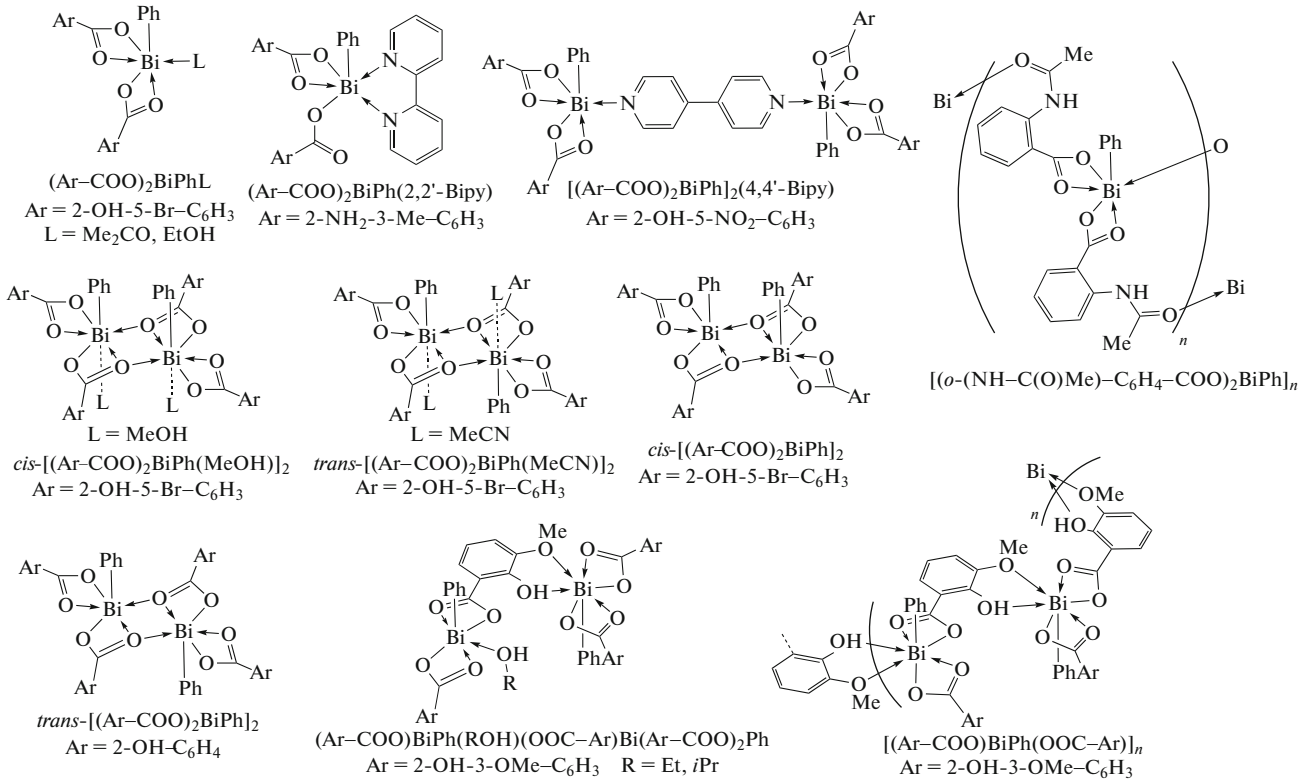

Scheme 39.

Compounds $(Ar{-}COO)_2BiPhL$ (L = $Me_2C{=}O$, EtOH) are monomeric and contain a molecule of the coordinated solvent in the equatorial position at the bismuth atom in the pentagonal pyramid. The same geometry was determined in $[(Ar\text{-}COO)_2BiPh]_2$(4,4'-Bipy), where two such units are linked together through the 4,4'-bipyridine ligand. Compounds (Ar−COO)BiPh(ROH)-(OOC−Ar)Bi$(Ar{-}COO)_2$Ph form dimers in which similar coordination polyhedra of Bi atoms are observed. Compounds $[(o\text{-}(NH{-}C(O)Me){-}C_6H_4{-}COO)_2\text{-}BiPh]_n$ and $[(Ar{-}COO)BiPh(OOC{-}Ar)]_n$ are polymeric. In $(Ar{-}COO)_2$BiPh(2,2'-Bipy), one of the carboxylate ligands is bidentate, whereas the second ligand remains monodentate reflecting the same structural geometry that was observed for the earlier described compounds. Compounds *cis/trans*-$[(Ar{-}COO)_2\text{-}BiPh(L)]_2$ (L = MeOH/MeCN), *cis*-$[(Ar{-}COO)_2\text{-}BiPh]_2$, and *trans*-$[(Ar{-}COO)_2BiPh]_2$) are dimeric structures linked with each other by common oxygen atoms of the carboxylate groups.

Three phenylbismuth dicarboxylates were synthesized by the dephenylation of triphenylbismuth with *o*-methoxybenzoic, *m*-methoxybenzoic, and 5-[(R/S)-2,3-dihydroxypropylcarbamoyl]-2-pyridinecarboxylic acids (molar ratio 1 : 2) on reflux of a mixture of the reactants in methanol or ethanol [46]. The addition of an equimolar amount of 2,2'-bipyridyl (Bipy) to the reaction mixture results in the synthesis of the stable $[PhBi(O_2CC_6H_4OMe\text{-}o)_2(Bipy)]\cdot 0.5EtOH$ complex. The synthesized complexes were character-

ized by NMR spectroscopy and tested to antileishmanial activity. Their toxicity toward mammalian cells was additionally evaluated. The bismuth complexes of substituted benzoic acid show a significant antileishmanial activity against promastigotes L, majorV121 at very low concentrations, while the corresponding free carboxylic acids exhibit no efficient activity. However, the bismuth compounds inhibit the growth of mammalian cells at all studied concentrations (from 1.95 to 500 μg/mL) after 48 h of incubation.

The reactions of triphenylbismuth with such heterocyclic carboxylic acids as 3-hydroxypicolinic, pyrazine-2-carboxylic, quinolone-2-carboxylic (quinaldinic), furan-2-carboxylic, and thiophene-2-carboxylic acids are shown to form diphenylbismuth carboxylates and phenylbismuth dicarboxylates [47]. According to the XRD data, the coordination number of bismuth in the synthesized complexes varies from 5 to 8 due to the coordination of the potential coordinating sites (heteroatoms and carbonyl oxygen atoms).

An increase in the coordination number of the bismuth atom is observed in phenylbismuth bis(chloroacetate), where the chloroacetate ligands are tridentate chelate-bridging and bind the adjacent molecules through the oxygen atoms into polymeric chains [48].

Two bismuth complexes $(MICA)_2BiPh$ and $(IGA)_2BiPh$ were synthesized from indolecarboxylic acids (MICAH = 1-methyl-1*H*-indole-3-carboxylic acid, and IGAH = 2-(1*H*-indol-3-yl)-2-oxoacetic acid) and triphenylbismuth in boiling ethanol (Scheme 40) [49].

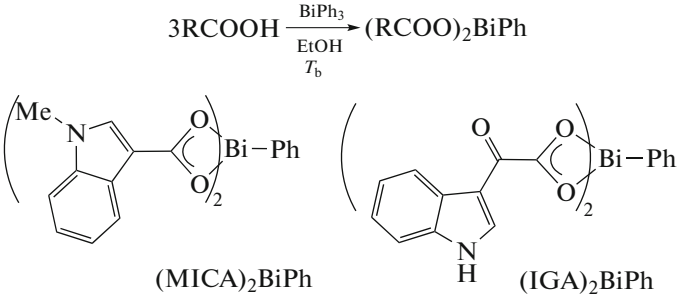

Scheme 40.

The complexes were characterized by elemental analysis, IR spectroscopy, mass spectrometry, and NMR (^1H, ^{13}C) spectroscopy. The $(IGA)_2BiPh$ complex in the solid state was characterized by X-ray crystallography as a dimer. The in vitro antibacterial activity of indolecarboxylic acids and their bismuth complexes was estimated against *Helicobacter pylori*. The compounds are highly active against leishmaniasis without any toxicity toward mammalian cells at their effective concentration.

Phenylbismuth dicarboxylate $(3\text{-Hpic})_2BiPh$ was obtained from triphenylbismuth and 3-hydroxypicolinic acid (3-HpicH) in the absence of solvent followed by recrystallization from DMF (Scheme 41) [50].

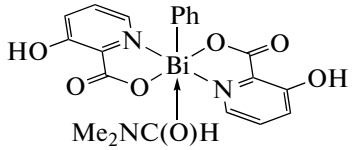

Scheme 41.

In molecules of the complex, the bismuth atoms are hexacoordinate in the distorted pentagonal pyramidal geometry with two N atoms, two O atoms of the chelating 3-Hpic ligands, and the oxygen atom of the solvent molecule in the equatorial plane and the phenyl substituent in the apical position.

The polynuclear bismuth oxoclusters were prepared from triphenylbismuth and *ortho*-nitrobenzoic acid under various conditions (Scheme 42) [51].

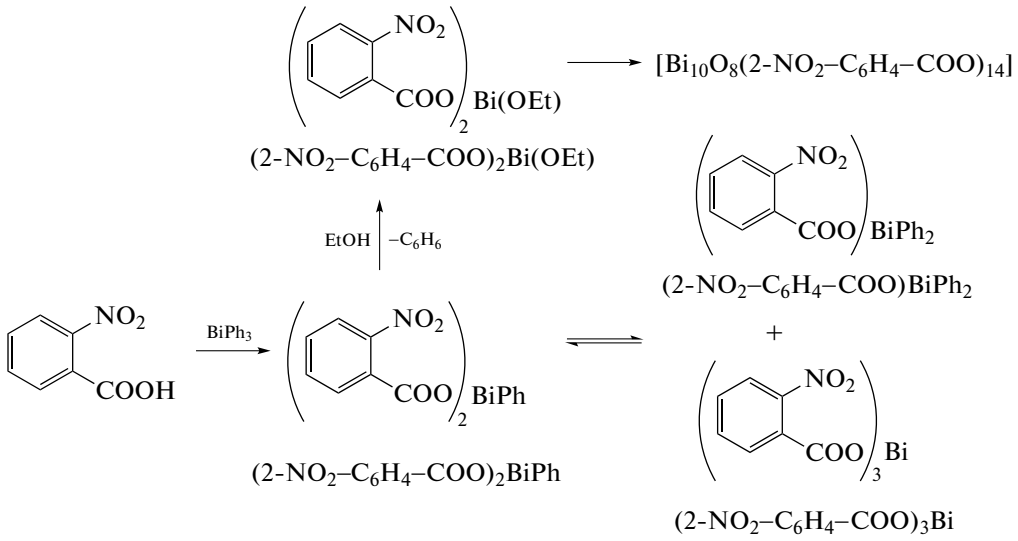

Scheme 42.

Compounds $(2\text{-}NO_2{-}C_6H_4{-}COO)_2Bi(OEt)\cdot EtOH$ and $(2\text{-}NO_2{-}C_6H_4{-}COO)BiPh_2$, which primarily crystallized together, were obtained at the 1 : 2 molar ratio of the starting reactants in ethanol, whereas $(2\text{-}NO_2{-}C_6H_4{-}COO)_3Bi\cdot H_2O$ was formed later from the filtered off mother liquor. Compound $(2\text{-}NO_2{-}C_6H_4{-}COO)_2Bi(OEt)\cdot EtOH$ is a result of the in situ ethanolysis of the $(2\text{-}NO_2{-}C_6H_4{-}COO)_2BiPh$ product and then undergoes hydrolysis with the formation of crystals of the $[Bi_{10}O_8(2\text{-}NO_2{-}C_6H_4{-}COO)_{14}](EtOH)_x$ oxocluster. The XRD studies of single crystals of four of the five compounds (except for $(2\text{-}NO_2{-}C_6H_4{-}COO)_2BiPh$) show that all of them are polymeric in the solid state and the coordination number of bismuth in them are 9, 8, and 5, respectively.

Bismuth(III) oxide $(ArBiO)_2$, which is coordinated via the N,C,N-intramolecular mode, where Ar = 2,6-$(Me_2NCH_2)_2C_6H_3$, reacts with 1,1'-ferrocenedicarboxylic acid to form the corresponding binuclear carboxylate $(Fc(COO)_2BiAr)_2$ (Scheme 43) [52].

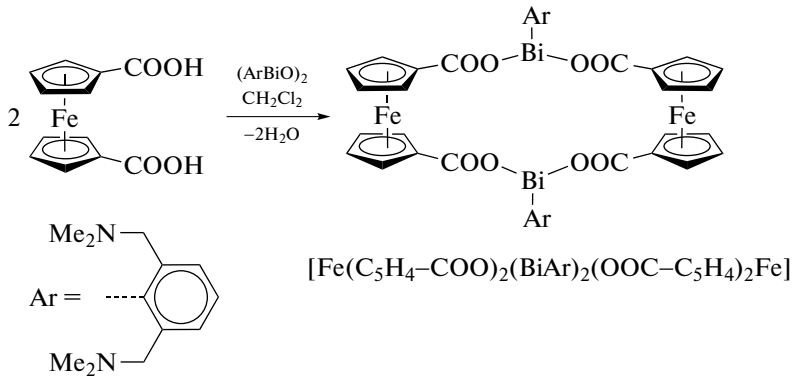

Scheme 43.

The compound was characterized by NMR, Raman, IR, and UV–VIS spectroscopy and XRD.

The phenanthrolinebismuth complex $[Bi(Phen)(C_6H_5COO)(C_6H_4COO)]$ (Phen = 1,10-phenanthroline) as brown crystals was synthesized from bismuth nitrate, 2-mercaptobenzoic acid, 1,10-Phen as the auxiliary ligand, nitric acid, and neodymium oxide in water at 160°C for 3 days (Scheme 44) [53]. The complex was characterized by XRD, IR spectroscopy, and thermogravimetric analysis.

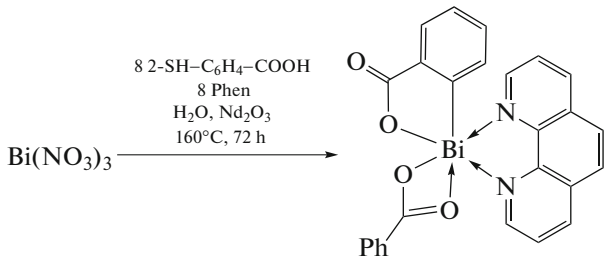

[Bi(Phen)(C_6H_5COO)(C_6H_4COO)]

Scheme 44.

Evidently, the appearance of the benzoate group in the complex is caused by the desulfonation of 2-mercaptobenzoic acid that occurs under the hydrothermal conditions.

Two bismuth complexes (Napht–C(O)S)$_2$BiPh (Scheme 45) and (4-BrC_6H_4–C(O)S)$_2$BiPh prepared from thionaphthoic and *p*-bromothiobenzoic acids and triphenylbismuth in a boiling ethanol solution (1 h) were characterized, and their in vitro activity against leishmaniasis and total toxicity toward human fibroblast cells were evaluated [54].

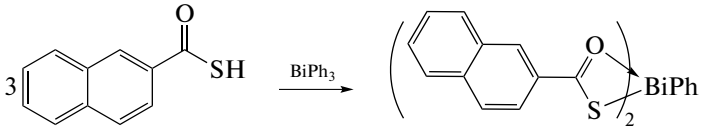

(Napht–C(O)S)$_2$BiPh

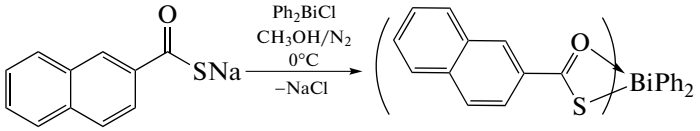

(Napht–C(O)S)$BiPh_2$

Scheme 45.

It should be mentioned that the thermolysis of the (R–C(O)S)$BiPh_2$ derivatives led to the formation of compounds $PhBiX_2$ and triphenylbismuth via the radical redistribution reaction (Scheme 46).

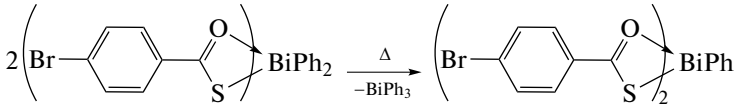

(4-Br–C_6H_4–C(O)S)$BiPh_2$ (4-Br–C_6H_4–C(O)S)$_2$BiPh

Scheme 46.

According to the XRD data, in the (4-Br–C_6H_4–C(O)S)$_2$BiPh complex two thiocarboxylate ligands coordinate to the bismuth atom with the formation of the distorted octahedral geometry of the coordination node in which the phenyl group and lone electron pair are oriented axially toward the plane formed by two thiocarboxylate ligands. The intermolecular Bi···S interactions (3.54 Å) bind these monomeric units into a single whole. It was shown that, in the biological respect, the bismuth thiocarboxylate derivatives turned out to be more active than the corresponding acids. The highest activity of the (Napht–C(O)S)$BiPh_2$ and (4-Br–C_6H_4–C(O)S)$_2$BiPh complexes was mentioned.

Several bismuth(III) compounds, (PhC(O)S)$_2$BiPh, *m*-NO_2–C_6H_4–C(O)S)$_2$BiPh, and (3-SO_3–C_6H_4–C(O)S)$_2$BiPh, were synthesized from thiobenzoic acids and triphenylbismuth (Scheme 47) [55]. The derivative with two phenyl groups at the bismuth

atom, $(Ph{-}C(O)S)BiPh_2$, was synthesized from diphenylbismuth chloride via the substitution reaction. The compound is readily transformed via ligand redistribution into the monophenyl complex $(Ph{-}C(O)S)_2BiPh$.

$$2Ph{-}C(O)SH + BiPh_3 \longrightarrow (Ph{-}C(O)S)_2BiPh$$

$$Ph{-}C(O)SNa + Ph_2BiCl \longrightarrow (Ph{-}C(O)S)BiPh_2$$

$$2(Ph{-}C(O)S)BiPh_2 \rightleftharpoons (Ph{-}C(O)S)_2BiPh + BiPh_3$$

Scheme 47.

The XRD data show that the $(Ph{-}C(O)S)_2BiPh$ complex forms discrete tetrameric units fastened by long intermolecular Bi···S bonds (3.774 Å). The activity of the $(Ph{-}C(O)S)_2BiPh$ and $(Ph{-}C(O)S)BiPh_2$ complexes against three strains of *Helicobacter pylori* was studied. The high level of bactericidal activity was shown to be insensitive to the degree of substitution at the bismuth atom.

A series of the monoorganic bismuth dithiocarboxylate complexes $(Ar{-}C(S)S)_2BiR$ (R = Me, Ph, *p*-Tol; Ar = Ph, *p*-Tol) was synthesized by the substitution reactions from triorganylbismuth or methylbismuth dichloride and dithiocarboxylic acids in the presence of trimethylamine as an acceptor of HCl (Scheme 48) [56].

$$R_3Bi + 2Ar{-}C(S)SH \xrightarrow[-2RH]{} (Ar{-}C(S)S)_2BiR$$

$$MeBiCl_2 + 2Ar{-}C(S)SH \xrightarrow[-2[Et_3NH]^+Cl^-]{2\ Et_3N} (Ar{-}C(S)S)_2BiMe$$

R = Me, Ph, *p*-Tol; Ar = Ph, *n*-Tol

Scheme 48.

The compounds were characterized by elemental analysis and spectroscopic studies. The molecular structure of $(p\text{-Tol}{-}C(S)S)_2BiR$ (R = Me or Ph) in the crystalline state was determined by XRD. It is shown that the bismuth atom in these compounds adopts the square pyramidal configuration with the R group in the apical position. The thermolysis of $(p\text{-Tol}{-}C(S)S)_2BiR$ (R = Me or Ph) on reflux in diphenyl ether resulted in the formation of nanocrystals of Bi_2S_3. The $(p\text{-Tol}{-}C(S)S)_2BiPh$ complex was used to precipitate thin films of Bi_2S_3.

The treatment of triphenylbismuth with 4-methyl-4*H*-1,2,4-triazole-3-thiol (4-MTTH) or 2-mercapto-1-methylimidazole (2-MMIH) in a toluene–ethanol mixture of solvents on reflux or under microwave irradiation results in the oxidation of the bismuth derivatives and formation (in both cases) of bright yellow substances: $(4\text{-MMT})_4BiPh$ and $(2\text{-MMI})_4BiPh$, respectively. The synthesis time was the shortest (7 min) in the case of microwave irradiation (Scheme 49) [57].

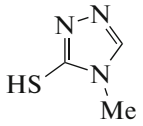

4-MMTH

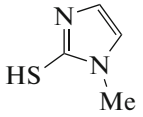

2-MMIH

$$4\ 4\text{-MMTH} \xrightarrow[\text{Reflux, 18 h}\ \text{or MW, 115°C, 7 min}]{BiPh_3,\ \text{toluene/EtOH}} (4\text{-MMT})_4BiPh \xrightarrow{DMSO} (4\text{-MMT})_2(4\text{-MMTH})_2BiPh$$

$$4\ 2\text{-MMIH} \xrightarrow[\text{Reflux, 18 h}\ \text{or MW, 115°C, 7 min}]{BiPh_3,\ \text{toluene/EtOH}} (2\text{-MMI})_4BiPh \xrightarrow{DMSO} (2\text{-MMI})_2(2\text{-MMIH})_2BiPh$$

Scheme 49.

However, the recrystallization of the $(4\text{-MMT})_4BiPh$ and $(2\text{-MMI})_4BiPh$ complexes from dimethyl sulfoxide (DMSO) resulted in the formation of the trivalent bismuth derivatives $[(4\text{-MMT})_2(4\text{-MMTH})_2BiPh]_3$ and $[(2\text{-MMI})_2(2\text{-MMIH})_2BiPh]_4$.

The products of the reactions of heterocyclic tetrazole-, imidazole-, and thiadiazole-thiols, namely, 1-methyl-1*H*-tetrazole-5-thiol (1-MMTZH), 4-MTTH, 5-methyl-1,3,4-thiadiazole-2-thiol (5-MMTDH), and 1,3,4-thiadiazole-2-dithiol ($2,5\text{-DMTDH}_2$),

with triphenylbismuth are heteroleptic complexes of thiolatophenylbismuth of the general formula $(RS)_2BiPh$, which were also obtained from phenylbismuth dichloride and thiol sodium salt (Scheme 50) [58]. The synthesized complexes were characterized by spectral methods and XRD.

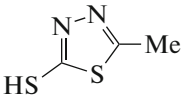

5-MMTDH

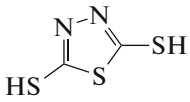

$2,5\text{-DMTDH}_2$

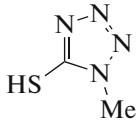

1-MMTZH

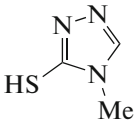

4-MMTH

$$2RSH + BiPh_3 \xrightarrow{\text{Toluene/EtOH}} (RS)_2BiPh$$

$$2RSNa + PhBiCl_2 \xrightarrow[-2NaCl]{\text{Toluene/EtOH}} (RS)_2BiPh$$

Scheme 50.

The bactericidal properties of the synthesized compounds against *Mycobacterium smegmatis* (*M. smegmatis*), *Staphyllococcus aureus* (*S. aureus*), methicillin-resistant *Staphyllococcus aureus* (MRSA), vancomycin-resistant enterococcus (VRE), *Enterococcus faecalis* (*E. faecalis*), and *Escherichia coli* (*E. coli*) were evaluated. Among them, the complexes containing the 1-MMTZ and 4-MTT ligands showed the highest efficiency: $(1\text{-MMTZ})_2(1\text{-MMTZH})_2BiPh$ and $(4\text{-MTT})_2(4\text{-MTTH})_2BiPh$. All complexes exhibited insignificant or zero toxicity against COS-7 cells of mammalia at 20 mg/mL.

The thiolatobismuth complex $(5\text{-MMTD})_2(4\text{-MMTH})BiPh$ was synthesized from heterocyclic thiadiazole- and triazole-thiones and structurally characterized (Scheme 51) [59].

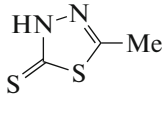

5-MMTDH

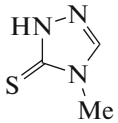

4-MMTH

$$2\ 5\text{-MMTDH} + 4\text{-MMTH} \xrightarrow[\substack{\text{toluene}\\ \text{Reflux, 12 h}\\ \text{or MW, 115°C, 10 min}}]{BiPh_3} (5\text{-MMTD})_2(4\text{-MMTH})BiPh$$

Scheme 51.

The complex was shown to exhibit antibacterial properties against *Staphyllococcus aureus*, VRE, *E. faecalis*, and *E. coli* and a low toxicity toward the mammalian COS-7 cell lines in a dose of 20 μg/mL.

Compound $(MBT)_2BiPh$ was obtained from 4-phenylthiazole-2-thiol (MBTH) and triphenylbismuth or from $BiPhCl_2$ and corresponding sodium thiolate (NaMBT) (Scheme 52) in the yield up to 89% under various conditions (without solvent, 100°C, 4 h; reflux of toluene solution, 6 h; microwave irradiation, toluene, 115°C, 15 min; methanol, 12 h, 24°C) and characterized by XRD [60].

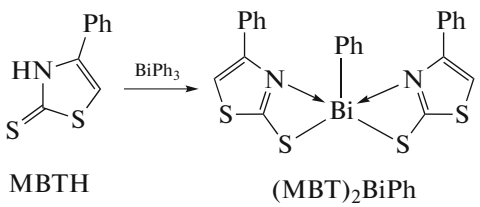

MBTH $(MBT)_2BiPh$

Scheme 52.

The $(MBT)_2BiPh$ complex, being dimeric in the crystal, was shown to manifest a high antileishmanial activity; exhibits active bactericidal properties against *Mycobacterium smegmatis*, MRSA, *E. faecalis* resistant

to VRE, and *E. coli*; and demonstrates a low toxicity toward the mammalian COS-7 cells at 20 μg/mL.

A series of 5-substituted phenylthiazoloxadiazolethiones of the $(X\text{-PTOT})_2BiPh$ type, where X = Me, MeO, MeS, F, Cl, Br, and CF_3; PTOTH = 5-(2-phenylthiazol-4-yl)-1,3,4-oxadiazole-2-thiol (Scheme 53), was synthesized from triphenylbismuth and corresponding thioamides or from phenylbismuth dichloride and sodium salts of thioamides [61].

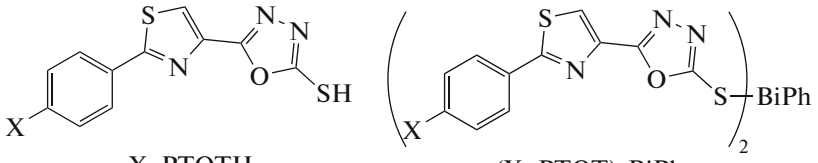

Scheme 53.

Complexes $(Cl{-}PTOT)_2BiPh$ and $(Br{-}PTOT)_2BiPh$ were recrystallized from DMSO and structurally characterized by XRD as $(X{-}PTOT)_2BiPh\cdot 2DMSO$ (X = Cl, Br). The antibacterial properties of the thiones and their Bi(III) complexes against *Mycobacterium smegmatis*, *S. aureus*, MRSA, VRE, *E. faecalis*, and *E. coli* were evaluated. All bismuth(III) complexes were shown to be highly efficient against all bacteria, since they have very low minimum inhibition concentrations (MIC) (1.1–2.1 μmol/L). These complexes exhibited an insignificant toxicity or the absence of toxicity toward the mammalian COS-7 cells at 20 μg/mL.

The bismuth(III) complexes $[(Sac)BiPh_2]_n$, $[(Sac)_2BiPh]_n$, $[(Tsac)BiPh_2]_n$, and $[(Tsac)_2BiPh]_n$ (SacH is saccharin, and TsacH is thiosaccharin) were synthesized and characterized [62]. The elimination of one phenyl group from the bismuth atom was observed upon reflux of equimolar amounts of triphenylbismuth and saccharin or thiosaccharin in ethanol for 30 min (Scheme 54).

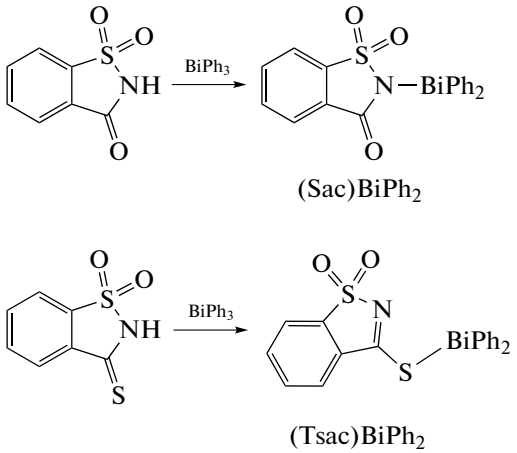

Scheme 54.

The $PhBiX_2$ derivatives were formed in the yield up to 73% at the 1 : 2 molar ratio and increasing heating time to 1 h. The structures of $[(Sac)BiPh_2]_n$ and $[(Tsac)BiPh_2]_n$ were confirmed by X-ray crystallography. In $[(Sac)BiPh_2]_n$, the Sac bridging ligands bind the Ph_2Bi groups to the tetracoordinate bismuth atom through the nitrogen atom (Bi–N 2.353(4) Å) and one of the oxygen atoms of the SO_2 group (Bi···O 2.605(4) Å). However, in the structure of $[(Tsac)BiPh_2]_n$, the thiosaccharin ligand is σ-bonded via the exocyclic sulfur atom to form the thiolate complex, thus confirming a more thiophilic character of bismuth(III). The crystal of the $[(Tsac)BiPh_2]_n$ complex also contains polymeric chains with formally tetracoordinate bismuth atoms. The activity of the complexes against *H. pylori* was estimated. The activity depends on both the ligand and degree of substitution of the ligand. The saccharinate complexes $[(Sac)BiPh_2]_n$ and $[(Sac)_2BiPh]_n$ manifest the activity comparable with the values standard for bismuth(III) tricarboxylates (6.25 μg/mL), whereas the activity of the thiolate bismuth complexes increased sharply with an increase in the number of thiolate groups. Saccharin, thiosaccharin, and triphenylbismuth were inactive.

The synthesis of phenylbismuth bis(2,5-dimethylbenzenesulfonate) in a yield of 94% from triphenylbismuth and 2,5-dimethylbenzenesulfonic acid in toluene was reported [63]. According to the XRD data and taking into account the stereochemically active lone electron pair, the bismuth atoms have a distorted octahedral coordination, which can be considered (without the "phantom"-ligand) as a square pyramid with the oxygen atoms in the equatorial positions and the carbon atom of the phenyl group in the axial position. The bismuth atom shifts from the mean equatorial O_4 plane by 0.19 Å in the direction opposite to the carbon atom. The trans angles in the equatorial OBiO plane are 177.7(1)° and 164.1(1)°. Two CBiO angles (89.0(5)°, 88.8(5)°) are close to the theoretical value, whereas other two CBiO angles (81.6(5)°, 82.5(5)°) significantly deviate from this value. The Bi–C bond length is 2.247(5) Å. The Bi–O bond lengths (2.394(9), 2.390(9) Å) and Bi···O coordination

bonds (2.396(10), 2.403(10) Å) almost do not differ from each other.

The synthesis and characteristics of two coordination polymers of vinylbismuth(III) sulfonates were reported [64]. The bismuth complexes were synthesized from triphenylbismuth and vinylsulfonic acid in ethanol or acetonitrile (Scheme 55).

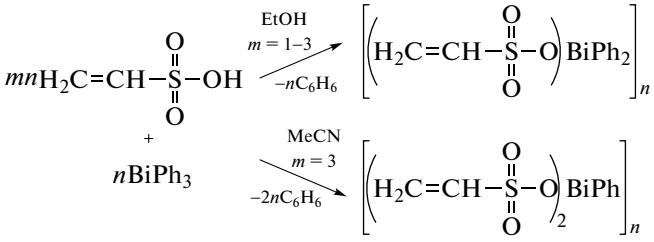

Scheme 55.

The structures of the compounds were proved by spectral methods and XRD. In the crystal of the coordination polymer $[(Vin\text{-}SO_3)BiPh_2]_n$ (Vin is vinyl), the bismuth atoms with allowance for the stereochemically active lone electron pair have the coordination of a distorted trigonal bipyramid in which the oxygen atoms occupy the apical positions with the OBiO angle equal to 164.7(3)°. One phenyl substituent of the adjacent molecule is oriented to the bismuth atom (Bi···arene 3.42 Å) at an almost perpendicular arrangement of the bismuth atom above the center of the phenyl ring (Scheme 56).

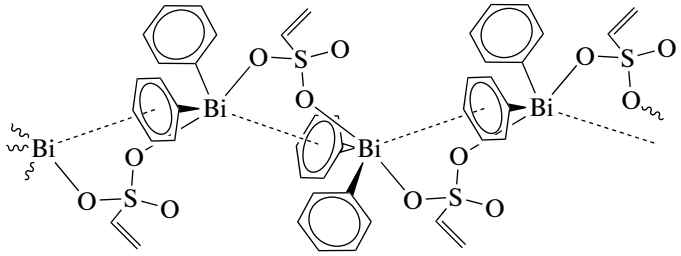

Scheme 56.

The crystal of the coordination polymer $[(Vin\text{-}SO_3)_2BiPh]_n$ contains crystallographically independent molecules of two types that do not interact with each other. The molecules of each type form a polymeric chain along the crystallographic *b* axis. In the polymeric chain, the bismuth atoms are bound to each other through the oxygen atoms of the sulfonate ligands. The coordination sphere of the bismuth atoms can be described best of all as a square pyramid with the phenyl substituent in the vertex. When taking into account the stereochemically active lone electron pair, the coordination sphere can be described as a pseudooctahedron.

Three diphenylbismuth organosulfonates $(R{-}SO_3)BiPh_2$, where R = *p*-tolyl (*p*-Tol), mesityl (Mes), or *S*-(+)-10-camphoryl (*S*-(+)-10-Camph), were synthesized by the reactions of equimolar amounts of triphenylbismuth and organosulfonic acid in alcohol with the yield of the target product up to 99% (Scheme 57) [65]. The recrystallization of the compounds from acetone is accompanied by ligand redistribution and formation of polymeric bis(organosulfonato)phenylbismuth $[(R{-}SO_3)_2BiPh]_x$ and triphenylbismuth.

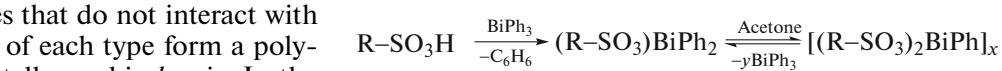

R = *p*-Tol, Mes, *S*-(+)-10-Camph

Scheme 57.

According to the XRD data, complexes $(Mes{-}SO_3)BiPh_2$ and $(S\text{-}(+)\text{-}10\text{-}Camph{-}SO_3)BiPh_2$ structurally resemble the polymeric spiral chains in which the bismuth atoms having the trigonal bipyramidal environment are bound to the oxygen atoms of the sulfonate groups with nearly linear OBiO angles. Two phenyl rings with the stereochemically active electron pair lie in the equatorial plane, and the axial positions are occupied by the oxygen atoms. The presence of one sulfonate ligand in the $(R{-}SO_3)BiPh_2$ compounds resulted in a sharp increase in the bactericidal activity toward bacterium *H. pylori* over triphenylbismuth and sulfonic acid, which were nearly inactive. In the $[(R{-}SO_3)_2BiPh]_x$ complexes (R = *p*-Tol, Mes), the bismuth atoms are

linked with each other by two bridging organosulfonate ligands through the oxygen atoms. The coordination mode of the bismuth atoms is octahedral, one position is occupied by a lone electron pair, and the Bi–C and Bi–O bond lengths are 2.226(7), 2.221(10) Å and 2.361(4)–2.384(7) Å, respectively. The eight-membered rings consisting of bismuth, oxygen, and sulfur atoms have a chair conformation, and two opposite oxygen atoms shift from the plane of other atoms (complanar within 0.09 Å) to opposite sides by 0.93 Å.

The treatment of triphenylbismuth with 5-sulfosalicylic acid (H_3Ssal) leads to the formation of phenylbismuth sulfosalicylate hydrate (HSsal)BiPh·H_2O and its ethanol-containing analog (HSsal)BiPh·EtOH [66]. According to the XRD data, both complexes in the solid state are polymers with the frameworks built of dimeric $[(HSsal)Bi]_2$. The former of these heteroleptic complexes demonstrates a remarkable solubility in water (10 mg/mL) due to which a transparent solution with pH 1.5 is formed. On the contrary, the second complex (with ethanol) is nearly insoluble in water. The complexes manifest a considerable activity toward bacterium *H. pylori*.

Diphenylbismuth triflate was synthesized from dimesityltellurium triflate and triphenylbismuth and by the counter synthesis from triphenylbismuth and trifluoromethanesulfonic acid (Scheme 58) [67].

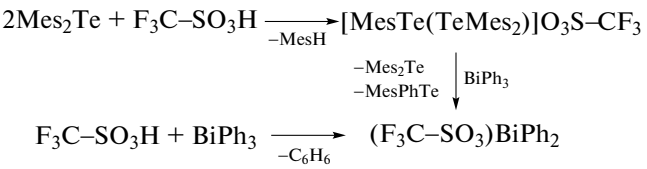

Scheme 58.

According to the XRD data, diphenylbismuth triflate represents a polymer in which the Ph_2Bi fragments are bound to each other via the bridging oxygen atoms of the triflate groups (2.531(6), 2.473(5) Å).

The reaction of triphenylbismuth with 1,1,2,3,3-pentamethyltrimethylenephosphinic acid {*cyc*-P(O)OH·$2H_2O$} in THF on heating and at room temperature affords the 16-membered macrocycle $[(cyc\text{-}PO_2)_8(BiPh)_4]$ and polymer $[(cyc\text{-}PO_2)BiPh_2]_n$, respectively (*cyc*-$PO_2$ is 1,1,2,3,3-pentamethyltrimethylenephosphinate) (Scheme 59) [68].

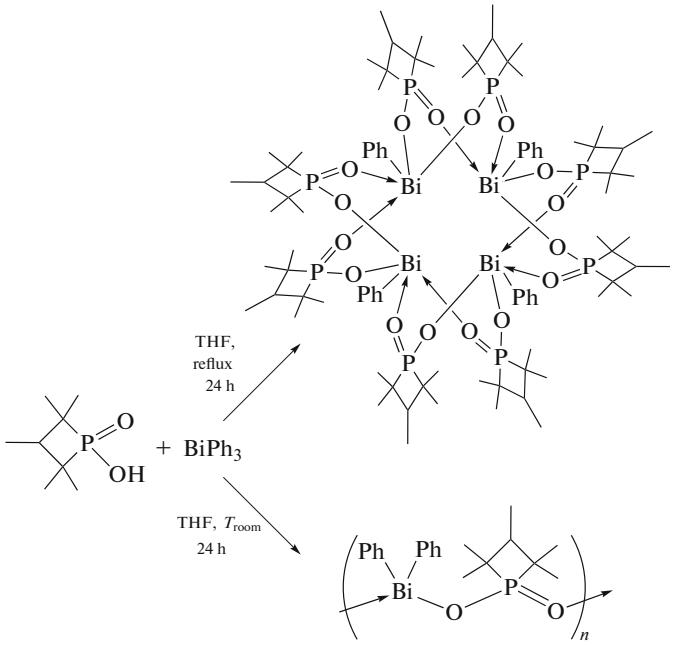

Scheme 59.

The anisobidentate phosphinate ligands are bridging in both complexes, which were characterized by XRD.

The reaction of phosphate diester $(t\text{BuO})_2PO(OH)$ with $BiPh_3$ in a ratio of 1 : 1 at room temperature in ethanol gives the coordination polymer $[((t\text{BuO})_2PO_2)BiPh_2]_n$ in which the bismuth atoms are linked with the isobidentate ligands $[(t\text{BuO})_2PO_2]$ (Scheme 60) [69].

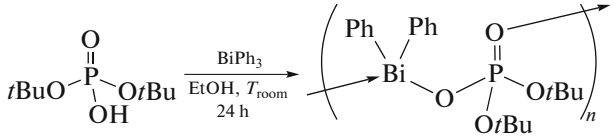

Scheme 60.

The thermolysis of the compound at 700°C gives the pure phase of $BiPO_4$.

New coordination polymer $[(Me_2N{-}C(S)S)BiPhCl]_n$ was synthesized from sodium dimethyl dithiocarbamate and triphenylbismuth (molar ratio 2 : 1) in a methanol–THF mixture of solvents (25°C, 24 h) and characterized by IR spectroscopy, ^{1}H NMR spectroscopy, and XRD [70]. In the crystal, the square pyramidal blocks with the phenyl ligand in the apical position are linked with each other by the bridging chlorine atoms to form a one-dimensional spiral chain (Scheme 61).

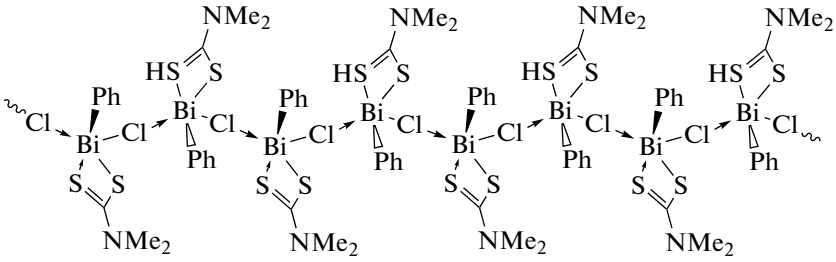

Scheme 61.

The complex is characterized by a high photocatalytic activity shown for methylene blue, rhodamine B, and methyl violet as examples.

Other methods for synthesis of bismuth derivatives $RBiX_2$ and R_2BiX. Compounds of trivalent bismuth with one or two organic substituents at the bismuth atoms can be synthesized by several methods among which the procedures based on the reactions of organic derivatives of active metals with bismuth trihalides are fairly efficient. For instance, a series of the trivalent bismuth derivatives tBu$_2$BiX (X = Cl, Br, I, CN, N_3, and SCN) was obtained [71]. Chloride tBu$_2$BiCl was synthesized by the reaction of bismuth trichloride with two equivalents of tBuMgCl, whereas compounds tBu$_2$BiX (X = Br, I, CN, and SCN) were produced from tBu$_3$BiX$_2$. Azide tBu$_2$BiN$_3$ was prepared by the reaction of tBu$_2$BiCl with NaN_3. The crystal of tBu$_2$Bi(CN) consists of polymeric chains in which the tBu$_2$Bi groups are bound to each other by the Bi–C≡N···Bi bridges (N···Bi distance 2.548 Å).

The approaches to the synthesis of the first adamantylbismuth complexes from adamantylmagnesium bromide or adamantyllithium and 1- and 2-adamantylzinc bromides (Scheme 62) were described [72].

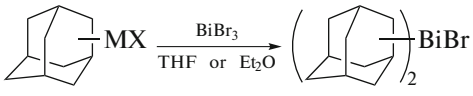

Scheme 62.

The molecular structure of bis(2-adamantyl)bismuth bromide in the crystalline state was confirmed by the XRD.

A series of pentafluoroethylbismuth derivatives $Et^F_nBiX_{3-n}$ ($Et^F = CF_2{-}CF_3$, X = F, Cl, Br, and I) was prepared via the schemes of classical organoelement synthesis, and the compounds were characterized by XRD [8]. Their chemical properties induced by the strong electron-acceptor character of the pentafluoroethyl groups are shown for the reactions with hydrohalic acids and salts of some elements used as examples (Scheme 63).

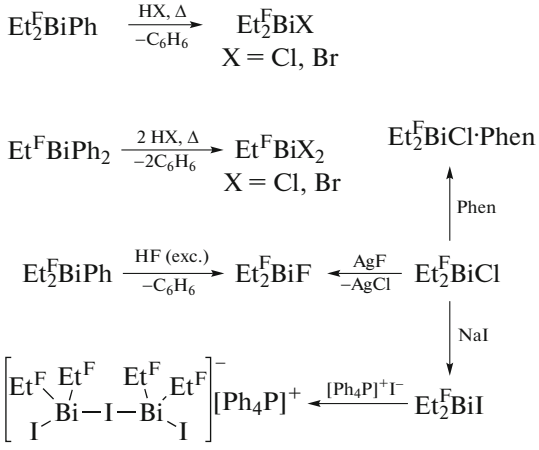

Scheme 63.

Four new sterically overloaded terphenyl-substituted bismuth dihalides of the $[Ar^mBiX_2]_2$ type (m = 1, 2 (Ar^1 = 2,6-Mes$_2$C$_6$H$_3$, X = Br, I; Ar^2 = 2,6-Mes$_2$-4-tBu-C$_6$H$_2$, X = Cl, Br)) were synthesized and structurally characterized (Scheme 64) [73]. Compounds $[Ar^1BiBr_2]_2$, $[Ar^2BiCl_2]_2$, and $[Ar^2BiBr_2]_2$ in the solid state are dimeric, whereas bismuth diiodide $[Ar^1BiI_2]_n$ is a one-dimensional coordination polymer.

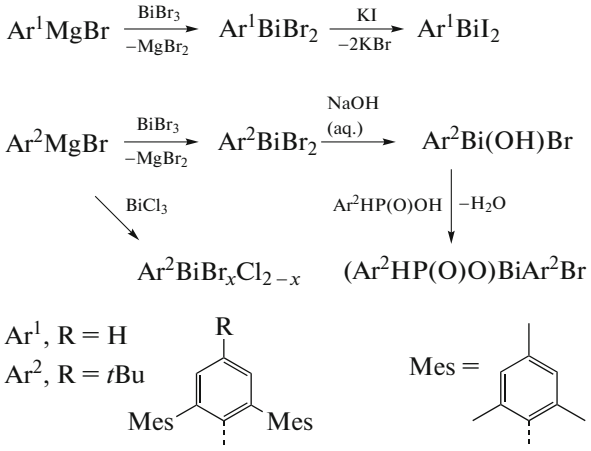

Scheme 64.

The hydrolysis of compound $[Ar^2BiBr_2]_2$ leads to the formation of bromoarylbismuth $Ar^2Bi(OH)Br$, which was isolated instead of the expected monoorganobismuth dihydroxide. The resistance of $Ar^2Bi(OH)Br$ to further hydrolysis can be explained by the intramolecular bismuth···arene π interactions. The reaction of $Ar^2Bi(OH)Br$ with sterically overloaded phosphinic acid $Ar^2PH(O)(OH)$ affords organobismuth phosphinate $(Ar^2HP(O)O)BiAr^2Br$. The XRD study of this compound revealed the unusual double π-intramolecular bismuth···arene coordination (Scheme 65).

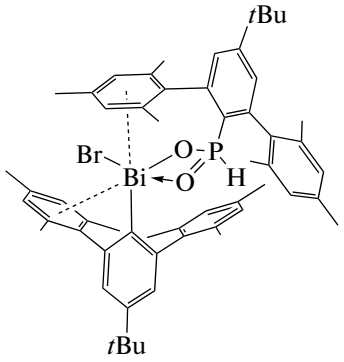

Scheme 65.

In order to study the Bi···π-arene intramolecular interactions, a series of nontransition metal compounds containing the bulky amide ligands $[(R_3Si)N(Ar^*)]$ (Ar^* = 2,6-$(CHPh_2)_2$-4-*t*Bu-C_6H_2, R = Me, Ph) were synthesized via Scheme 66 [74].

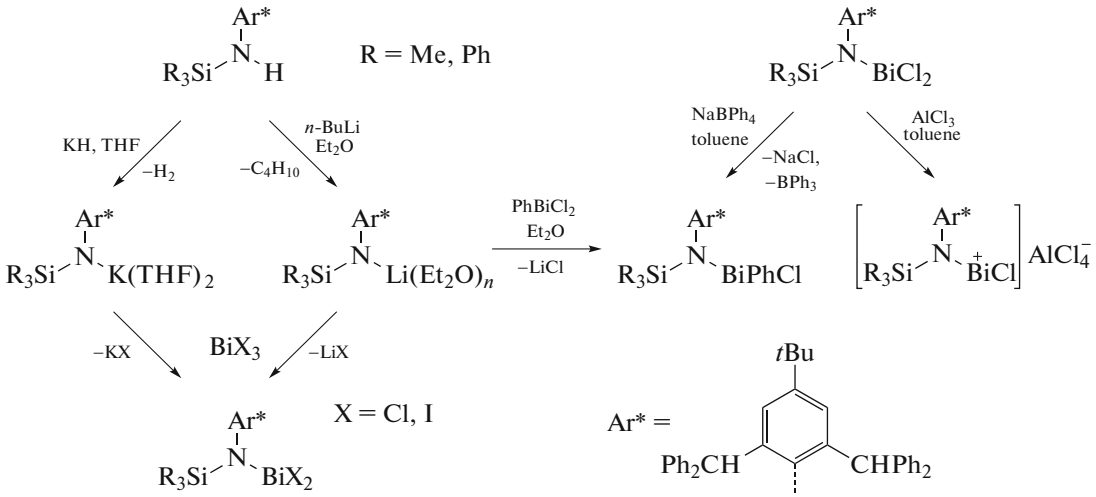

Scheme 66.

The shortest Bi···η⁶—π-arene contact is observed in the cationic complex $[(R_3Si)N(Ar^*)BiCl]^+[AlCl_4]^-$ (2.85—2.98 Å). In other bismuth complexes, the Bi···C (η⁶—π-arene) distances approach the sum of van der Waals radii of bismuth and carbon, indicating a weak interaction between them. Note that a similar contact was observed in the tetranuclear bismuth 3,4,5-trifluorobenzoate complex with toluene $Bi_4(O)_2(O_2CC_6H_2F_3\text{-}3,4,5)_8\cdot 2(\eta^6\text{-}C_6H_5Me)$ in which the Bi···C (η⁶—π-arene) distance reached 3.02 Å [75].

The reaction of Ph_2BiCl with PhSLi or (2,6-$Me_2C_6H_3$)SLi gives Ph_2BiSPh or $Ph_2Bi(SC_6H_3Me_2$-2,6), respectively [76]. Both compounds were characterized by IR, Raman, and ^1H and ^{13}C NMR spectroscopy and XRD. It is shown that the structure of Ph_2BiSPh is polymeric with the Bi(1)···S(2) intermolecular interactions (3.309(1) Å) and the Bi—S bond length equal to 2.588(1) Å. The complex crystallizes as a monomer with an increase in the volume of the phenylthiolate ligand in $Ph_2Bi(SC_6H_3Me_2$-2,6).

Poorly soluble in organic solvents colorless crystals of dimethylbismuth methoxide $[Me_2BiOMe]_\infty$ are formed upon the interaction of a benzene solution of trimethylbismuth with air oxygen (12 h) [77]. According to the XRD data, the complex is a coordination

polymer in which the MeO ligands link the Me_2Bi fragments into chains. The Bi–O bond lengths are equal to 2.359(6) and 2.344(6) Å, which is more than the sum of covalent radii of Bi and O (2.18 Å [20]), and the C–Bi distances (2.243(6), 2.243(6) Å) are usual for compounds of this type [78].

The method for the synthesis of some organobismuth compounds is based on the insertion of small molecules. It is shown that carbon monoxide is inserted into cationic bismuthamide at the Bi–N bond under mild conditions (Scheme 67) [79].

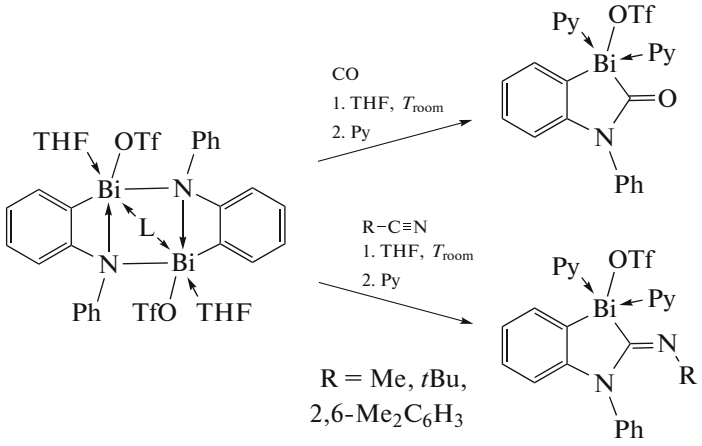

Scheme 67.

The combined experimental and theoretical approach made it possible to understand the mechanism of CO insertion that can be extended over isonitriles.

It is found that bismuth amide 1,8-$C_{10}H_6$-$(NSiMe_3)_2Bi–NMe_2$ derived from 1,8-bis((trimethylsilyl)amino)naphthalene and tris(dimethylamide)bismuth reacts with 2-benzoylpyridine, 3-pyridinecarboxaldehyde, 2-methyl-2-propenenitrile, and diethylacetylenedicarboxylate to form addition products at the Bi–N bond (Scheme 68) [80]. The synthesized compounds were characterized by XRD and spectral methods.

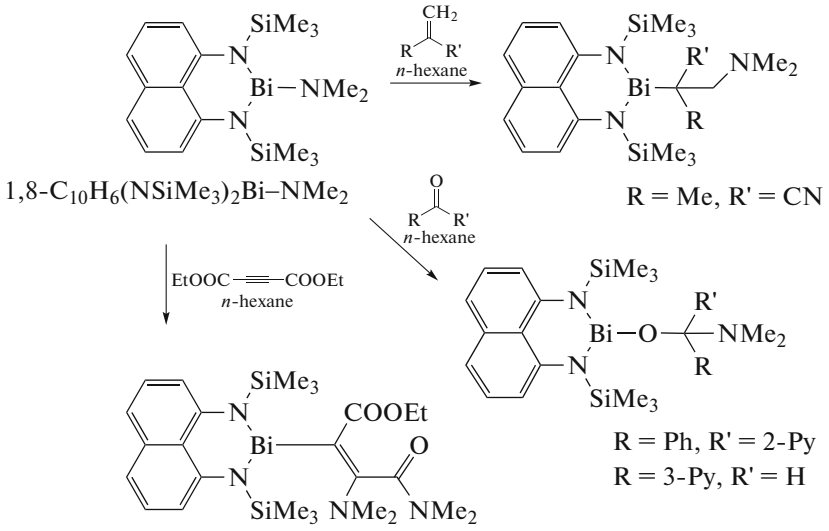

Scheme 68.

Using bismuth amide 1,8-$C_{10}H_6(NSiMe_3)_2$-$Bi–NMe_2$, one can synthesize trivalent bismuth derivatives with such hydrocarbon substituents as Me, C_5Me_5, and C≡CPh (Scheme 69) [81].

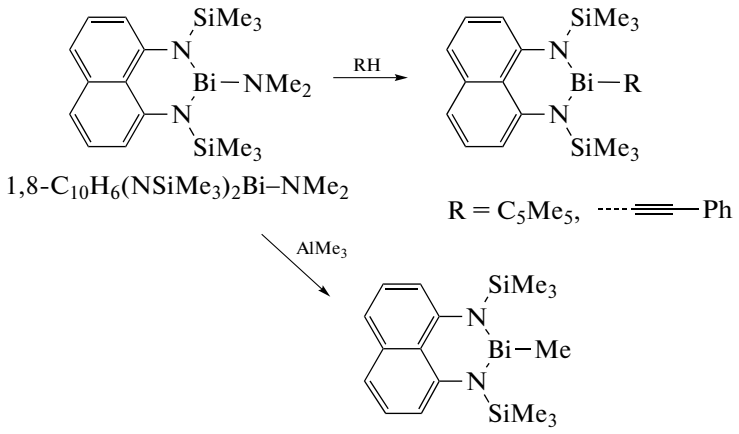

Scheme 69.

The structures of the compounds were proved by ^{1}H, ^{13}C, and ^{29}Si NMR spectroscopy and XRD.

It is shown that 1,2,4,3-triazaborol-3-yldiphenylbismuth $(L^{N3B})BiPh_2$ is characteristic of the insertion of small arylisonitrile (ArNC) and carbon monoxide molecules at the B—Bi bond (Scheme 70) [82].

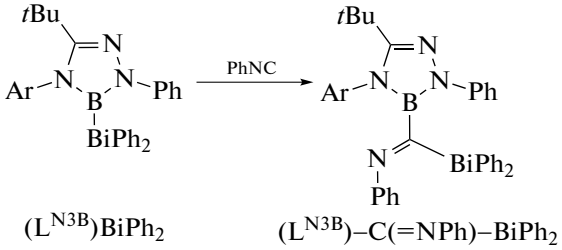

Scheme 70.

The starting compound $(L^{N3B})BiPh_2$ was prepared from amidrazone (Scheme 71), and complexes $(L^{N3B})BiPh_2$ and (L^{N3B})–C(=NPh)–$BiPh_2$ were characterized by XRD.

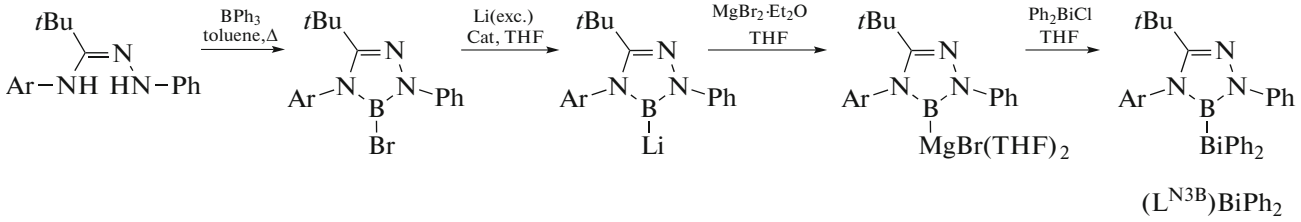

Scheme 71.

The reactivity of bismuth tribromide toward N-heterocyclic carbene 1,3-bis(2,6-diisopropylphenyl)-imidazol-2-ylidene (Dipp-NHC) was studied [83]. The addition of one molar equivalent of bismuth tribromide to a solution of IPr in diethyl ether was shown to form the (Dipp-NHC)·$BiBr_3$ adduct, which instantly precipitated from the reaction mixture as bright yellow crystals in a yield of 90% (Scheme 72). It is shown that the 1 : 1 (Dipp-NHC)·$BiBr_3$ adduct readily isomerizes on heating to 75°C (12 h) to form colorless crystals of the zwitter on (Scheme 72, bottom left), and its reaction with aluminum bromide leads to the ionic complex $[(Dipp\text{-}NHC)BiBr_2]^+[AlBr_4]^-$ (Scheme 72, bottom right).

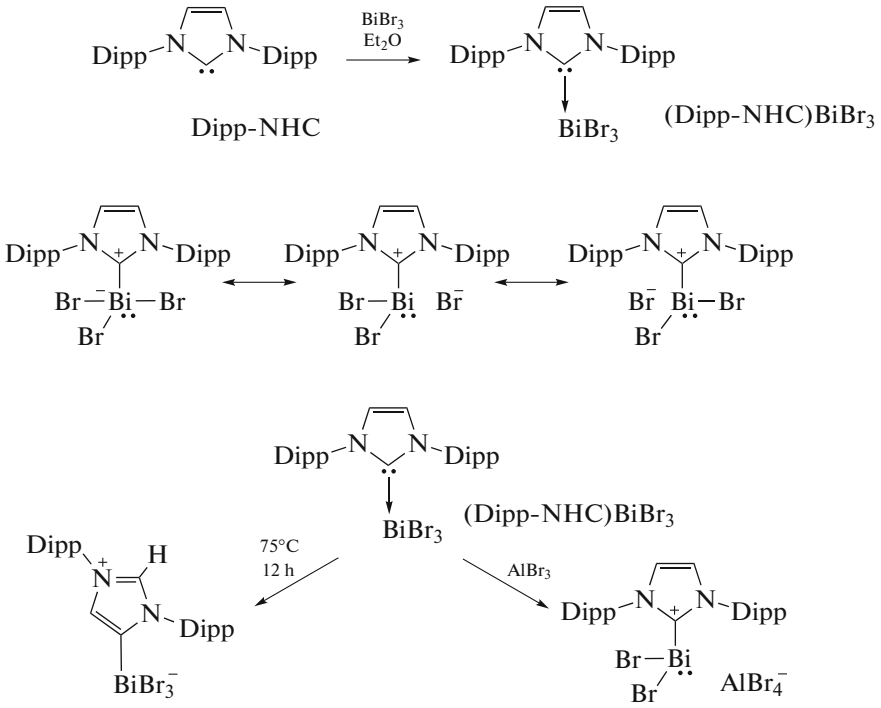

Scheme 72.

The synthesis and structural characteristics of the first adducts of N-heterocyclic carbene with bismuth chloride (Scheme 73) were described [84]. Compound (iPr–NHC^{Me})$BiCl_3$ was synthesized via the reaction of N-heterocyclic carbene iPr–NHC^{Me} with $BiCl_3$ (Scheme 73), and the addition of trimethylsilyltrifluoromethanesulfonate to a solution of this compound resulted in the (iPr–NHC^{Me})$BiCl_2$(OTf)(THF) adduct, whose dimeric structure in the crystalline form was proved by XRD.

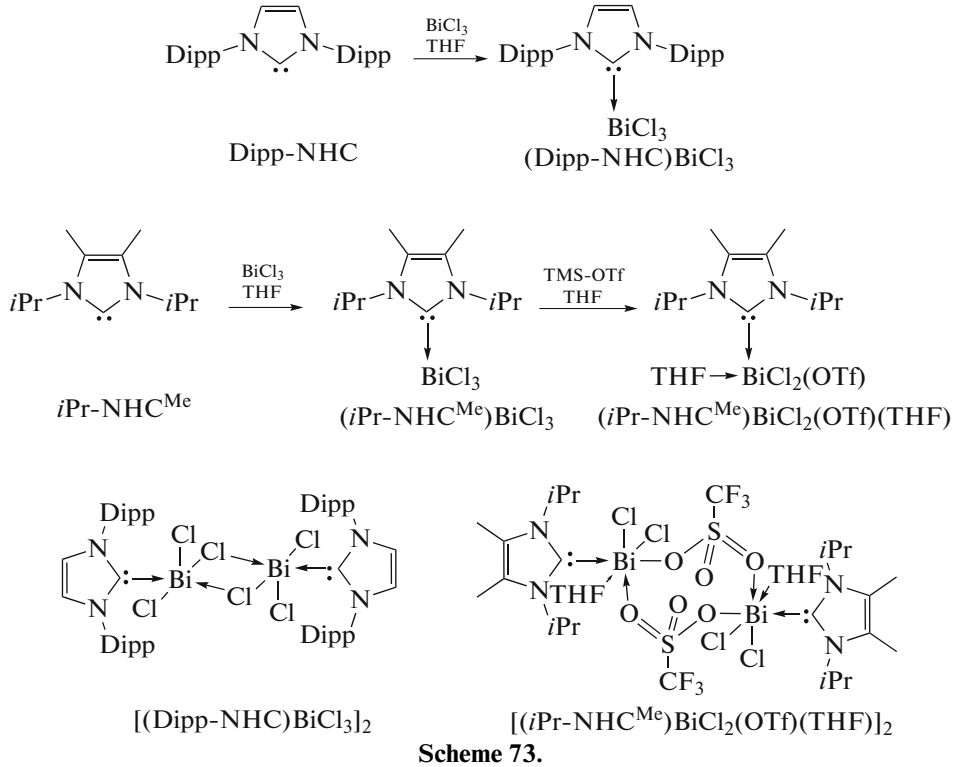

Scheme 73.

The synthesis of the first cyclic (alkyl)(amino)carbenes (^{Et2}CAAC)Bi(Ph)Cl_2 and (^{Cy}CAAC)Bi(Ph)Cl_2 stabilized by the bismuth complexes, which were prepared from carbenes and phenylbismuth dichloride (Scheme 74), was described in ref. [85].

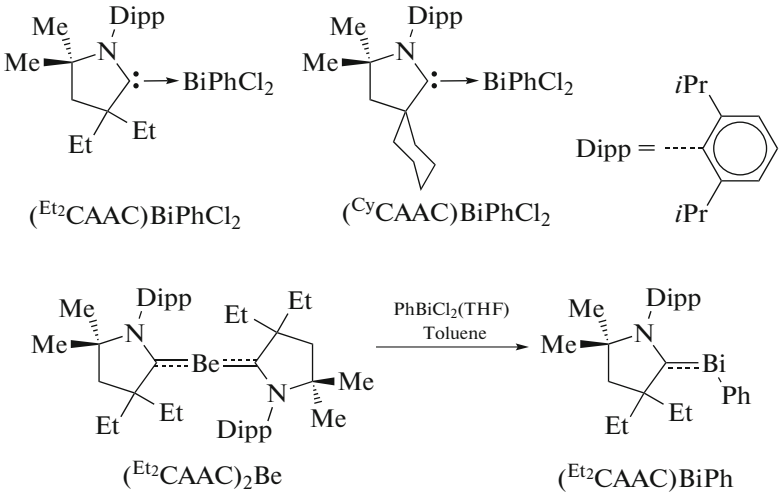

Scheme 74.

The bismuth complexes can also be prepared by the deprotonation of stable in air salts $[^{Et2}CAAC{-}H]_2^{2+}[Cl_2(Ph)Bi(\mu\text{-}Cl_2)Bi(Ph)Cl_2]^{2-}$ and $[^{Cy}CAAC{-}H]_2^{2+}[Cl_2(Ph)Bi(\mu\text{-}Cl_2)Bi(Ph)Cl_2]^{2-}$ using potassium bis(trimethylsilyl)amide $K[N(SiMe_3)_2]$. The same authors report in another work on the synthesis of the carbene-stabilized bismuthinidene complex (^{Et2}CAAC)BiPh from the beryllium complex (^{Et2}CAAC)$_2$Be, which is used as a reducing agent and ligand transfer reagent (Scheme 74) [86].

Adduct $(CDP^{Ph})BiCl_3$ of hexaphenylcarbodiphosphorane (CDP^{Ph}) with bismuth trichloride was obtained in a THF solution at room temperature (Scheme 75) [87]. The treatment of $(CDP^{Ph})BiCl_3$ with triflate TMS–OTf afforded complex $(CDP^{Ph})BiCl(OTf)_2$.

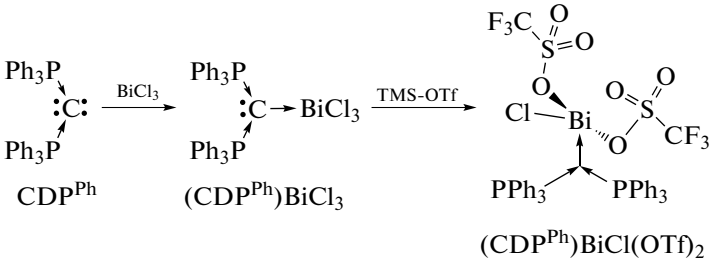

Scheme 75.

All compounds were characterized by spectral methods and XRD.

The kinetically stabilized carbene analog containing the bismuthenium ion $[(2,6\text{-}Mes_2C_6H_3)_2Bi]^+[BAr^F_4]^-$ (Mes = 2,4,6-$Me_3C_6H_2$, Ar^F = 3,5-$(CF_3)_2C_6H_3$) was obtained from diarylbismuth hydride and triphenylcarbenium salt (Scheme 76) [88].

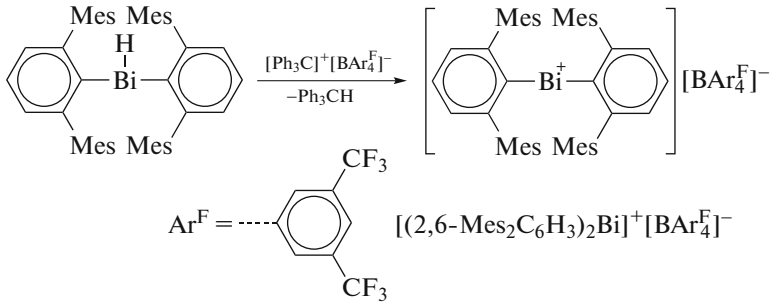

Scheme 76.

The reactions of [2+2] addition using acetylene or tolane were carried out for the heavy $[Bi(\mu\text{-}N(2,6\text{-}Mes_2C_6H_3))]_2$ biradical (Scheme 77) affording heterocyclic compounds, whose structures were proved by XRD [89].

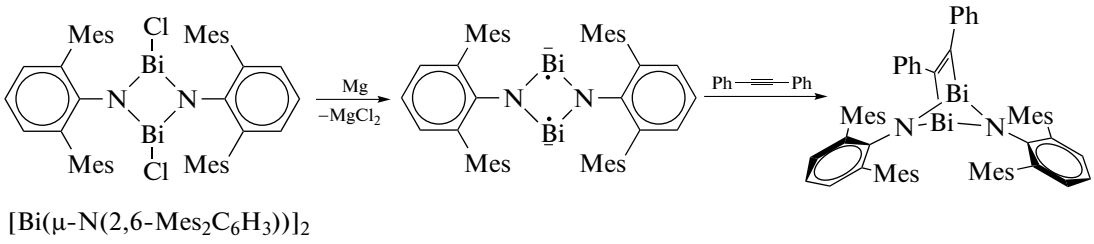

Scheme 77.

The reactions of the organobismuth derivatives accompanied by the formation of organic compounds of nonordinary structure are very interesting. For example, the reactivity of aminobismuthane $Mes^*N(SiMe_3)BiCl_2$ (Mes^* is 2,4,6-tri-*tert*-butylphenyl) with the organic metal derivatives was studied [90]. The synthesis of $Mes^*N(SiMe_3)BiCl_2$ in a yield of 33% is accompanied by the formation of the coupling product of two $Mes^*N(SiMe_3)H$ molecules in a yield of 60% (Scheme 78).

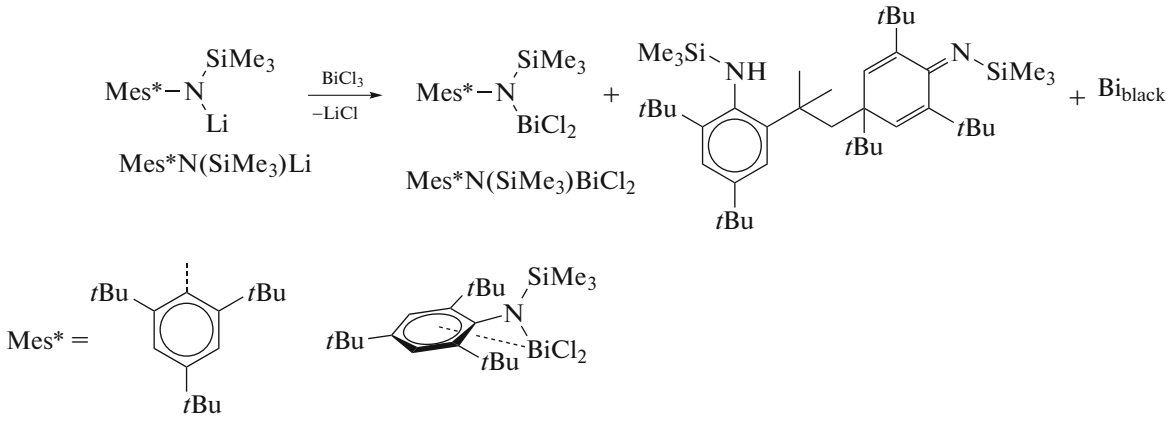

Scheme 78.

The reaction of $Mes^*N(SiMe_3)BiCl_2$ with $GaCl_3$ resulted in the formation of $[Mes^*N(SiMe_3)BiCl]^+[GaCl_4]^-$ only (Scheme 79). The use of the Ag[WCA] salt (WCA is the weakly coordinating anion) for binding chlorides made it possible to isolate the C–C coupling product. Diiodide $Mes^*N(SiMe_3)BiI_2$ and azidochloride compound $Mes^*N(SiMe_3)Bi(N_3)Cl$ were also synthesized, but the synthesis of these derivatives was not accompanied by the formation of coupling products.

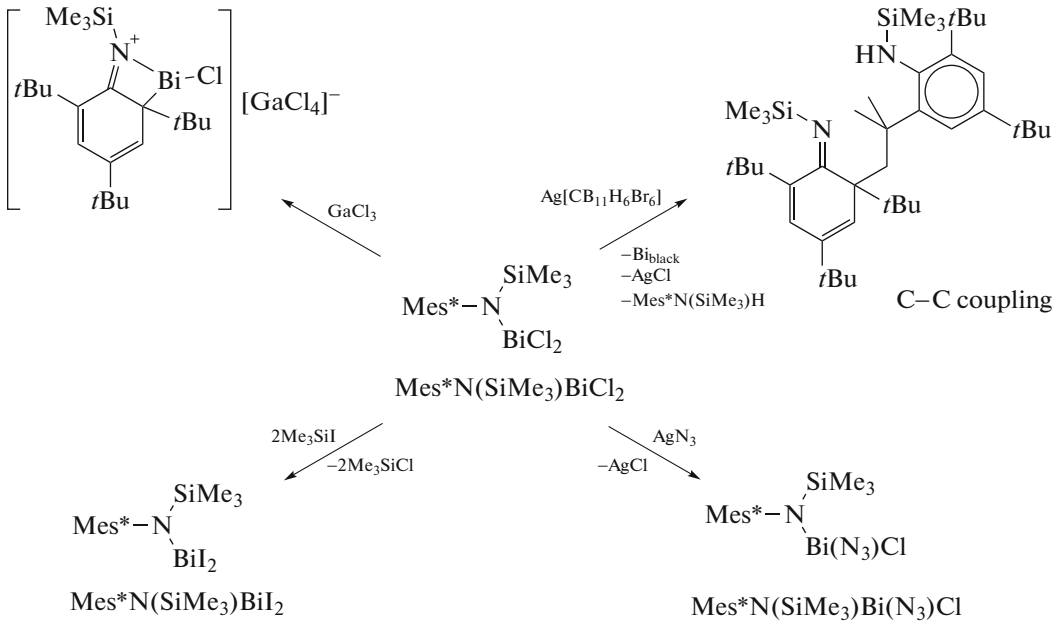

Scheme 79.

The synthesis and properties of bismuth(III) phosphinates were described [91]. When triphenylbismuth is treated with perfluoroalkylphosphinic acid, one or two phenyl groups are eliminated from the bismuth atom (Scheme 80).

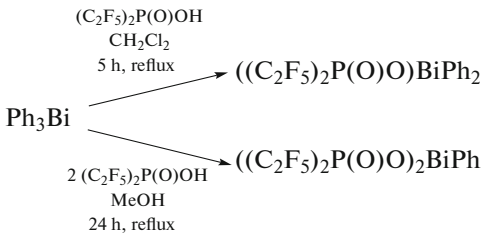

Scheme 80.

The examples for the successful application of the obtained bismuth phosphinates in the formation of carbon–carbon bonds are presented (e.g., Scheme 81).

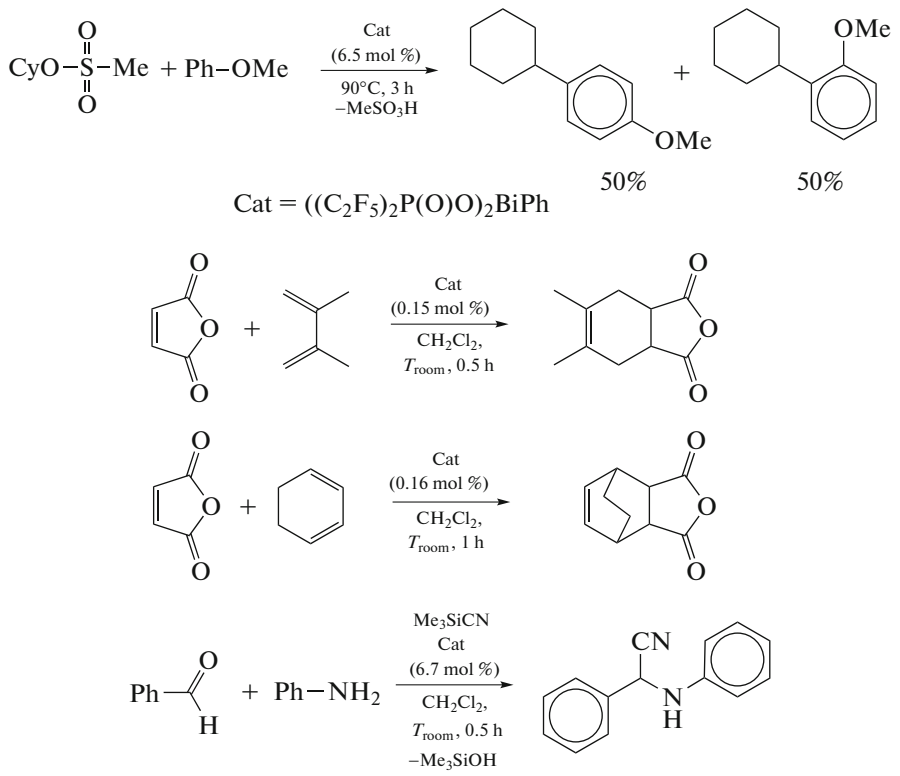

Scheme 81.

The carbometallation reactions conducted by mixing bismuth halide, carbon nucleophile, and unsaturated hydrocarbon were described [92], and a change in the type of halogen and bismuth salt switches regioselectivity of the reaction (Scheme 82).

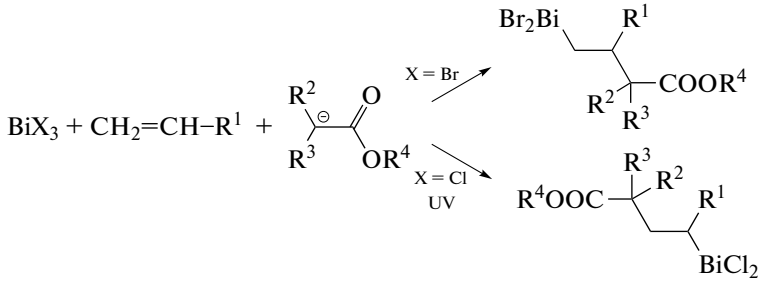

Scheme 82.

It should be mentioned that the reaction conditions determine the quantitative composition of the products (Scheme 83).

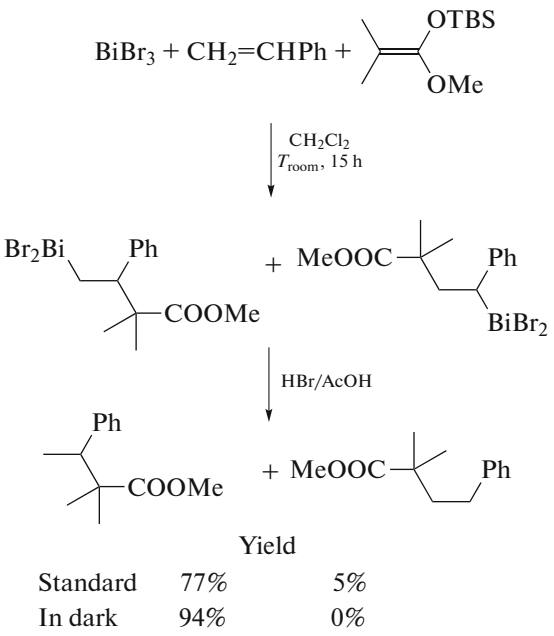

Scheme 83.

The carbobismuthination of alkyne was confirmed by the XRD study of the product of the reaction of bismuth tribromide with 3,5-di(*tert*-butyl)phenylacetylene and dimethylketenetrimethylsilylmethylacetal in dichloromethane at room temperature, when the single product is monoalkenylbismuth dibromide isolated from the reaction mixture as colorless crystals in a quantitative yield (Scheme 84) [93].

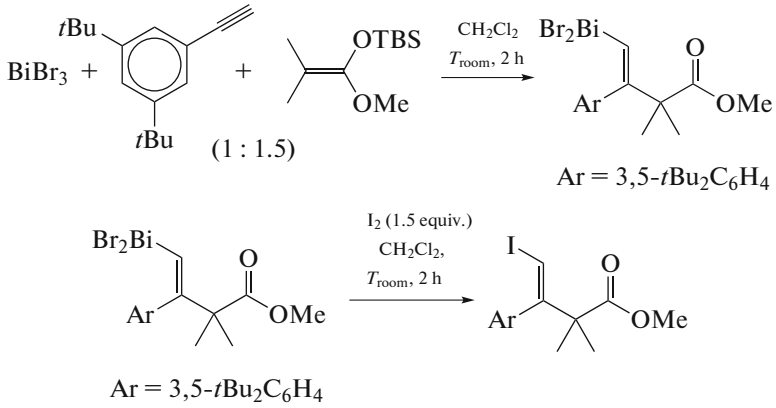

Scheme 84.

The XRD study of this monoalkenylbismuth dibromide revealed the cis conformation of the bismuth atom and aromatic substituent at the double bond, which confirms the regio- and stereoselective character of carbobismuthination. The crystal consists of tetramers formed due to the bromide bridges. The geometry of the bismuth atoms is a distorted trigonal bipyramid with the bromine atoms in the axial positions. The alkenyl group, bromine atom, and lone electron pair occupy the equatorial positions. It is shown that alkenylbismuth readily reacts with iodine to form alkenyl iodide with the retention of stereochemistry.

The transformation of C–H bonds into more reactive C–M bonds that are amenable to further functionalization, which is of fundamental significance in synthetic chemistry, was described [94]. It was shown that the transformation of the neutral bismuth compounds into their cationic analogs can be used as a strategy for the facilitation of C–H bond activation (Scheme 85).

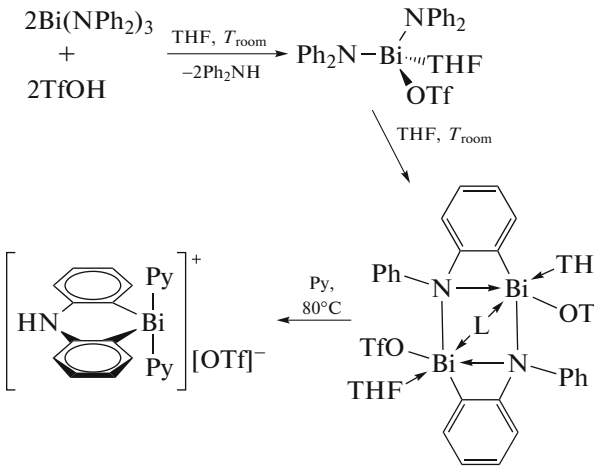

Scheme 85.

The organometallic products of the first and second stages of the activation of the C–H bonds were isolated in high yields. The XRD data and DFT calculations showed the unusual properties of the ground state of these compounds (ring deformation and moderate heteroaromaticity).

Synthesis of bismuth compounds with polydentate aryl ligands. The chemistry of the arylbismuth compounds with polydentate ligands at the central metal atom has recently been developed intensively. The simplest representatives of this class are the β-diketonate bismuth derivatives that can be synthesized from triphenylbismuth and β-diketone. For example, the first examples of the F-containing diketonate complexes of arylbismuth, namely, phenylbismuth(III) bis(hexafluoroacetylacetonate) $(Hfac)_2BiPh$ and its adducts $(Hfac)_2BiPh(L)$ (HfacH is 1,1,1,5,5,5-hexafluoro-2,4-pentanedione; L = H_2O, Me_2CO, THF, DMAA (*N*,*N*-dimethylacetamide), DMSO, and PhCN) and mixed complex of phenylbismuth hexafluoroacetylacetonatotrifluoroacetate $[(Hfac)BiPh(CF_3COO)]_2$, were synthesized (Scheme 86) and characterized by XRD [95].

$$Ph_3Bi \xrightarrow[-2C_6H_6]{2HfacH} (Hfac)_2BiPh \xrightarrow{L} (Hfac)_2BiPh(L)$$

$$L = H_2O, Me_2CO, THF, DMAA, DMSO, PhCN$$

$$Ph_3Bi \xrightarrow[-2C_6H_6]{\substack{HfacH\\CF_3COOH}} 0.5\,[(Hfac)BiPh(CF_3COO)]_2 \xleftarrow[-C_6H_6]{HfacH} Ph_2Bi(CF_3COO)$$

Scheme 86.

Complex $(Hfac)_2BiPh$ is isolated from the reaction mixture of triphenylbismuth with 1,1,1,5,5,5-hexafluoro-2,4-pentanedione (molar ratio 1 : 2) in anhydrous hexane. Compound $[(Hfac)BiPh(O_2CCF_3)]_2$ was synthesized from equimolar amounts of Ph_3Bi, HfacH, and CF_3COOH, whereas diphenylbismuth trifluoroacetate $Ph_2BiO_2CCF_3$ and β-diketone (Hhfac) were used in the second method. Attempts to grow single crystals of $(Hfac)_2BiPh$ from solutions of noncoordinating solvents turned out to be unsuccessful. However, in the presence of coordinating solvents, $(Hfac)_2BiPh$ forms yellow crystals of the corresponding $(Hfac)_2BiPh(L)$ adducts isolated from a hexane solution of $(Hfac)_2BiPh$ in the presence of small amounts of H_2O, Me_2CO, THF, DMAA, DMSO, and PhCN. All isolated complexes are sensitive to air; moderately soluble in methanol, acetone, dichloromethane, and chloroform; and soluble, to a lower extent, in diethyl ether and hydrocarbons. The synthesized compounds were characterized by IR and NMR spectroscopy and XRD. As it was expected, the IR spectra exhibited the bands corresponding to stretching vibrations of C=O groups in a range of 1634–1640 cm^{-1}, which differs considerably from an analogous band observed in the IR spectrum of free HfacH (1689 cm^{-1}), and indicate the chelating character of the ligand. It follows from the XRD data that the configuration of the metal atom in the $(Hfac)_2BiPh(L)$ adducts represents a pentagonal pyramid. The binuclear $[(Hfac)BiPh(CF_3COO)]_2$ complex consists of two distorted pentagonal pyramids linked into dimers by the bridging carboxylate groups.

The bismuth compounds containing the bidentate C,N-ligands at the bismuth atom are presented in the literature by somewhat higher number. They are synthesized, as a rule, from bismuth halides and active

metal derivatives. For instance, bromide (2-(iPr$_2$NCH$_2$)C$_6$H$_4$)$_2$BiBr was prepared from the Grignard reagent and bismuth trichloride (Scheme 87) [96].

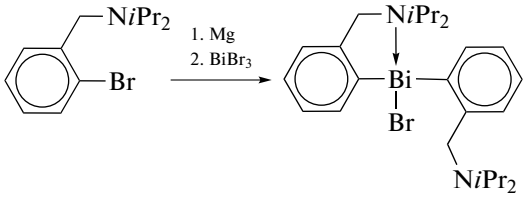

Scheme 87.

Compound (2-(iPr$_2$NCH$_2$)C$_6$H$_4$)$_2$BiBr was characterized by multinuclear NMR spectroscopy, mass spectrometry, and XRD. The Bi–Br bond (2.7294(10) Å) is shorter than that in other related R$_2$BiBr derivatives (for R = 2-(Me$_2$NCH$_2$)C$_6$H$_4$ 2.8452(7), and for 2-(Et$_2$NCH$_2$)C$_6$H$_4$ 2.7517(10), 2.7484(10), and 2.8084(11) Å) [78]. One of the nitrogen atoms is not coordinated to the central metal atom, but the distance between the second nitrogen atom and bismuth atom (Bi···N 2.737(6) Å) is somewhat longer than the sum of their covalent radii (2.19 Å, [20]) and substantially shorter than the sum of van der Waals radii of the indicated elements (3.94 Å, [20]), which shows an interaction between them. The BrBiN bond angle (164.80(13)°) is smaller than an ideal value of 180° and comparable with those found in the R$_2$BiBr compounds.

Diarylbismuth chlorides were synthesized using a combination of the above indicated methods [13]. For instance, the reaction of RLi or RMgBr (R = 2-(Et$_2$NCH$_2$)C$_6$H$_4$) with bismuth trichloride in a molar ratio of 2 : 1 gives R$_2$BiCl or R$_2$BiBr, respectively (Scheme 88). The reaction of redistribution of radicals can produce arylbismuth dichloride RBiCl$_2$ in which the chlorine atoms can readily be replaced by bromine or iodine atoms under the action of aqueous solutions of potassium bromide or iodide.

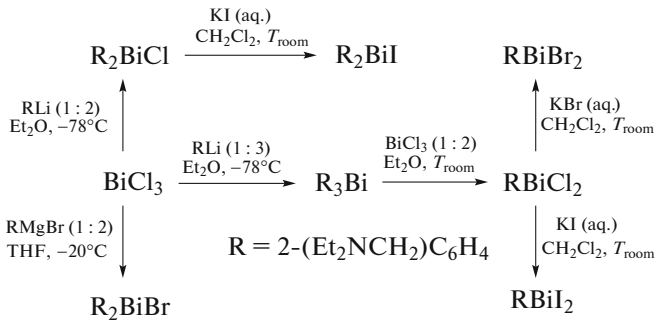

Scheme 88.

In the synthesized monohalides, one nitrogen atom coordinates to the bismuth atom (2.557(8)–2.645(6) Å), whereas the second nitrogen atom is not almost coordinated to the central metal atom (2.992(12)–3.170(8) Å). The common core (C,N)$_2$BiX (X = Cl, Br, and I) has a distorted square pyramidal geometry.

Bromides R(C$_6$F$_5$)BiBr, R(Mes)BiBr, and R(Ph)-BiBr (R = 2-(Me$_2$NCH$_2$)C$_6$H$_4$) were synthesized similarly from equimolar amounts of RBiBr$_2$ and C$_6$F$_5$MgBr, MesMgBr, or PhMgBr or from PhBiBr$_2$ and RLi in a molar ratio of 1 : 1 (Scheme 89) [12].

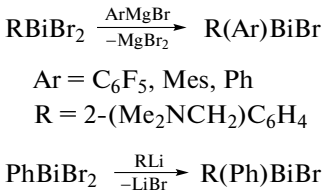

Scheme 89.

Bis(2-((dimethylamino)methyl)phenyl)azidobismuth (2-(Me$_2$NCH$_2$)C$_6$H$_4$)$_2$BiN$_3$ and (2-(dimethylaminomethyl)phenyl)bismuth diazide (2-(Me$_2$NCH$_2$)-C$_6$H$_4$)Bi(N$_3$)$_2$ were synthesized via similar schemes and structurally characterized [14]. Triarylbismuth was used as an intermediate product from which the corresponding aryl- and diarylbismuth chlorides were synthesized via the radical redistribution reaction. The

latter were transformed into iodides by the treatment with a sodium iodide excess in THF, and the subsequent treatment with silver azide gave the target products (Scheme 90).

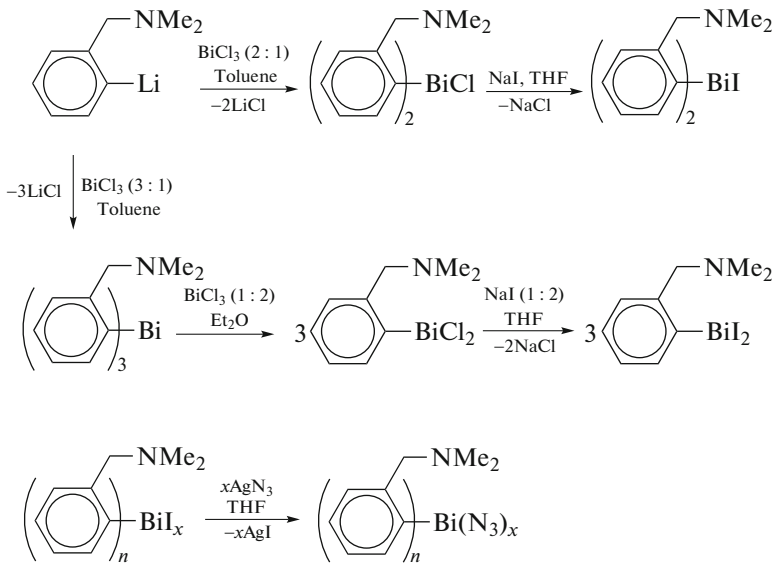

$n = 2, x = 1$ $(2\text{-}(Me_2NCH_2)C_6H_4)_2BiN_3$

$n = 1, x = 2$ $(2\text{-}(Me_2NCH_2)C_6H_4)Bi(N_3)_2$

Scheme 90.

The synthesized compounds represent rare examples of bismuth azides. The crystal of monoazide $(2\text{-}(Me_2NCH_2)C_6H_4)_2BiN_3$ contains monomeric molecules with the coordination of the nitrogen atoms of the amino groups to the central atom (2.555(2), 3.131(3) Å), whereas diazide $(2\text{-}(Me_2NCH_2)C_6H_4)Bi(N_3)_2$ in which the coordination of the nitrogen atoms of the amino group with the central metal atom is rather substantial (2.568(2) Å) is presented as a dimer with two types of linking of the azido groups. In addition, weak van der Waals interactions between these centrosymmetric dimers lead to the chain structure in the crystal.

Triorganobismuthines $R(C_6F_5)_2Bi$ and $R[2,4,6\text{-}(C_6F_5)_3C_6H_2]_2Bi$, where R = $2\text{-}(Me_2NCH_2)C_6H_4$, were synthesized from $RBiBr_2$ and C_6F_5MgBr or $2,4,6\text{-}(C_6F_5)_3C_6H_2Li$, respectively, in a molar ratio of 1 : 2 (Scheme 91) [12].

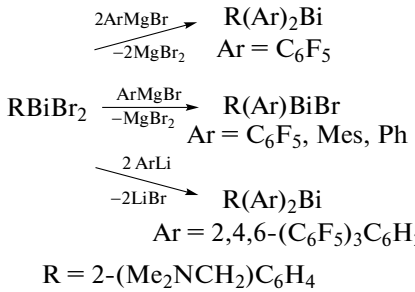

Scheme 91.

Bromides $R(C_6F_5)BiBr$, R(Mes)BiBr, and R(Ph)BiBr were synthesized similarly from $RBiBr_2$ and C_6F_5MgBr, MesMgBr, and PhMgBr or from $PhBiBr_2$ and RLi in the equimolar ratio (Scheme 91). The molecular structures of these compounds were determined by XRD. Chiral bromides $R(C_6F_5)BiBr$, R(Mes)BiBr, and R(Ph)BiBr (R = $2\text{-}(Me_2NCH_2)\text{-}C_6H_4$) in the solid state exhibit a strong intramolecular coordination N→Bi. In these compounds, the N–Bi distances are approximately equal, indicating the absence of the influence of the second organic substituent (C_6F_5, Ph, Mes) on the length of the coordination N···Bi bond.

Chlorides $(2\text{-}\{E(CH_2CH_2)_2NCH_2\}C_6H_4)_2BiCl$ (where E = O, MeN) and dichlorides $(2\text{-}\{E(CH_2CH_2)_2\text{-}$

$NCH_2\}C_6H_4)BiCl_2$ (where E = O, MeN) were synthesized by the reaction of the corresponding *ortho*-lithium derivative with bismuth trichloride in the corresponding molar ratios (Scheme 92) [23].

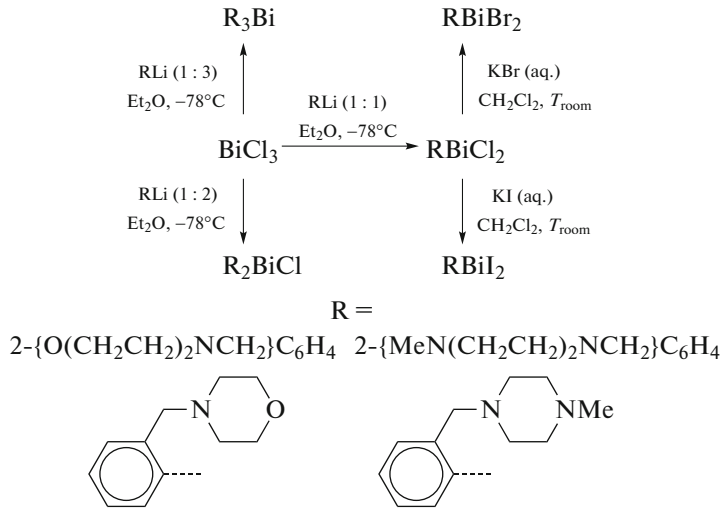

Scheme 92.

Dihalides $(2\text{-}\{E(CH_2CH_2)_2NCH_2\}C_6H_4)BiX_2$ (X = Br, E = O, MeN; X = I, E = O, MeN) and $(2\text{-}(Me_2NCH_2)C_6H_4)BiBr_2$ were synthesized by the reactions of halide exchange between $RBiCl_2$ and an excess of an aqueous solution of KX. In all compounds, the nitrogen atoms are coordinated to the bismuth atoms. In the monochlorides, one nitrogen atom is strongly coordinated to the bismuth atom (2.660(11) Å in $(2\text{-}\{O(CH_2CH_2)_2NCH_2\}C_6H_4)_2BiCl$ and 2.744(14) Å in $(2\text{-}\{MeN(CH_2CH_2)_2NCH_2\}C_6H_4)_2BiCl$), whereas the second nitrogen atom is involved in the weak intramolecular interaction N → Bi (3.095(11) Å in $(2\text{-}\{O(CH_2CH_2)_2NCH_2\}C_6H_4)_2BiCl$ and 3.061(14) Å in $(2\text{-}\{MeN(CH_2CH_2)_2NCH_2\}C_6H_4)_2BiCl$). As a whole, the $(C,N)_2BiCl$ core is a tetragonal pyramid. The crystals of dihalides $(2\text{-}\{O(CH_2CH_2)_2NCH_2\}C_6H_4)_2BiCl_2$ and $(2\text{-}(Me_2NCH_2)C_6H_4)BiBr_2$ contain discrete dimeric units. The nitrogen atom of the amino groups in the $(C,N)BiX_2$ cores (X = Cl, Br) coordinates to the metal atom (2.548(9) Å in $(2\text{-}\{O(CH_2CH_2)_2NCH_2\}C_6H_4)_2BiCl_2$ and 2.485(13) Å in $(2\text{-}(Me_2NCH_2)C_6H_4)BiBr_2$). Supramolecular architectures based on intermolecular Bi···Br, Cl···H, and Br···H interactions are formed in the crystals of these two compounds and $(2\text{-}\{O(CH_2CH_2)_2NCH_2\}C_6H_4)_2BiCl$. The six-membered morpholine and piperazine rings adopt the chair conformation that prevents the intramolecular coordination of the oxygen or nitrogen atoms to the bismuth atom.

Four resistant to air hypervalent compounds of organobismuth R_2BiCl with the (C,O)- or (C,S)-chelating ligands, where $R = 2\text{-}(MeECH_2)C_6H_4$ (E = O or S), as well as $(2\text{-}(MeOCH_2)C_6H_4)_2Bi(OTf)$ and $[\{2\text{-}(MeSCH_2)C_6H_4\}_2Bi]^+[OTf]^-$, were synthesized from bismuth trichloride and aryllithium (Scheme 93) [97].

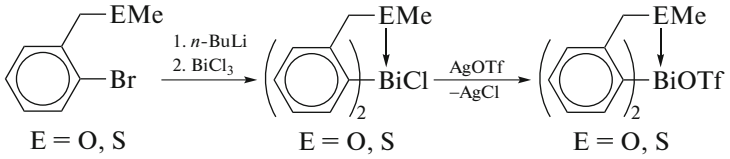

Scheme 93.

Unlike the former three compounds, the ionic complex $[\{2\text{-}(MeSCH_2)C_6H_4\}_2Bi]^+[OTf]^-$ consists of the bismuth-containing cations and triflate anions. Compound $[2\text{-}(MeOCH_2)C_6H_4]_2Bi(OTf)$ showed a high catalytic efficiency and possibility of the repeated use in the allylation of various aldehydes by tetraallyltin in methanol (or THF, MeCN, EtOH, T_{room}, 1 h) for the production of the corresponding homoallyl alcohols in the yield up to 96% (Scheme 94).

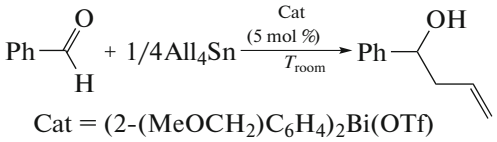

Scheme 94.

The reactions of organobismuth(III) chlorides R_2BiCl and $RBiCl_2$, where R = 2-$(Me_2NCH_2)C_6H_4$, with alkaline metal pseudohalides in a molar ratio of 1 : 1 and 1 : 2, respectively, afforded hypervalent bismuth compounds R_2BiX (X = NCO, SeCN) and $RBiX_2$ (X = NCO, NCS, and SeCN) (Scheme 95) [98].

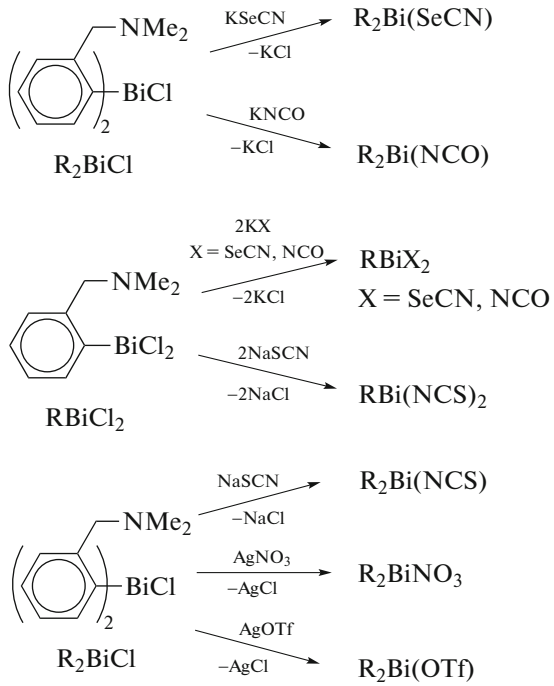

Scheme 95.

The molecular structures of compounds $R_2Bi(NCO)$ and $R_2Bi(SeCN)$ were determined. In all complexes, the nitrogen atoms of the amino groups are involved in the intramolecular coordination with the metal, resulting in a distorted square coordination geometry of the bismuth atom.

The reactions of equimolar amounts of chloride R_2BiCl, where R = 2-$(Me_2NCH_2)C_6H_4$, with sodium or silver salts (NaSCN, AgOTf, or $AgNO_3$) result in the substitution of the chlorine atom by another electronegative substituent and formation of the bismuth derivatives $R_2Bi(NCS)$, $R_2Bi(OTf)$, and R_2BiNO_3, respectively (Scheme 95). The structures of these compounds were determined by XRD [99]. Both nitrogen atoms of the amino groups participate in the intramolecular N···Bi coordination of different strengths. For isothiocyanate $R_2Bi(NCS)$, this results in a distorted square pyramidal core $(C,N)_2BiN$. In the case of triflate $R_2Bi(OTf)$ and nitrate R_2BiNO_3, the oxo anions are strongly coordinated asymmetrically to the Bi atom via the oxygen atoms (Bi···O 2.337(12)–3.317(15) Å in $R_2Bi(OTf)$ and 2.476(5)–3.088(5) Å in R_2BiNO_3). Thus, the pentagonal pyramidal coordination of the bismuth atom is observed for the $R_2Bi(OTf)$ and R_2BiNO_3 compounds.

Mesityl(2-dimethylaminomethylphenyl)bismuth chloride R(Mes)BiCl, where R = 2-(Me_2NCH_2)-C_6H_4, was synthesized from mesityl-bismuth dichloride (Scheme 96) [100].

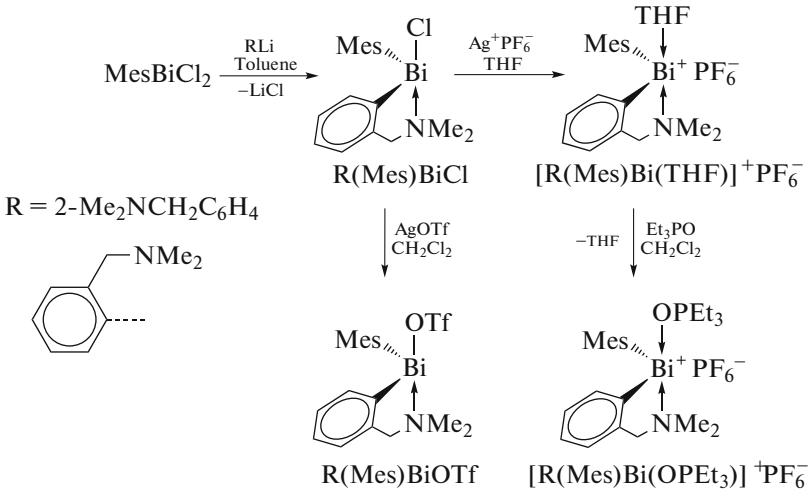

Scheme 96.

Complex R(Mes)BiCl treated with silver triflate is transformed into R(Mes)BiOTf. The consecutive reactions of R(Mes)BiCl with $AgPF_6$ and Et_3PO lead to the synthesis of $[R(Mes)Bi(OPEt_3)]^+PF_6^-$ in which the Bi–N bond (2.501(5) Å) is longer than that in R(Mes)BiOTf (2.446(2) Å).

The ambiguous character of the reactions of the organolithium compounds with bismuth trichloride was shown [101]. For example, the reactions of equimolar amounts of $BiCl_3$ with (Dipp–NacNac)Li (Dipp-NacNac = Dipp–N–C(Me)=CH–C(Me)=N–Dipp, Dipp = 2,6-iPr$_2$C$_6$H$_3$) under various conditions led to the synthesis of diverse bismuth compounds: $[(Dipp–NacNac)BiCl_2]_2$, [(Dipp–NacNac)Bi,Cl(μ-Cl)Bi(n-Bu)Cl(μ-Cl)]$_2$, $[LBiCl(\mu\text{-}Cl)]_2$ (L = N(Ar)=C(Me)CH=C(NHAr)CH$_2$), and L'Bi$_2$Cl$_4$ (L' = N(Ar)=C(Me)CC(Me)=N(Ar)) (Scheme 97).

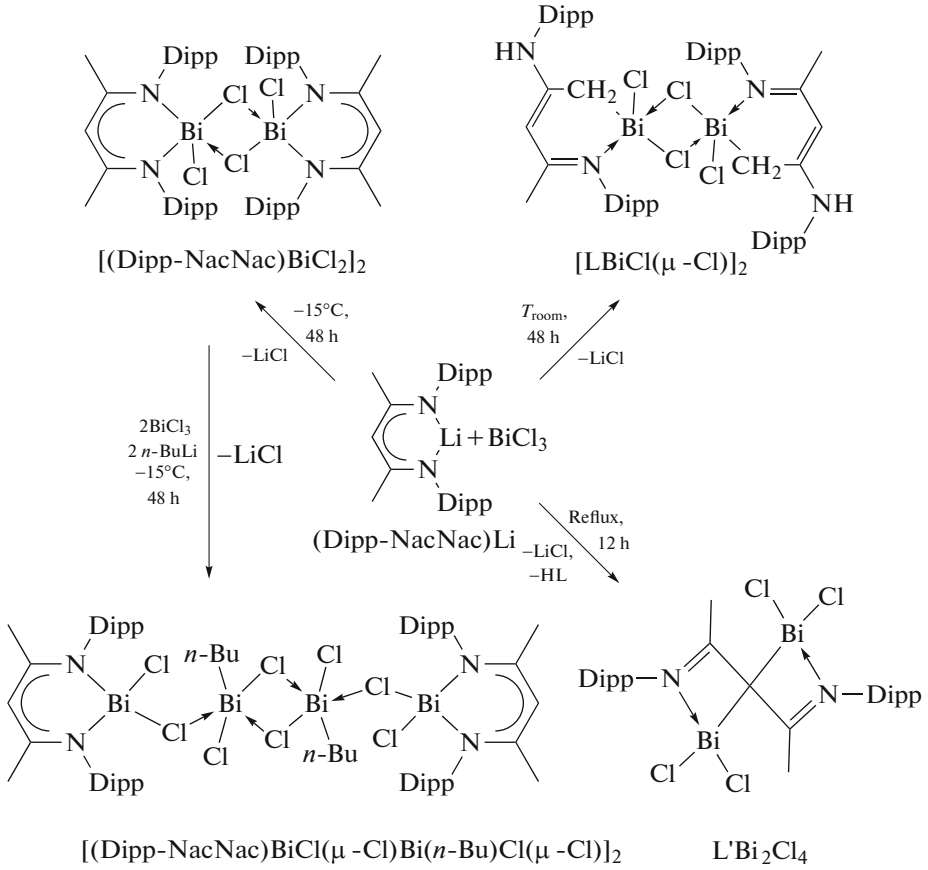

Scheme 97.

Compounds $[(Dipp–NacNac)BiCl_2]_2$ and $[LBiCl(\mu\text{-}Cl)]_2$ are isomers, and the thermal conversion of $[(Dipp–NacNac)BiCl_2]_2$ to $[LBiCl(\mu\text{-}Cl)]_2$ was carried out. In this reaction system at a minor excess of n-BuLi and $BiCl_3$, [(Dipp–NacNac)BiCl(μ-Cl)Bi(n-Bu)Cl(μ-Cl)]$_2$ was isolated as a by-product after $[(Dipp–NacNac)BiCl_2]_2$ was isolated. The structures of the complexes were confirmed by the data of ^{1}H and ^{13}C NMR spectroscopy and X-ray crystallography.

Arylbismuth dichloride $LBiCl_2$ (L = o-(CH=N-2,6-iPr$_2$C$_6$H$_3$)C$_6$H$_4$]) reacts with diphenyl dichalcogenide PhEEPh (E = S, Se, or Te) to form the corresponding complexes LBi(EPh)$_2$ (E = S, Se, or Te) from which the bismuth derivatives with one or two EPh groups can be synthesized under different conditions (Scheme 98) [102].

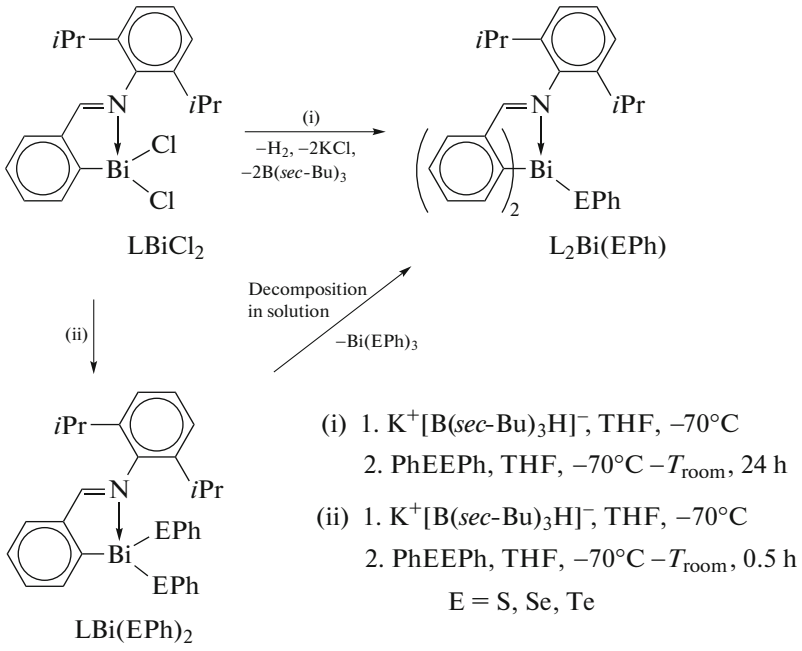

Scheme 98.

The stability of compounds $L_2Bi(EPh)$ is caused by the rigid coordination of both atom-nitrogen donors of ligand L with the bismuth atom.

Arylbismuth dichloride $LBiCl_2$ containing the N,C,N-ligand was obtained via a similar scheme from equimolar amounts of LLi (where L = 2,6-$(MeN(CH_2CH_2)_2NCH_2)_2C_6H_3$) and $BiCl_3$ (Scheme 99). Compounds $LBiBr_2$ and $RBiI_2$ were synthesized from $LBiCl_2$ by halogen exchange reactions [103].

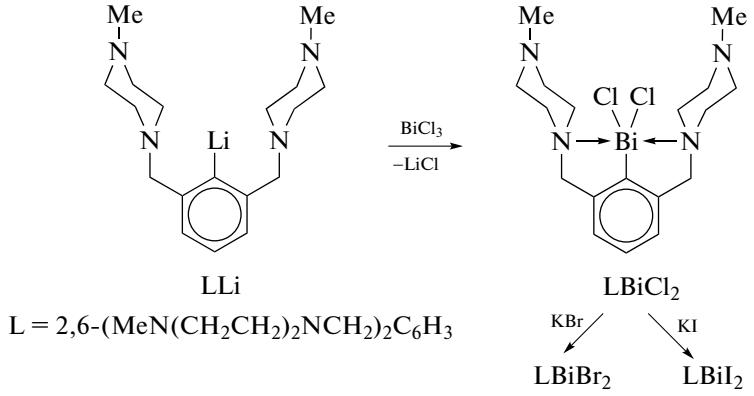

Scheme 99.

These arylbismuth(III) dihalides $LBiHal_2$ were characterized in both the solution and solid state. The molecular structures of the compounds in the crystalline state were determined by the XRD. All of them have the T-like core $CBiHal_2$ stabilized by two strong intramolecular interactions N → Bi in the *trans* positions to each other. The common $(N,C,N)BiHal_2$ core has a distorted square pyramidal coordination geometry with the aryl ligand in the vertex. The NMR spectroscopic studies confirm the nitrogen–bismuth internal coordination in the solution.

Arylbismuth dichloride of the L^*BiCl_2 type containing the tridentate N,C,N-ligand L* (Scheme 100) was used as a precursor for the synthesis of the monomeric bismuth compound L*Bi [104].

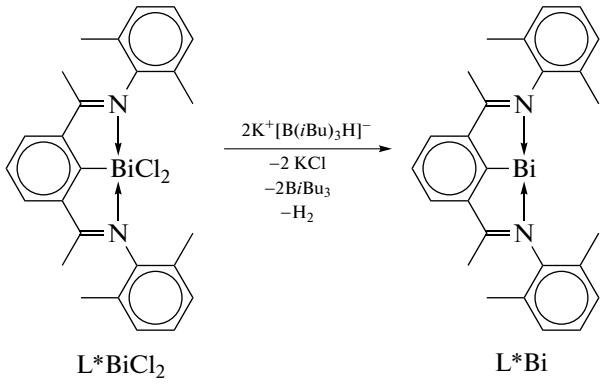

Scheme 100.

The reaction of L^*BiCl_2 with two equivalents of $K[B(i\text{Bu})_3H]$ in THF occurs with a change in the color of the reaction mixture to dark blue and a noticeable gas release, which indicated the formation of unstable hydride $LBiH_2$ that immediately loses hydrogen. Compound L*Bi was isolated by crystallization from a saturated hexane solution as a dark blue microcrystalline powder in a yield of 35%. The compounds were characterized by elemental analysis and ^1H and ^{13}C NMR spectra in deuterated benzene. The spectra exhibited the signals corresponding to ligand L*.

Some reactions of diarylbismuth chloride bearing N,C,N-ligands, $(2,6\text{-}(Me_2NCH_2)_2C_6H_3)_2BiCl$ (L_2BiCl), were studied in order to compare the coordination chemistry of Bi^{3+} and lanthanides Ln^{3+} having similar ion sizes (Scheme 101) [6].

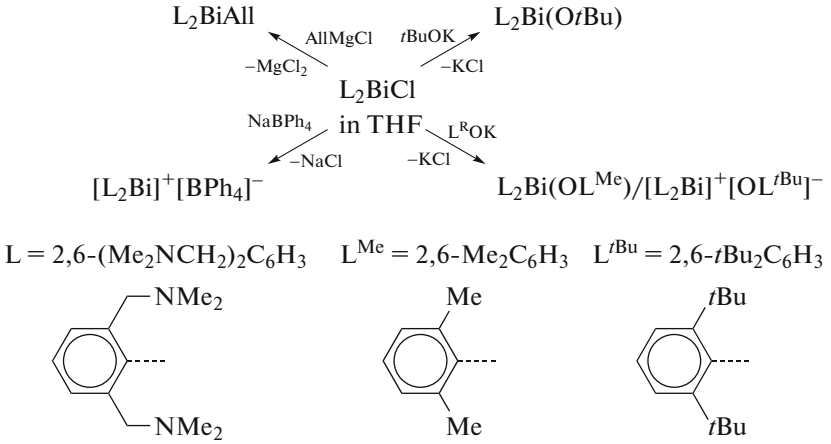

Scheme 101.

Complex L_2BiCl ($L = 2,6\text{-}(Me_2NCH_2)_2C_6H_3$) reacts with *t*BuOK and $L^{Me}OK$ to form alkoxide $L_2Bi(O\text{t}Bu)$ and aryl oxide $L_2Bi(OL^{Me})$, respectively, but an analogous reaction with potassium salt of more bulky phenol $L^{t\text{Bu}}OK$ resulted in the formation of the ionic complex $[L_2Bi]^+[OL^{t\text{Bu}}]$ in which the aryloxide ligand acts as an anion of the external sphere. The Cl substituent is removed from L_2BiCl by $NaBPh_4$ to form another ionic complex $[L_2Bi]^+[BPh_4]^-$.

The synthesis and molecular structures of the bismuth derivatives with the O,C,O-ligand, $(4\text{-}t\text{Bu-}2,6\text{-}[(EtO)_2P{=}O]_2C_6H_2)BiCl_2$ and $(4\text{-}t\text{Bu-}2,6\text{-}[(EtO)_2P{=}O]_2C_6H_2)BiCl$, (Scheme 102) were described [105].

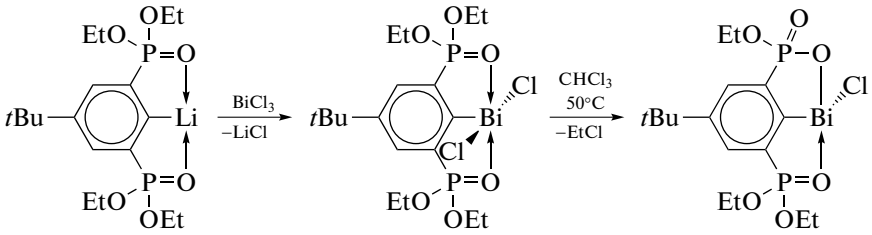

Scheme 102.

Compound $(4\text{-}t\text{Bu-}2,6\text{-}[(EtO)_2P{=}O]_2C_6H_2)BiCl_2$ crystallizes in the triclinic space group with two pairs of crystallographically independent molecules per unit cell. Each bismuth atom has a distorted octahedral configuration CCl_2O_2Bi with the chlorine and oxygen atoms in the *trans* position. The intramolecular Bi···O distances range from 2.378(5) to 2.414(5) Å. The phosphabismol derivative $(4\text{-}t\text{Bu-}2,6\text{-}[(EtO)_2P{=}O]_2C_6H_2)BiCl$ forms a dimer according to the "head-to-tail" type via the intermolecular Bi···O bonds (2.426(2), 2.278(3) Å) (Scheme 103).

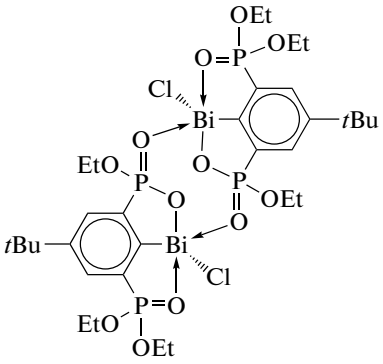

Scheme 103.

The DFT calculations show a high *s* character of lone electron pairs on the bismuth atoms in (4-*t*Bu-2,6-$[(EtO)_2P{=}O]_2C_6H_2)BiCl_2$ and (4-*t*Bu-2,6-$[(EtO)_2P{=}O]_2C_6H_2)BiCl$.

The reaction of equimolar amounts of aryllithium LLi (L = 2-(Me_2NCH_2)-6-$(MeOCH_2)$-C_6H_3) with bismuth trichloride afforded the corresponding arylbismuth dichloride $LBiCl_2$ in a high yield (Scheme 104) [106].

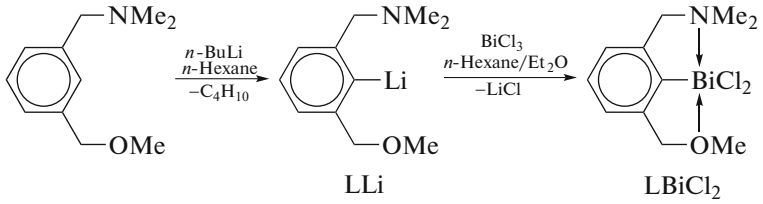

Scheme 104.

New chelating ligand L (2-(Me_2NCH_2)-6-$(MeOCH_2)$-C_6H_3) was obtained from *m*-toluenenitrile. The subsequent lithiation of this ligand by butyllithium in hexane and the addition of bismuth trichloride to the reaction mixture were completed by the synthesis of the target product, whose structure was proved by XRD.

The synthesis and structural peculiarities of the bismuth derivatives with the C,E,C-ligands (E = N, O, and S) were described in several publications. For instance, some compounds of cyclic bismuth(III) chlorides and triphenylgermyl propionates $[(C_6H_4CH_2)_2X]BiCl$ and $[(C_6H_4CH_2)_2X]BiOC(O)$-$CH_2CH_2GePh_3$ (X = S or NR with the nitrogen or sulfur atom as an additional intramolecular coordinating center) were synthesized from the dilithium derivative and bismuth chloride (Scheme 105) [107].

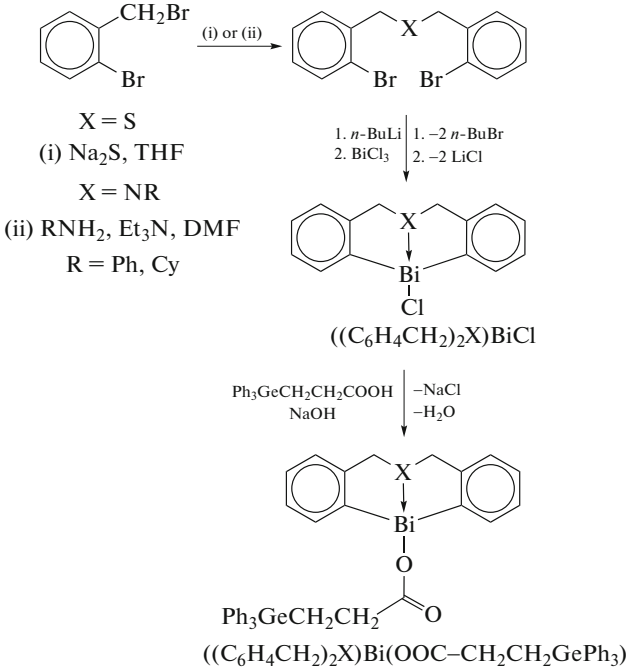

Scheme 105.

The XRD results show that the Bi–S or Bi–N bond lengths in the eight-membered rings of thiabismocin or azabismocin depend on the nature of substituted groups at the Bi atoms. The replacement of the chlorine atom in azabismocin and thiabismocin by the triphenylgermylpropionic group ($Ph_3GeCH_2CH_2COO$) results in the elongation of the Bi–N and Bi–S bonds. The compounds were found to exhibit a higher antiproliferative activity toward stomach carcinoma cells than that of cisplatin. Moreover, the antiproliferative activity is enhanced when the chlorine atom of the bismocin compounds is replaced by the triphenylgermylpropionic substituent.

Several other diorganobismuth(III) compounds, for example, $[(C_6H_4CH_2)_2S]BiX$ based on the heterocyclic cage of the butterfly type: tetrahydrodibenzo[c,f][1,5]-thiabismocin (Scheme 106), were also synthesized and structurally characterized [108].

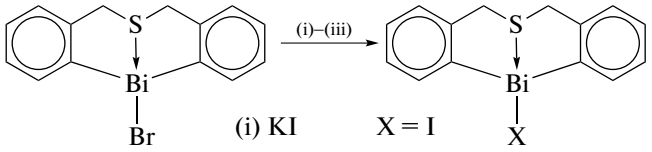

Scheme 106.

The reaction of the dilithium derivative of bis(2-bromobenzyl) sulfide with bismuth tribromide in a molar ratio of 1 : 1 led to the formation of $((C_6H_4CH_2)_2S)BiBr$. The subsequent exchange reactions of $[(C_6H_4CH_2)_2S]BiBr$ with KI, $AgNO_3$, and AgOTf gave the hypervalent bismuth compounds $[(C_6H_4CH_2)_2S]BiX$ (X = I, ONO_2, and OTf, respectively). In all compounds, the sulfur atom is intramolecularly coordinated to bismuth and the X···HC, Bi···Ar, and Bi···O intermolecular interactions result in the formation of polymeric chains in the crystals.

The same authors in another work report on the synthesis of diorganobismuth(III) bromides $[(C_6H_4CH_2)_2NR]BiBr$ (R = $C_6H_5CH_2$, $C_6H_5CH_2CH_2$, and $MeOCH_2CH_2$) containing the heterocyclic cage of dibenzo[1,5]azabismocin from the corresponding dibromide $(2\text{-}BrC_6H_4CH_2)_2NR$ by the consecutive reactions, including *ortho*-lithiation and treatment of the dilithium derivative in a molar ratio of 1 : 1 (Scheme 107) [109].

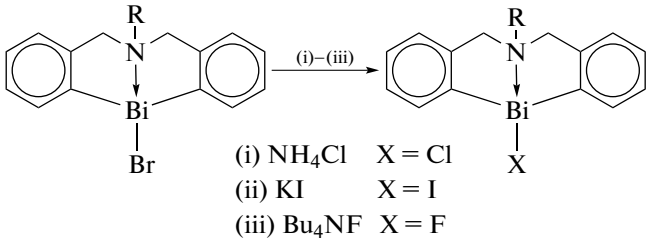

R	X
$C_6H_5CH_2$	Cl, I
$C_6H_5CH_2CH_2$	Cl, I
$MeOCH_2CH_2$	F, Cl, I

Scheme 107.

The further exchange reactions between the bromides and corresponding metal halides or ammonium fluoride (Scheme 107) afforded $[(C_6H_4CH_2)_2\text{-}NR]BiX$, where R = $C_6H_5CH_2$, X = Cl, I; R = $C_6H_5CH_2CH_2$, X = Cl, I; and R = $MeOCH_2CH_2$, X = F, Cl, I. All ten compounds were characterized by the NMR and XRD methods. The strong transannular N → Bi interactions were observed in all studied diorganobismuth(III) halides. The molecules are bound into dimers by strong Bi···π-arene interactions in $[(C_6H_4CH_2)_2N(CH_2CH_2OMe)]$-BiBr, $[(C_6H_4CH_2)_2N$-

$(CH_2C_6H_5)]BiCl$, and $[(C_6H_4CH_2)_2N(CH_2CH_2OMe)]BiI$ (about 3.50 Å) and Bi···X interactions in $[(C_6H_4CH_2)_2N$-$(CH_2C_6H_5)]BiBr$, $[(C_6H_4CH_2)_2N(CH_2C_6H_5)]BiI$, and $[(C_6H_4CH_2)_2N(CH_2CH_2C_6H_5)]BiI$.

Two precursors of the asymmetric tridentate C,E,C-chelating ligand 1-Br-2-$[(2'$-$BrC_6H_4CH_2E)$-$CH_2]C_{10}H_6$ (E = O, S) were obtained in a high yield (Scheme 108) [110].

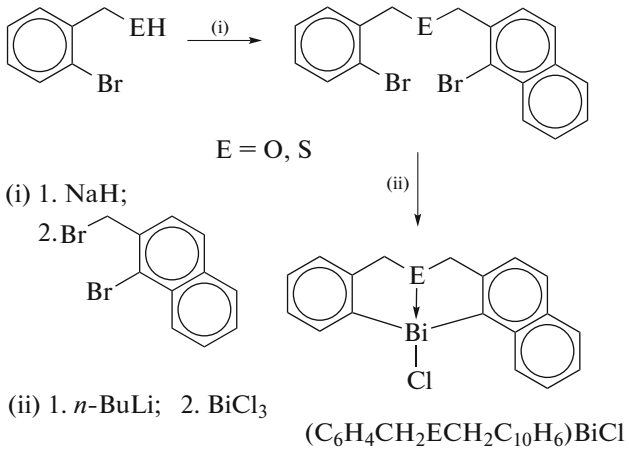

Scheme 108.

After lithiation by butyllithium and treatment with bismuth trichloride, two hypervalent bismuth chlorides with the asymmetric C,E,C-chelating ligand were obtained: $(C_6H_4CH_2OCH_2C_{10}H_6)BiCl$ and $(C_6H_4CH_2SCH_2C_{10}H_6)BiCl$ (E = O, S). The XRD method revealed that the donor atoms (O, S) are strongly coordinated to the bismuth atoms.

Note that some of the bismuth compounds with the C,E,C-ligands are efficient catalysts for various reactions of organic synthesis. For instance, the stable in air triflate complex of organobismuth $\{[(C_6H_4$-$CH_2)_2O]Bi(H_2O)\}^+[OTf]^-$ with the dibenzo[1,5]oxabismocin cage manifests a high catalytic activity toward ring opening in the reactions of epoxides in aqueous media with aromatic amines at room temperature (Scheme 109) [111].

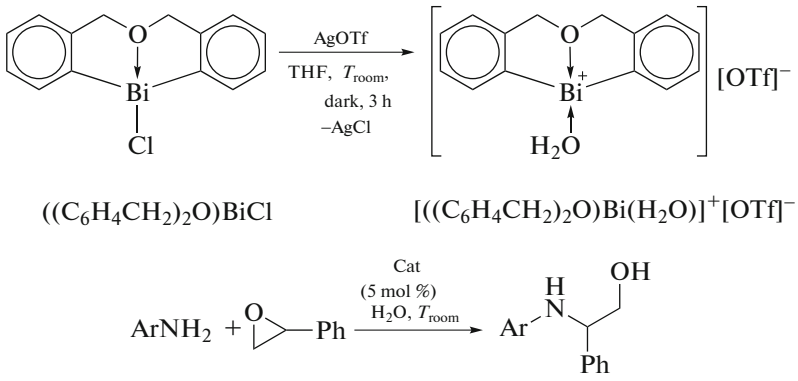

Scheme 109.

This catalyst demonstrates a high stability and applicability to regeneration and repeated use. The catalytic system provides a simple and efficient method for the synthesis of β-aminoalcohols in the yield to 93%.

Another work reported on the synthesis of the binuclear organobismuth complexes $\{[(C_6H_4CH_2)_2NR]Bi\}_2E$ (E = O, S; R = *t*Bu, Cy, Ph) with two dibenzo[1,5]azabismocin cages cros-slinked through the sulfur or oxygen atom by the treatment of organobismuth chlorides with sodium hydroxide or $Na_2S{\cdot}9H_2O$ (Scheme 110) [112].

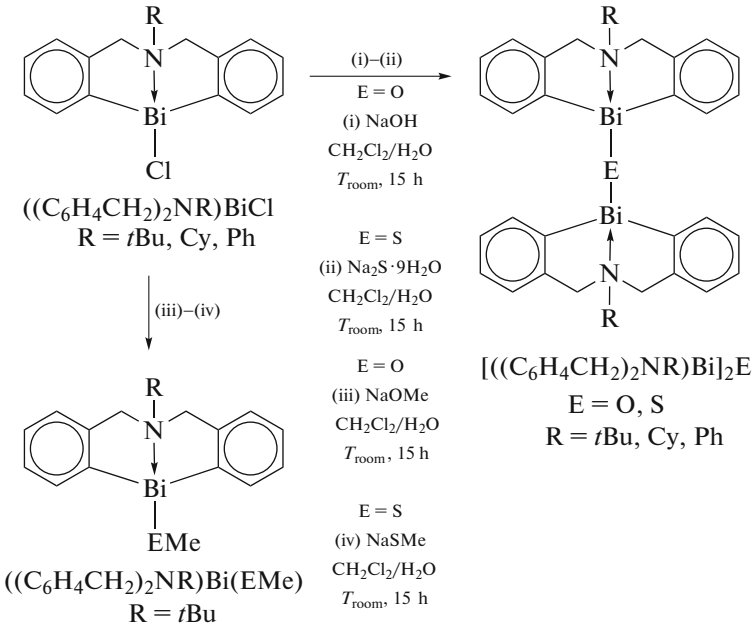

Scheme 110.

Complexes $\{[(C_6H_4CH_2)_2NR]Bi\}_2E$ show a high catalytic efficiency in the synthesis of cyclic carbonates from 2-(chloromethyl)oxirane and CO_2. Among them, the $\{[(C_6H_4CH_2)_2NtBu)Bi]_2S$ complex exhibits the highest activity (Scheme 111).

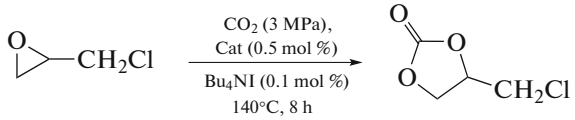

Cat = $[((C_6H_4CH_2)_2NtBu)Bi]_2S$

Scheme 111.

The binuclear organobismuth complexes show a higher catalytic activity over their precursors, chloride $[(C_6H_4CH_2)_2NR]BiCl$, methoxide $[(C_6H_4CH_2)_2NtBu]BiOMe$, and methanethiolate $[(C_6H_4CH_2)_2NtBu]BiSMe$, which are mononuclear organobismuth complexes. However, the complexes with the oxygen bridge $[((C_6H_4CH_2)_2NR)Bi]_2O$ are instable in air and lose their catalytic efficiency because of hydrolysis or adsorption of CO_2 (with the formation of organobismuth carbonates in the last case). Nevertheless, the binuclear organobismuth complexes with the sulfur bridge $\{[(C_6H_4CH_2)_2NR]Bi\}_2S$ are very stable in air and can be applied for the synthesis of cyclic carbonates (in the presence of Bu_4NI) via various types of epoxides, demonstrating satisfactory efficiency and selectivity.

The ionic complexes containing the C,S,C-ligands manifest a high catalytic activity in the Mannich reactions for the preparation of α,β-unsaturated ketones [113]. The precursor for catalyst preparation is organobismuth chloride $[(C_6H_4CH_2)_2S]BiCl$, which is synthesized from the butterfly-shaped ligand with sulfur, *n*-BuLi, and bismuth trichloride in diethyl ether. Complex $[(C_6H_4CH_2)_2S]BiCl$ contains the tridentate ligand in which the sulfur atom has two pairs of electrons: one pair coordinates to the bismuth center, and another pair is free. The complexes with the counterion of the general formula $\{[(C_6H_4CH_2)_2S]Bi(H_2O)\}^+X^-$ (X^- = ClO_4^-, BF_4^-, $OSO_2C_4F_9^-$,

$OSO_2C_8F_{17}^-$) were derived from this compound and showed a high electron-acceptor ability and properties of efficient catalysts in the Mannich reaction (Scheme 112).

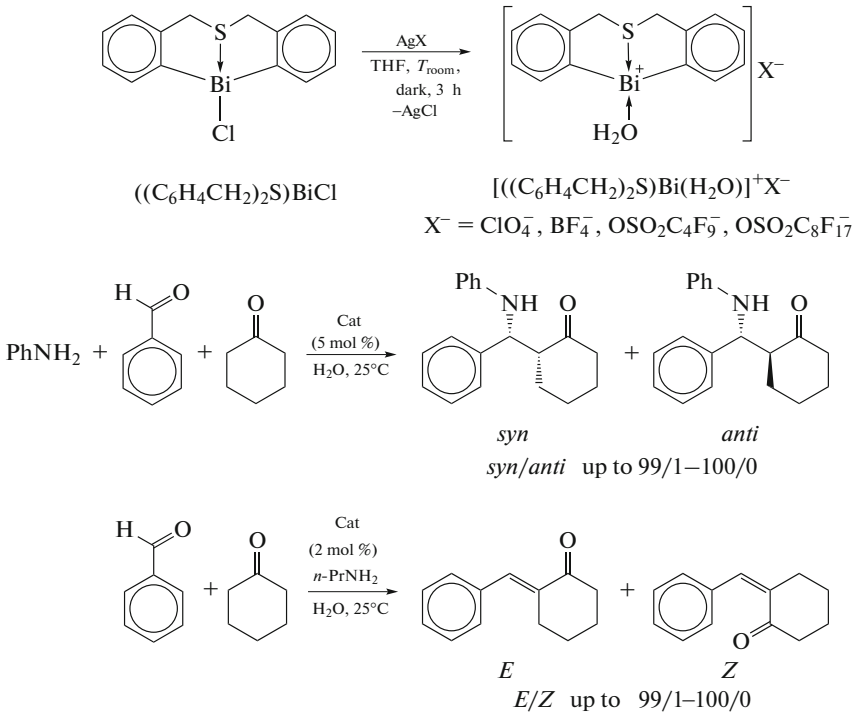

Scheme 112.

In this case, a high diastereoselectivity is observed and the *trans*-conformation products are isolated from the reaction mixture in the yield up to 99%.

The N,C,N-chelate bismuth complexes with the bulky bis(diphenyl(arylamino)phosphorano)methane substituents $H_2C(Ph_2PN\text{-}Dipp)_2$ can be prepared from bismuth trichloride and corresponding lithium compounds (Scheme 113) [114].

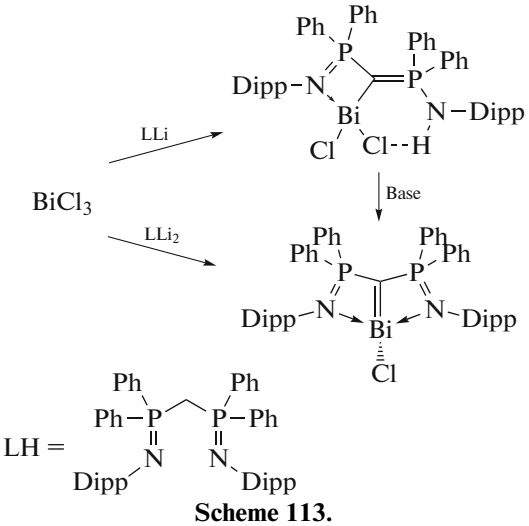

Scheme 113.

The complexes were characterized by the XRD and NMR methods. It is found that the dianionic complex has a rare structural motif of the formally double carbon–bismuth(III) bond.

Arylbismuth oxides bearing tridentate aryl ligands are used as the starting organic compounds of metal in many works devoted to the synthesis of the aryl derivatives of trivalent bismuth. For example, the reaction of $RBiCl_2$

(R = 2,6-MeN$(CH_2CH_2)_2NCH_2]_2C_6H_3$) with KOH affords oxide *cyclo*-$R_2Bi_2O_2$ (Scheme 114) [115]. The cyclic oxide can capture gaseous CO_2 with the formation of "$RBiCO_3$." The reactions of dichloride $RBiCl_2$ with ethylene glycol, pinacol, or pyrocatechol ($CatH_2$) in the presence of KOH result in the formation of 2-organo-1,3,2-dioxabismolanes $RBi(OCH_2)_2$, $RBi(OCMe_2)_2$, or 2-organo-1,3,2-dioxabismol RBi(Cat), respectively.

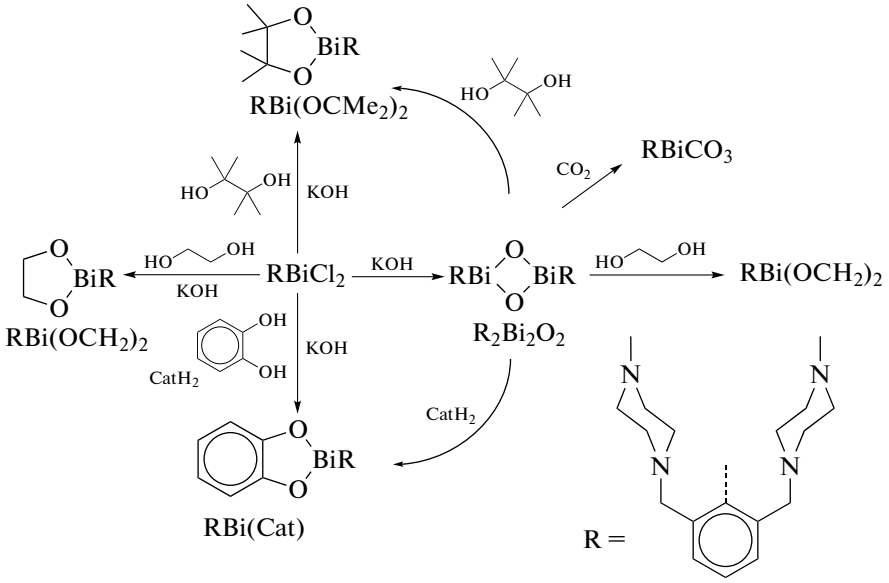

Scheme 114.

The structures of the synthesized compounds were studied by NMR spectroscopy and XRD. The organic group R was elucidated to act as the chelate N,C,N-ligand. The nonplanarity of the five-membered chelate cycles BiC_3N is explained by the intramolecular interactions N → Bi. The molecules of compounds $R_2Bi_2O_2$, $RBi(OCH_2)_2$, and RBi(Cat) are distorted square pyramids regardless of the nature of the oxo ligand.

The reactions of organobismuth oxide $(LBiO)_2$ (L = [2,6-bis(dimethylamino)methyl]phenyl) with organoboric acids (1 : 4 mol/mol) give heteroboroxines $LBi[(OBR)_2O]$, where R = Ph, 4-$CF_3C_6H_4$ and Fc (Scheme 115) [116].

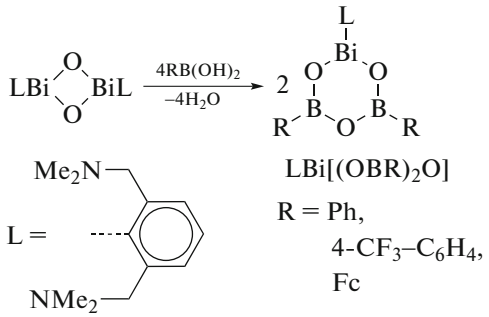

Scheme 115.

The compounds were characterized by elemental analysis and NMR spectroscopy. Their structures were described in both the solution (NMR studies) and solid state. According to the XRD data, all complexes contain the central BiB_2O_3 fragment, whose nonaromatic character was confirmed by the DFT calculations.

The synthesis and structures of bismaheteroboroxines of the general formula $LBi[(OBR)_2O]$ with the N,C,N-chelating ligand L = 2,6-$(Me_2NCH_2)_2C_6H_3$ (Scheme 116) were described [117]. The target compounds were derived from the oxide $(LBiO)_2$ and corresponding organoboric acid (1 : 4 mol/mol).

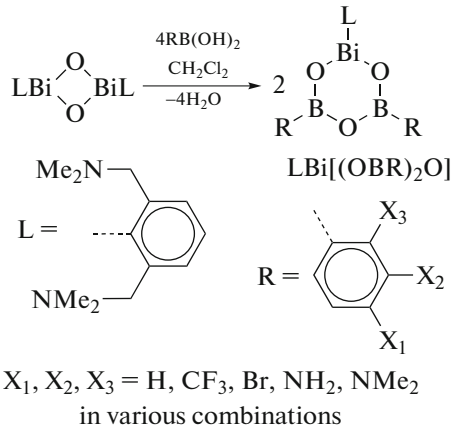

Scheme 116.

Heteroboroxine $LBi[(OBR)_2O]$ containing the donor group (R = 4-pyridyl) in boric acid was synthesized via a similar scheme (Scheme 117).

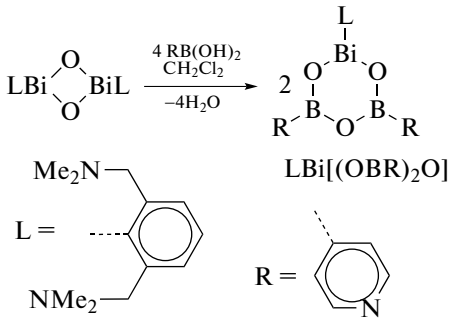

Scheme 117.

The synthesized compounds were characterized by multinuclear NMR spectroscopy and XRD.

The reaction of N,C,N-intramolecularly coordinated bismuth(III) oxide $(LBiO)_2$, where L = 2,6-$(Me_2NCH_2)_2C_6H_3$), with $(HO)SiPh_2OSiPh_2(OH)$ at a molar ratio of 1 : 2 afforded *cyclo*-$LBi[(OSiPh_2)_2O]$ containing the six-membered $BiSi_2O_3$ cycle (Scheme 118) [118].

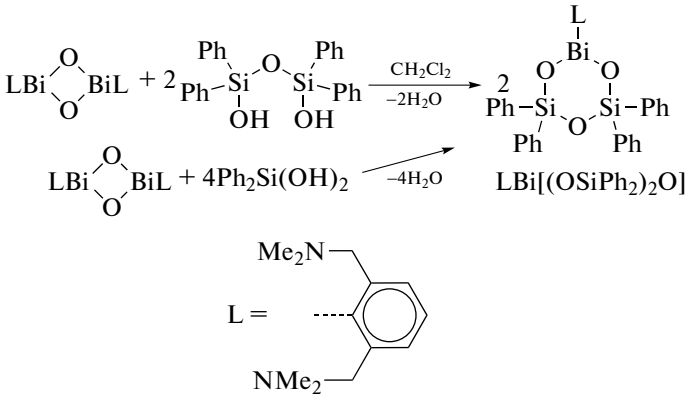

Scheme 118.

Alternatively, *cyclo*-$LBi[(OSiPh_2)_2O]$ can be obtained from diphenyltin dihydroxide $Ph_2Si(OH)_2$ and $(LBiO)_2$ at a molar ratio of 4 : 1. Compound $(LBiO)_2$ reacts with cyclosiloxane $(Me_2SiO)_3$ to form six-membered bismuthsiloxane *cyclo*-$LBi(OSiMe_2)_2O$ (Scheme 119).

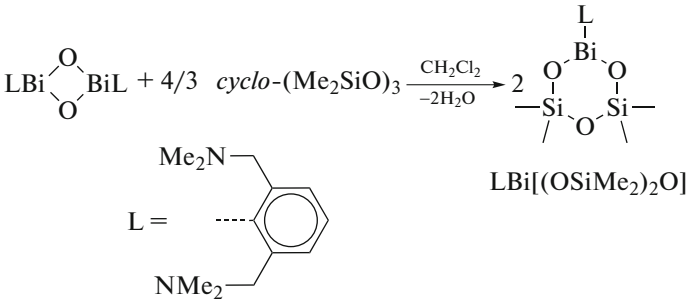

Scheme 119.

The compounds were characterized using elemental analysis, ^1H, ^{13}C, and ^{29}Si NMR spectroscopy, and XRD.

Crystals with the solvate benzene molecule were obtained for the bismuth(III) heteroboroxine complex $LBi[(OBDipp)_2O]$ derived from oxide $(LBiO)_2$ (R = 2,6-

$(Me_2NCH_2)_2C_6H_3$) and substituted boric acid (Scheme 120). However, the found nonplanarity of the benzene ring in the crystal of the solvate of the chelate complex was not confirmed by the DFT-D quantum-chemical calculations [119]. The observed bent structure of benzene, in fact, is a superposition (thermal average) of an ensemble of the thermopopulated benzene structures in the complex.

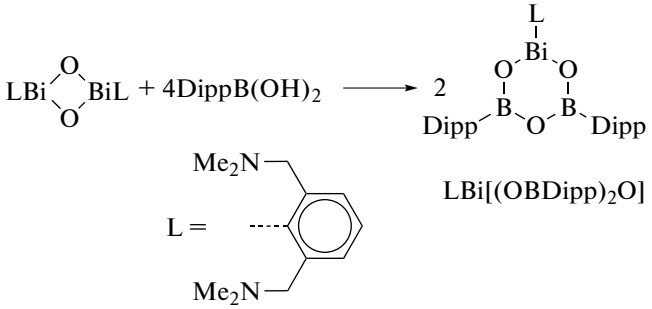

Scheme 120.

The unexampled transfer of the aryl group from boron to the bismuth atom is observed in the reactions of heteroboroxines of the general formula LBi[$(OBR)_2O$] (L = 2,6-$(Me_2NCH_2)_2C_6H_3$; R = Ph, 4-$CF_3C_6H_4$, and 4-BrC_6H_4) with the corresponding boric acid $RB(OH)_2$ (Scheme 121) [120].

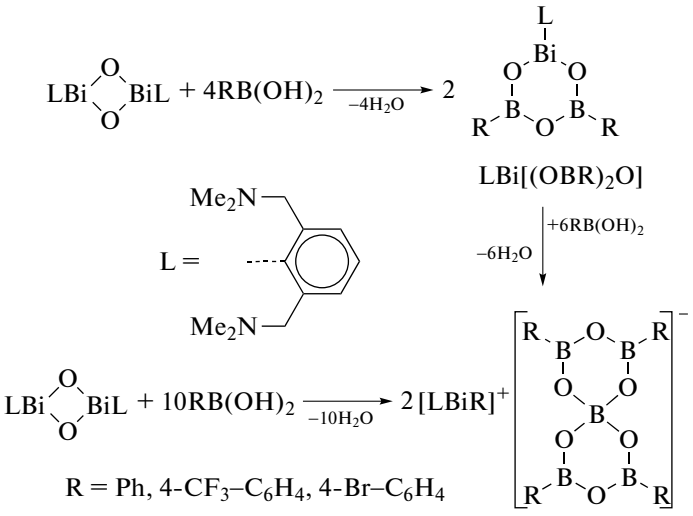

Scheme 121.

Ion pairs $[LBiR]^+[R_4B_5O_6]^-$ (R = Ph, 4-$CF_3C_6H_4$, and 4-BrC_6H_4) were obtained, and the structure of the phenyl-containing complex was proved by the XRD method.

The reaction of dimeric bismuth(III) oxide $(LBiO)_2$ (R = $(Me_2NCH_2)_2C_6H_3$) with acetic acid afforded acetate $LBi(OAc)_2$ [121]. Hydroxide LBi(OH)(OTf) was obtained using trifluoromethanesulfonic acid (Scheme 122).

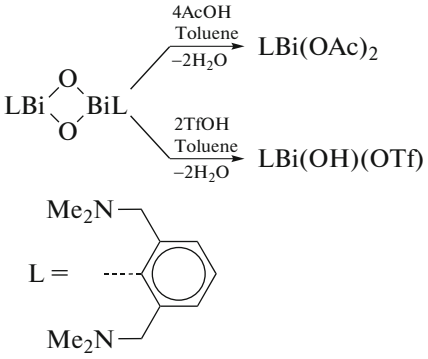

Scheme 122.

Complexes $LBi(OAc)_2$ and LBi(OH)(OTf) were characterized by mass spectrometry, ^1H and ^{13}C NMR spectroscopy, and XRD. The crystal of LBi(OH)(OTf) contains weakly bound dimeric $LBi(\mu\text{-}OH)_2BiL$ units, and the triflate anions are linked with the bridging OH fragments by hydrogen bonds along with the Bi···O interactions leading to the infinite chain of the supramolecular LBi(OH)(OTf) structure.

The reactions of $(LBiO)_2$, where R = $(Me_2NCH_2)_2C_6H_3$, with organophosphorus acids at a molar ratio of 1 : 4 gave organobismuth phosphonates $LBi[OP(tBu)(O)(OH)]_2$ (Scheme 123) [122]. When a molar ratio of 1 : 2 is used, $[LBi(O(O)P(tBu)O)]_3$ is formed. The reaction of $[LBi(O(O)P(tBu)O)]_3$ with $EtP(O)(OH)_2$ afforded mixed phosphonate LBi-[OP(Et)(O)(OH)][OP(*t*Bu)(O)(OH)].

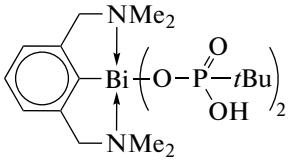

$LBi[OP(tBu)(O)(OH)]_2$

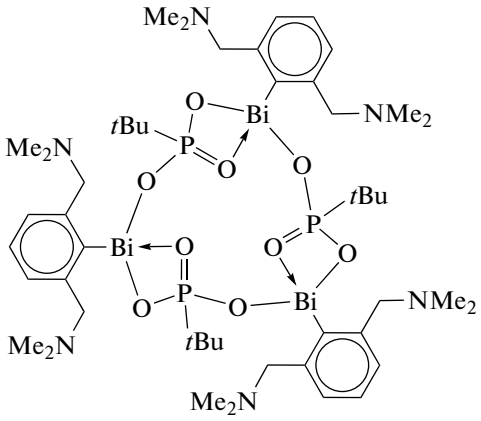

$[LBi(O(O)P(tBu)O)]_3$

Scheme 123.

All compounds were characterized by elemental analysis, mass spectrometry, ^1H, ^{13}C, and ^{31}P NMR spectroscopy, and IR spectroscopy. On the one hand, secondary phosphonate $LBi[OP(tBu)(O)(OH)]_2$ consists of dimeric units weakly bound via hydrogen bridges of the PO–H···O=P type. On the other hand, complex $[LBi(O(O)P(tBu)O)]_3$ is a trimer with the central 12-membered ring formed by three LBi(O(O)P(*t*Bu)O) blocks via the intermolecular Bi···O=P contacts.

The same oxide $(LBiO)_2$ reacts with arsenic oxides As_2O_5 and As_2O_3 to form molecular compounds $(LBi)_3(AsO_4)_2$ and $(LBi)_2(As_2O_5)$ (Scheme 124) [123].

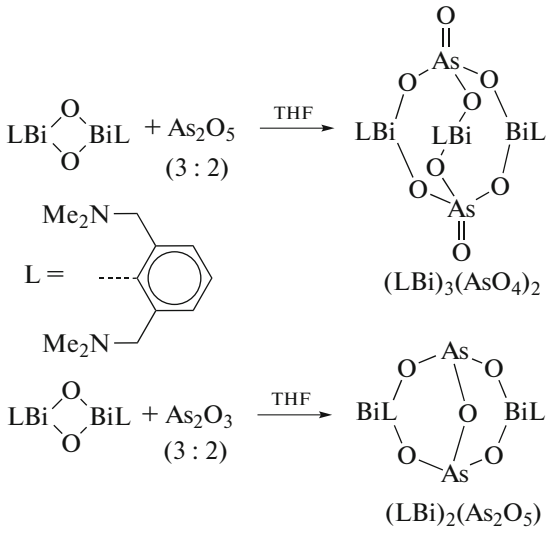

Scheme 124.

The obtained complexes were characterized by mass spectrometry and ^1H and ^{13}C NMR spectroscopy, as well as by XRD in the case of $(LBi)_2(As_2O_5)$.

The synthesis of the N→Bi-intramolecularly coordinated bismuth selenite $[LBi(O(O)SeO)]_3$ (Scheme 125) was reported [124].

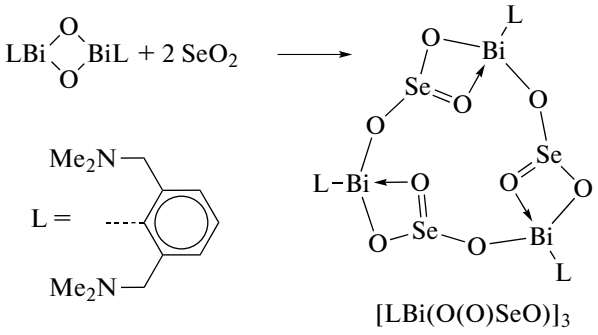

Scheme 125.

Organobismuth selenite $[LBi(O(O)SeO)]_3$ is a rare example of mixed selenium oxide and bismuth, which was characterized by ^1H, ^{13}C, and ^{77}Se NMR spectroscopy, IR spectroscopy, and XRD.

Arylbismuth sulfides, which are prepared from arylbismuth dichlorides and sodium or lithium sulfides, are used more rarely in the synthesis of trivalent bismuth derivatives with tridentate ligands. For example, the reaction of arylbismuth(III) dichloride $LBiCl_2$ containing the O,C,O-chelating ligand L = 2,6-$(tBuOCH_2)_2C_6H_3$ with sodium sulfide in a toluene–water mixture afforded bismuth sulfide $(LBiS)_2$ (Scheme 126) stable at −30°C but decomposed at room temperature [125].

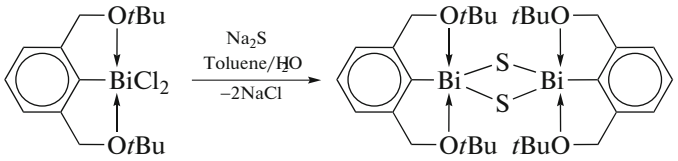

$LBiCl_2$, L = 2,6-(tBuOCH$_2$)$_2$C$_6$H$_3$ $(LBiS)_2$

Scheme 126.

Sulfide $(LBiS)_2$ was characterized by elemental analysis, mass spectrometry, ^{1}H and ^{13}C NMR spectroscopy, and XRD.

Organobismuth(III) sulfide $(LBiS)_2$ (L = 2,6-(Me_2NCH_2)$_2$C$_6$H$_3$), which was synthesized from arylbismuth dichloride and lithium sulfide, is also dimeric in the solid state (Scheme 127) [126].

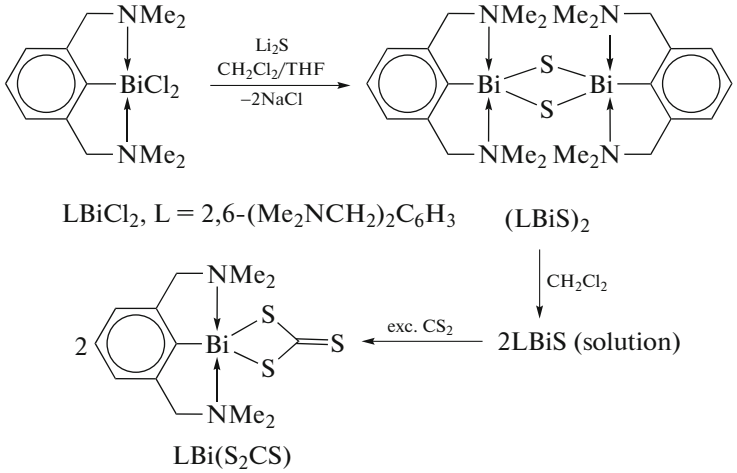

Scheme 127.

Nevertheless, the presence in the solution of the monomeric structure with the Bi–S terminal bonds was proved by [2+2] cycloaddition to CS_2 leading to the formation of molecular trithiocarbonate $LBi(S_2CS)$. Both compounds in the solid state were characterized by single-crystal X-ray diffraction and IR spectroscopy. Carbon disulfide can be removed from trithiocarbonate $LBi(S_2CS)$ on heating to 160°C with reduction to the starting sulfide. In a solution, trithiocarbonate $LBi(S_2CS)$ exists at equilibrium with the starting sulfide, but this equilibrium can be shifted to the left by the addition of a carbon disulfide excess.

Arylbismuth sulfide $(LBiS)_2$ can also be used in organoelement synthesis. For instance, $(LBiS)_2$ containing the NCN-chelating ligand L = 2,6-(Me_2NCH_2)$_2$C$_6$H$_3$ reacts with one molar equivalent of elemental sulfur to form cyclic bis(pentasulfide) $LBi(\mu\text{-}S_5)_2BiL$ with the central 12-membered ring Bi_2S_{10} (Scheme 128) [127].

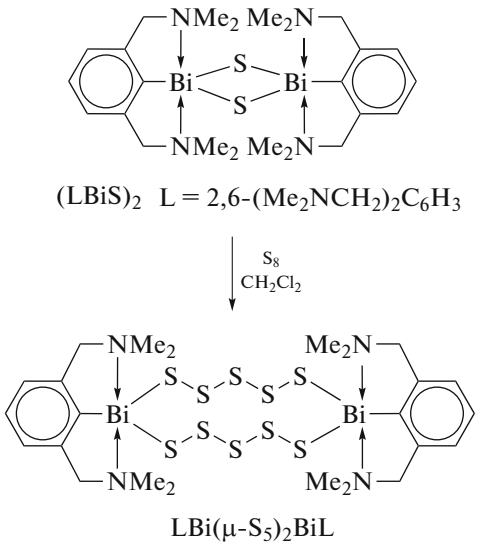

Scheme 128.

Compound $LBi(\mu\text{-}S_5)_2BiL$ was obtained as stable orange crystals and characterized by XRD, IR spectroscopy, and Raman spectroscopy.

The reactivity of the bismuth complexes with polydentate ligands is poorly studied, except for substitution reactions that are most widely presented by the reactions of organic bismuth halides with silver salts of various acids. For example, the reaction of 12-chloro-6-cyclohexyl-5,6,7,12-dibenzo[1,5]azabismocin and silver triflate afforded the corresponding triflate of the heterocyclic bismuth compound $[(C_6H_4CH_2)_2NCy]Bi(OTf)$ (Scheme 129), and its crystal structure was determined [128].

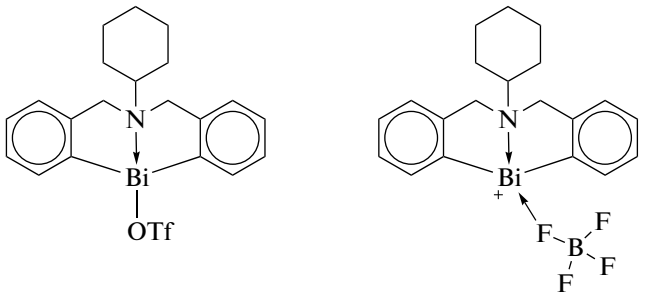

$((C_6H_4CH_2)_2NCy)Bi(OTf)$ $[((C_6H_4CH_2)_2NCy)Bi]^+BF_4^-$

Scheme 129.

The central bismuth-containing moiety of the complex has a distorted pseudotrigonal bipyramidal structure. The carbon atoms and lone electron pair of Bi are arranged in the equatorial plane, whereas the nitrogen and oxygen atoms lie in the apical positions. The Bi–C distances are 2.216(9) and 2.219(9) Å. The CBiC angle is 96.3(3)°, and the NBiO angle is equal to 151.7(2)° (rather than 180°). The Bi–N distance is 2.430(6) Å, and the cyclohexyl group is disordered over two positions.

Stable in air heterocyclic arylbismuth tetrafluoroborate $[(C_6H_4CH_2)_2NCy]Bi\}^+BF_4^-$ was synthesized via the same scheme (Scheme 129) and turned out to manifest the catalytic activity in the allylation of diverse aldehydes by tetraallyltin in aqueous methanol (Scheme 130) to give the corresponding homoallyl alcohols with excellent selectivity [129]. This activity of the $\{[(C_6H_4CH_2)_2NCy]Bi\}^+BF_4^-$ complex is close to the catalytic activity of the earlier described $[2\text{-}(MeOCH_2)C_6H_4]_2Bi(OTf)$ compound (Scheme 94) [97].

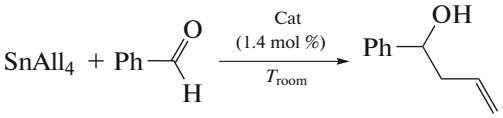

Up to 97%

Cat = $[((C_6H_4CH_2)_2NCy)Bi]^+BF_4^-$

Scheme 130.

Air-resistant organobismuth perfluorooctanesulfonate $\{[(C_6H_4CH_2)_2S]Bi(H_2O)\}^+[OSO_2C_8F_{17}]^-$ was synthesized similarly and characterized by a high catalytic activity and possibility of repeated use in the synthesis of (*E*)-α,β-unsaturated ketones due to the highly selective cross condensation of ketones and aldehydes in water [130]. The stable in air cationic organobismuth complex prepared from silver perchlorate and diarylbismuth chloride was used as a highly efficient catalyst of the direct diastereoselective Mannich reaction in water (Scheme 112) [131].

The organobismuth complex, 5*H*-dibenzo[1,5]oxabismocin-12(7*H*)-yl nitrate $[(C_6H_4CH_2)_2O]BiONO_2$, was synthesized by the addition of a solution of arylbismuth chloride in THF to a solution of silver nitrate in water [132]. This complex was found to manifest anticancer activity and has a high potential in cancer treatment.

The reactions of organylbismuth bromides $[(C_6H_4CH_2)_2NR]BiBr$ (R = $C_6H_5CH_2$, $C_6H_5CH_2CH_2$) and corresponding silver salts resulted in the formation of bismuth compounds of the general formula $[(C_6H_4CH_2)_2NR]BiX$ (Scheme 131) [133].

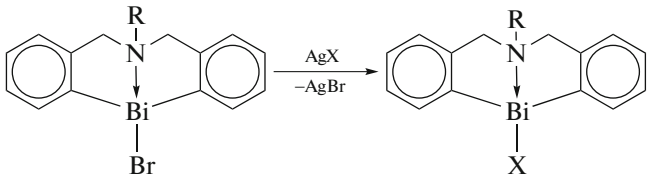

$((C_6H_4CH_2)_2NR)BiBr$ $((C_6H_4CH_2)_2NR)BiX$

R

$C_6H_5CH_2$

$C_6H_5CH_2CH_2$

$R = C_6H_5CH_2$

$X = ONO_2$, OTf,

$4\text{-}(CH_2{=}CH){-}C_6H_4{-}OSO_2$

$R = C_6H_5CH_2CH_2$

$X = ONO_2$

$$2\ Ph{-}SH + 1/2O_2 \xrightarrow[-H_2O]{\text{Cat (5 wt \%)}} Ph{-}S{-}S{-}Ph$$

$Cat = ((C_6H_4CH_2)_2NR)BiX$

Scheme 131.

The obtained compounds catalyze the oxidation of thiophenol to diphenyl disulfide using air as an oxidant in cyclohexane at temperatures below 100°C, which provides high reaction rates (100% conversion in 5 h).

Similarly prepared stable in air organobismuth(III) perfluorooctyl sulfonate $[(C_6H_4CH_2)_2NCy]BiO\text{-}SO_2C_8F_{17}$ manifests a high catalytic activity in the Mannich reactions with aromatic aldehydes and aromatic amines in water (Scheme 132) [134] (like its sulfur-containing analogs $\{[(C_6H_4CH_2)_2S]Bi(H_2O)\}^+X^-$ ($X^- = ClO_4^-$, BF_4^-, $OSO_2C_4F_9^-$, and $OSO_2C_8F_{17}^-$) presented in Scheme 113).

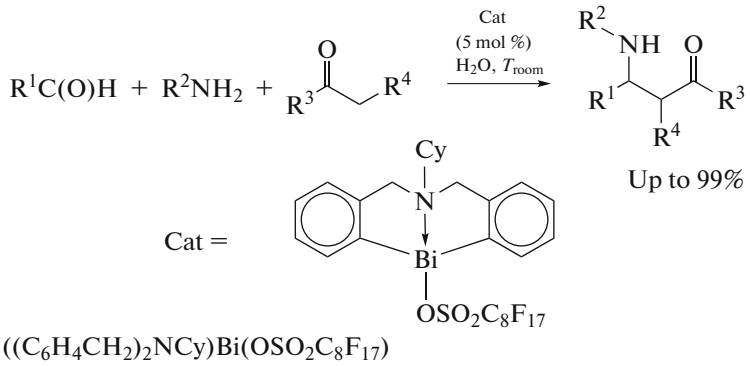

$((C_6H_4CH_2)_2NCy)Bi(OSO_2C_8F_{17})$

Scheme 132.

This catalyst also shows a good recirculation and possibility of repeated use in the synthesis of β-aminoketones.

The bismuth complex of 6-phenyldibenzo[1, 5]azabismocin-12(5*H*)-yl perchlorate was synthesized from 12-chloro-6-phenyldibenzo[1,5]azabismocin and silver perchlorate in THF in a yield of 93% [135]. According to the XRD data, the central atom has the trigonal bipyramidal environment with the oxygen and nitrogen atoms in the axial positions and two carbon atoms and lone electron pair in the equatorial positions. The Bi–C bond lengths are 2.250(13) and 2.204(12) Å; the CBiC and NBiO angles are 92.5(5)° and 154.0(3)°, respectively; and the Bi···N distance (2.388(10) Å) is shorter than that in the precursor $C_6H_5N(CH_2C_6H_4)_2BiCl$ (2.607(5) Å).

A series of heterocyclic organobismuth(III) carboxylates $[(C_6H_4)_2SO_2]BiOC(O)R$ (Scheme 133) was synthesized to determine the influence of the carboxylate ligand structure on the lipophilicity and antifungal activity toward yeast *Saccharomyces cerevisiae* [136].

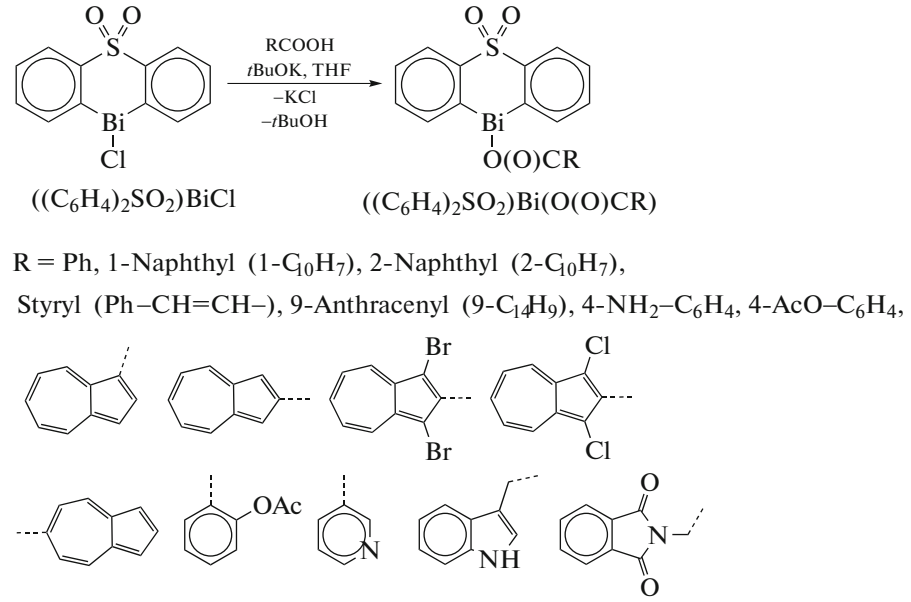

Scheme 133.

The reaction of arylbismuth dichloride $LBiCl_2$ (L = 2,6-$(Me_2NCH_2)_2C_6H_3$) with Na_2CO_3 or Ag_2SO_4 (molar ratio 1 : 1) afforded arylbismuth carbonate $RBiCO_3$ and sulfate $RBiSO_4$, respectively (Scheme 134) [137]. Arylbismuth dinitrate $RBi(NO_3)_2$ was synthesized from arylbismuth dichloride and silver nitrate at the molar ratio of the starting reagents 1 : 2.

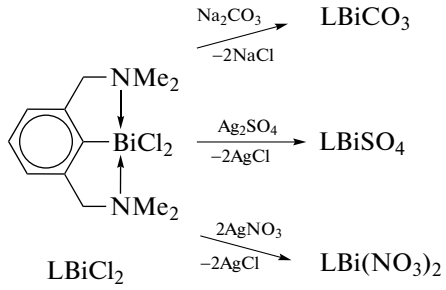

Scheme 134.

The molecular structures of $RBiCO_3 \cdot 0.5CH_2Cl_2$, $RBiSO_4$, and $RBi(NO_3)_2 \cdot H_2O$ were determined by the XRD method. The carbonate and sulfate have polymeric structures based on the bridging oxo anions, whereas the dinitrates are dimers with the bridging and terminal nitrate anions.

Two ionic bismuth complexes of the $[LBiCl]^+X^-$ type were synthesized (Scheme 135) from arylbismuth dichloride with the aryl NCO-ligand L = 2-(Me_2NCH_2)-6-$(tBuOCH_2)C_6H_3$ and silver salts [138].

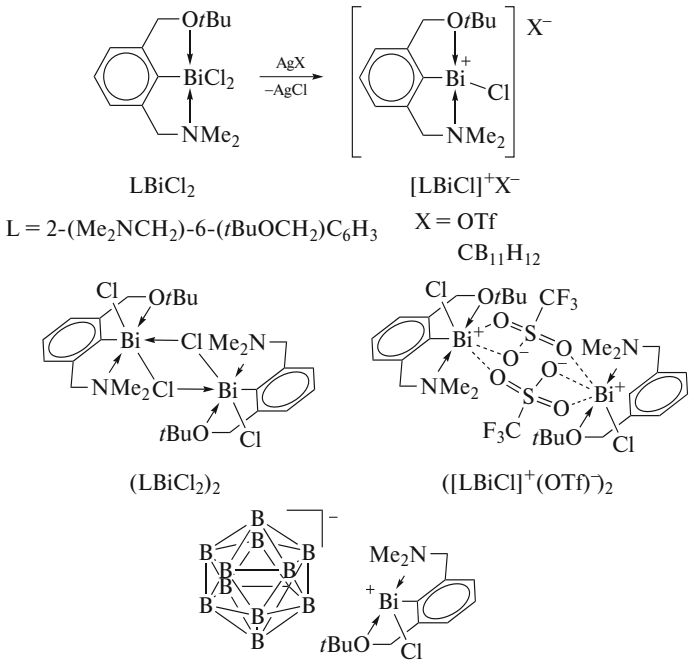

Scheme 135.

The crystals of the $LBiCl_2$ and $[LBiCl]^+(OTf)^-$ complexes in the solid state are dimers, whereas the ionic $[LBiCl]^+(CB_{11}H_{12})^-$ complex consists of monomeric structural units. All studied compounds were characterized by ^1H and ^{13}C NMR spectroscopy, ESI mass spectrometry, and single-crystal X-ray diffraction analysis.

Diarylbismuth nitrate with potential coordinating centers in the aryl ligands, $[(C_6H_4CH_2)_2NCy]Bi(NO_3)$, was prepared from diarylbismuth chloride and silver nitrate in water [139]. In the crystal, the bismuth atoms have the trigonal bipyramidal environment with the N (Bi···N 2.495(3) Å) and O atoms in the apical positions and two aryl ligands and lone electron pair in the equatorial plane. The nitrate group is a nonsymmetric bidentate ligand (Bi–O 2.416(3) and 3.0451(4) Å).

The treatment of N,C,N-chelate bismuth dichloride $LBiCl_2$ (L = 2,6-(R-N=CH)$_2$C$_6$H$_3$, R = *t*Bu, 2,6-$Me_2C_6H_3$) with one molar equivalent of $Ag[CB_{11}H_{12}]$ results in the formation of ion pairs $[LBiCl]^+[CB_{11}H_{12}]^-$ [140]. A similar reaction of the C,N-chelate analog $L'BiCl_2$ (L' = 2-(Dipp–N=CH)-4,6-(*t*Bu)$_2$C$_6$H$_2$) gives compound $[L'BiCl]^+[CB_{11}H_{12}]^-$ (Scheme 136).

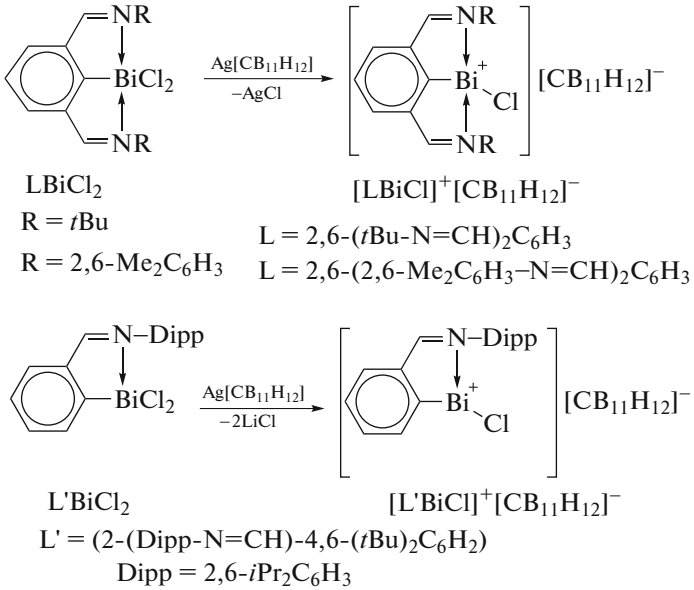

Scheme 136.

The treatment of the $[LBiCl]^+[CB_{11}H_{12}]^-$ complex (L = 2,6-(*t*Bu–N=CH)$_2$C$_6$H$_3$) with the second equivalent of $Ag[CB_{11}H_{12}]$ gave the adduct of the starting material with $Ag[CB_{11}H_{12}]$, namely, $[(2,6\text{-}(t\text{Bu–N=CH})_2C_6H_3)BiCl]^+[Ag(CB_{11}H_{12})_2]^-$. The crystals of this ionic compound decompose under daylight to the initial compounds as indicated by the ^{1}H NMR spectra.

Organobismuth carbonate $\{[(C_6H_4CH_2)_2O]\text{-}Bi\}_2CO_3$ in which the planar CO_3 group is attached to two benzo[1,5]oxabismocin cages (Scheme 137) was synthesized from diarylbismuth chloride and sodium carbonate in a water–dichloromethane mixture of solvents [141]. The lengths of two covalent bismuth–oxygen bonds are 2.217(3) and 2.223(3) Å.

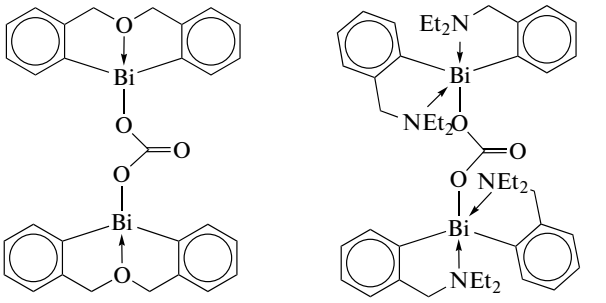

$[((C_6H_4CH_2)_2O)Bi]_2CO_3$ $[(2\text{-}Et_2NCH_2C_6H_4)_2Bi]_2CO_3$

Scheme 137.

The Bi···O distances with the CH_2OCH_2 group (2.587(4) and 2.618(3) Å) indicate the strong O→Bi coordination in the complex.

Another diarylbismuth carbonate $[(2\text{-}Et_2NCH_2C_6H_4)_2Bi]_2CO_3$ in which the bridging carbonate group links two $(2\text{-}Et_2NCH_2C_6H_4)_2Bi$ groups was synthesized similarly (Scheme 138). The shift of the bismuth atoms and *ipso*-carbon atoms from the plane of the carbonate group is 0.323(1) and 0.330(9) Å, respectively. The aryl ligands are arranged in the trans position relative to the quasi-planar groups $(CBi)_2CO_3$ [142]. The metal atom strongly coordinates to the N atom of one amino group (Bi···N 2.739(6) Å), whereas the N atom of another amino group is weakly bound to the metal atom (Bi···N 3.659(7) Å). Taking into account these intramolecular interactions, one can consider that the general coordination geometry of bismuth becomes a distorted square pyramid.

The reactions of N,C,N-chelate arylbismuth(I) $[LBi]_n$, which was prepared in situ from $LBiCl_2$ [L = 2,6-$C_6H_3(CH_2NMe_2)_2$] and K[B(*sec*-Bu)$_3$H], and diorganodisulfides ArSSAr result in the formation of organobismuth compounds $LBi(SAr)_2$ (Ar is 2-pyridyl, 4-methylthiazol-2-yl, thiophen-2-yl, 4-*tert*-butyl-1-isopropyl-1*H*-imidazol-2-yl, 1-phenyl-1*H*-tetrazol-5-yl, and 2-aminophenyl) (Scheme 138) [143].

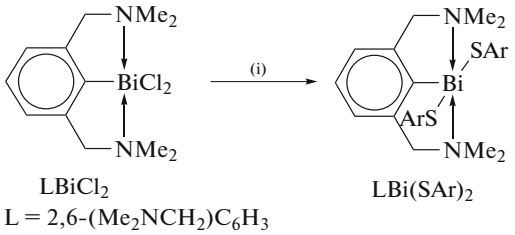

$LBiCl_2$ $LBi(SAr)_2$

L = 2,6-$(Me_2NCH_2)C_6H_3$

(i) 1. 2K[B(*sec*-Bu)$_3$H], THF, –70°C

2. ArSSAr, THF, –70°C – T_{room}

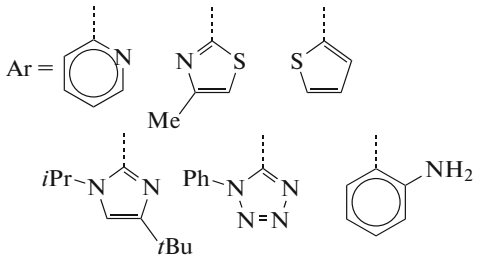

Scheme 138.

The compounds were characterized by ^1H and ^{13}C NMR spectroscopy and by XRD in the case of the 2-pyridyl, 4-methylthiazol-2-yl, and 1-phenyl-1*H*-tetrazol-5-yl derivatives. The complex based on *o*-aminothiophenol is unstable in the solution and decomposes to compound $LBi[S(NH)C_6H_4]$ containing the five-membered $BiSNC_2$ ring and 2-aminothiophenol (Scheme 139).

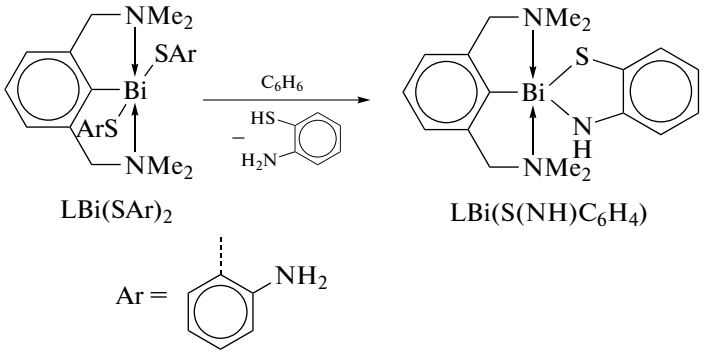

Scheme 139.

Attempts of selective cleavage of the Bi–N bond in this ring by hydrochloric or acetic acid led to the isolation of $LBiCl_2$ or diacetate $LBi(OAc)_2$ and 2-aminothiophenol only.

The N,C,N-pincer complex of arylbismuth dichloride $LBiCl_2$, where L = 2,6-$(Me_2NCH_2)_2C_6H_3$, reacts with two equivalents of potassium salts of phenols $(2,6\text{-}Me_2C_6H_3O)K$ and $(2,6\text{-}i Pr_2C_6H_3O)K$ to form the expected bismuth diaryl oxides $LBi(OAr^R)_2$, where $Ar^R = 2,6\text{-}R_2C_6H_3$; R = Me, *i*Pr (Scheme 140) [144].

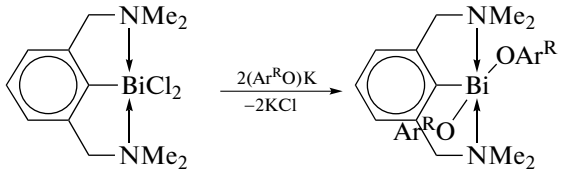

Scheme 140.

However, a similar reaction with two equivalents of $(Ar^{t\mathrm{Bu}}O)K$, where $Ar^{t\mathrm{Bu}}$ = 2,6-$t Bu_2C_6H_3O$, affords phenol $Ar^{t\mathrm{Bu}}OH$ and dark orange arylbismuth aroxide $LBi(C_6H_2tBu_2O)$, which is the product of *para*-CH bond activation (Scheme 141).

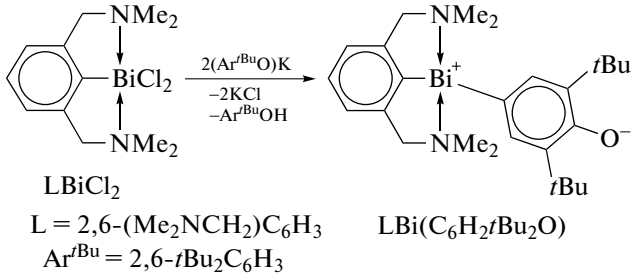

Scheme 141.

Complex $LBi(C_6H_2tBu_2O)$, where L = 2,6-$(Me_2NCH_2)_2C_6H_3$, transforms into ionic complex $[LBi(C_6H_2tBu_2OH)]^+[BPh_4]^-$ under the action of an equimolar amount of triethylammonium tetrafluoroborate in THF (Scheme 142).

The reactions of the bismuth complexes containing tridentate ligands with small molecules are rather interesting. For instance, the reactions of the pincer bismuth complex $LBi(C_6H_2tBu_2O)$, where L = 2,6-$(Me_2NCH_2)_2C_6H_3$, with CO_2 and COS in acetonitrile were studied (Scheme 142) [145]. It is shown that the red color of a solution of $LBi(C_6H_2tBu_2O)$ changes within 1 h to the yellow color inherent in solutions of the oxyaryl carboxylate complexes $LBi[O(E)C\text{–}C_6H_2tBu_2O]$, where E = O, S. These reactions of CO_2 and COS insertion at the Bi–C bond generate new dianions of the quinoid character resembling that of the oxyaryl dianionic ligand in $LBi(C_6H_2tBu_2O)$.

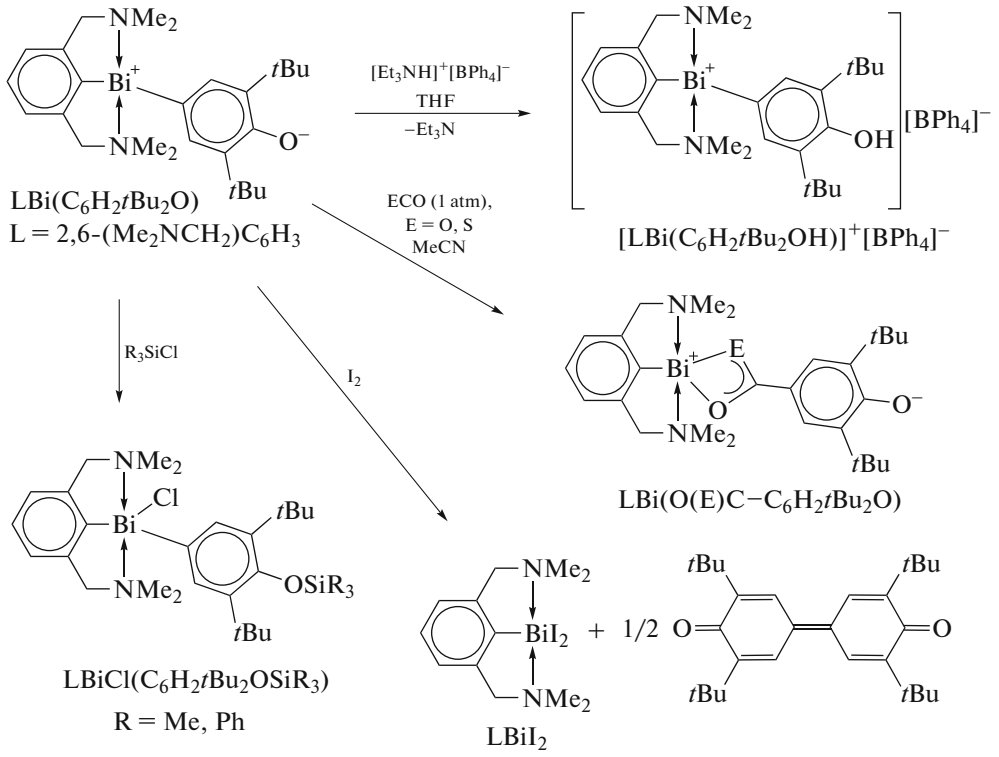

Scheme 142.

Silyl halides and pseudohalides R_3SiX (X = Cl, CN, N_3; R = Me, Ph) react with $LBi(C_6H_2tBu_2O)$, where L = 2,6-$(Me_2NCH_2)_2C_6H_3$, with the addition of X to form complexes $LBiX(C_6H_2tBu_2OSiR_3)$ (Scheme 142) in which the coordination number of the central metal atom increased to five. They react with an additional amount of R_3SiX to form complexes $LBiX_2$, where L = 2,6-$(Me_2NCH_2)_2C_6H_3$ and 2,6-$tBu_2C_6H_3$–$OSiR_3$. The reaction of $LBi(C_6H_2tBu_2O)$ (L = 2,6-$(Me_2NCH_2)_2C_6H_3$) with iodine proceeds via the oxidative cross-coupling scheme to form diiodide $Ar'BiI_2$ and 3,3',5,5'-tetra-*tert*-butyl-4,4'-diphenoquinone (Scheme 142).

A red acetonitrile solution of the oxyaryl complex $LBi(C_6H_2tBu_2O)$, where L = 2,6-$(Me_2NCH_2)_2C_6H_3$, interacts with NO at 1 atm to form a dark green solution containing several products identified using ^1H NMR spectroscopy (Scheme 143). The reactions carried out at a low temperature (−35°C) and with the stoichiometric amounts of gaseous NO gave complicated mixtures of products [146].

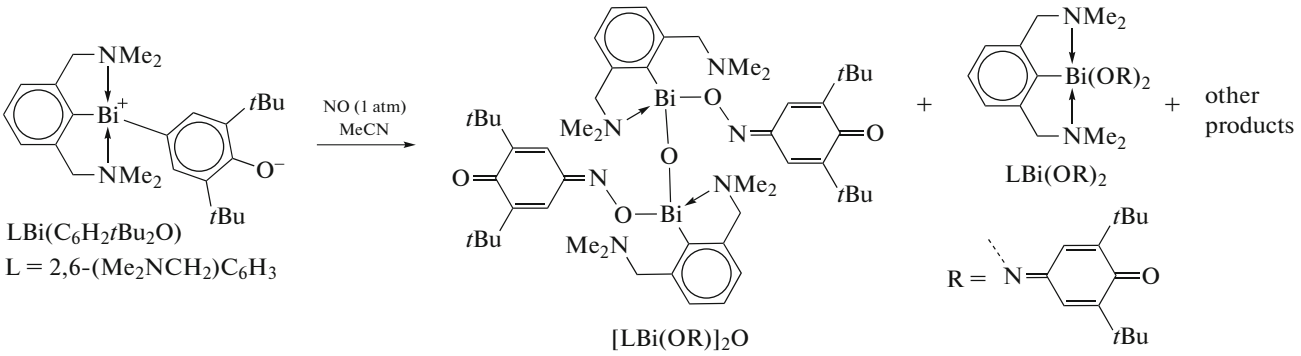

Scheme 143.

Yellow crystals of $[LBi(OR)]_2O$ were isolated from crude acetonitrile after the temperature of the reaction mixture was brought to room temperature, the solvent was removed, and the residue was recrystallized

(Scheme 143). Yellow crystals of $LBi(OR)_2$ (R = $-N{=}C_6H_2tBu_2{=}O$) were isolated from anhydrous acetonitrile.

ARYLBISMUTH(V) DERIVATIVES

The halogenation of the aryl compounds of trivalent bismuth with bromine, sulfuryl chloride, and xenon difluoride was reported. For example, tri-*p*-tolylbismuth was obtained from tri-*p*-tolylbismuth and bromine in a solution of carbon tetrachloride [147]. Diarylbismuth trihalides cannot be obtained by this method. However, in the case where the N,C-chelate ligand L (L = (2-Dipp−N=CH)C_6H_4, Dipp = 2,6-diisopropylphenyl) is present at the bismuth atom and the starting chloride LBi(Ph)Cl is treated with sulfuryl chloride, complex $LBi(Ph)Cl_3$, which was isolated and structurally characterized (Scheme 144), is stabilized [11].

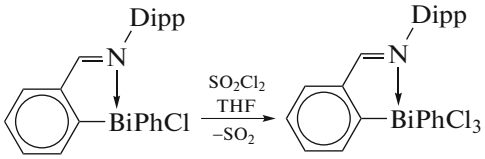

LBi(Ph)Cl LBi(Ph)Cl_3

Scheme 144.

Note that the $LBiPh_2Cl_2$ derivative was synthesized similarly.

The efficient fluorination with xenon difluoride of diphenylarylbismuth [2-(Me_2NCH_2)C_6H_4]$BiPh_2$ containing the dimethylaminomethyl substituent in the *ortho*-position of the aryl ligand (Scheme 145) was reported [148].

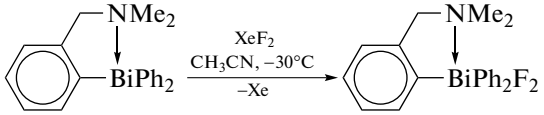

$LBiPh_2$ $LBiPh_2F_2$

Scheme 145.

Compounds [2-(Me_2NCH_2)C_6H_4]$_2BiN_3$ and [2-(Me_2NCH_2)C_6H_4]$Bi(N_3)_2$ are rare examples of bismuth azides [14]. The crystal of monoazide [2-(Me_2NCH_2)C_6H_4]$_2BiN_3$ contains monomeric molecules, whereas diazide [2-(Me_2NCH_2)C_6H_4]$Bi(N_3)_2$ is presented as a dimer with the linkage of azido groups of two types. In addition, weak van der Waals interactions between these centrosymmetric dimers lead to the chain structure in the crystal.

Triorganylbismuth dicarboxylates form a very large class of organic bismuth compounds. They are primarily presented by the aryl derivatives. It is known that triarylbismuth dicarboxylates are successfully prepared by oxidative addition from triarylbismuth and carboxylic acid in diethyl ether in the presence of hydroperoxides [149–156]. The synthesis of triarylbismuth dicarboxylates was conducted, as a rule, using *tert*-butyl hydroperoxide in diethyl ether (Scheme 146).

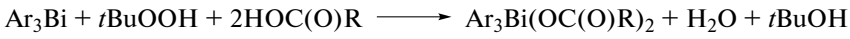

Scheme 146.

However, it seems more reasonable to use hydrogen peroxide as an oxidant in the reaction in the case of triarylbismuth containing potential coordinating centers, for example, tris(2-methoxy-5-bromophenyl)bismuth [31]. The target products were isolated from the reaction mixture in the yield not lower than 70%.

A series of triphenylbismuth dicarboxylates of the general formula $(RCOO)_2BiPh_3$ (Scheme 147) was obtained via the same scheme in order to determine their antileishmanial activity [157, 158].

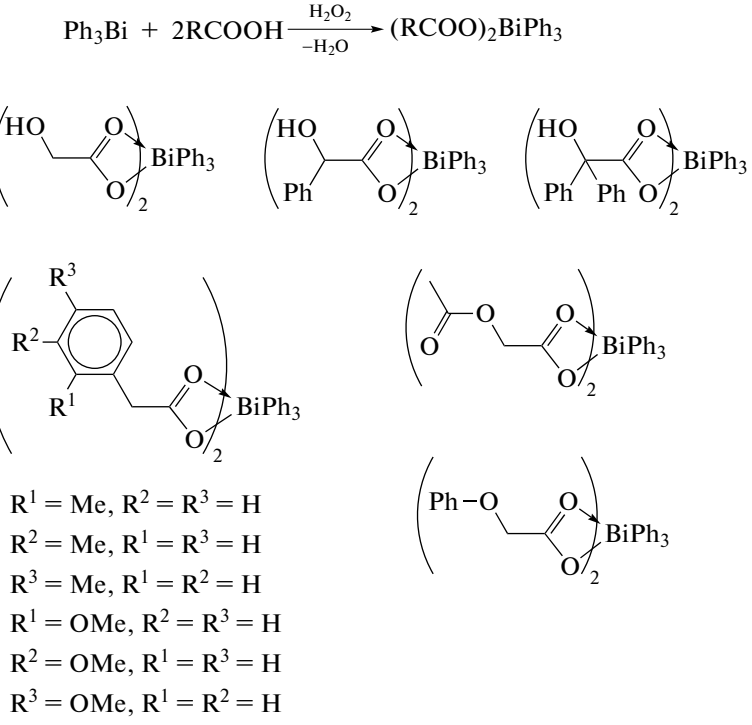

Scheme 147.

They were shown to be less active than similar antimony derivatives.

Eleven triphenylbismuth dicarboxylates were synthesized via the same scheme from the functionalized derivatives of benzoic or salicylic acid (Scheme 148), and they showed a high activity against leishmaniasis [159].

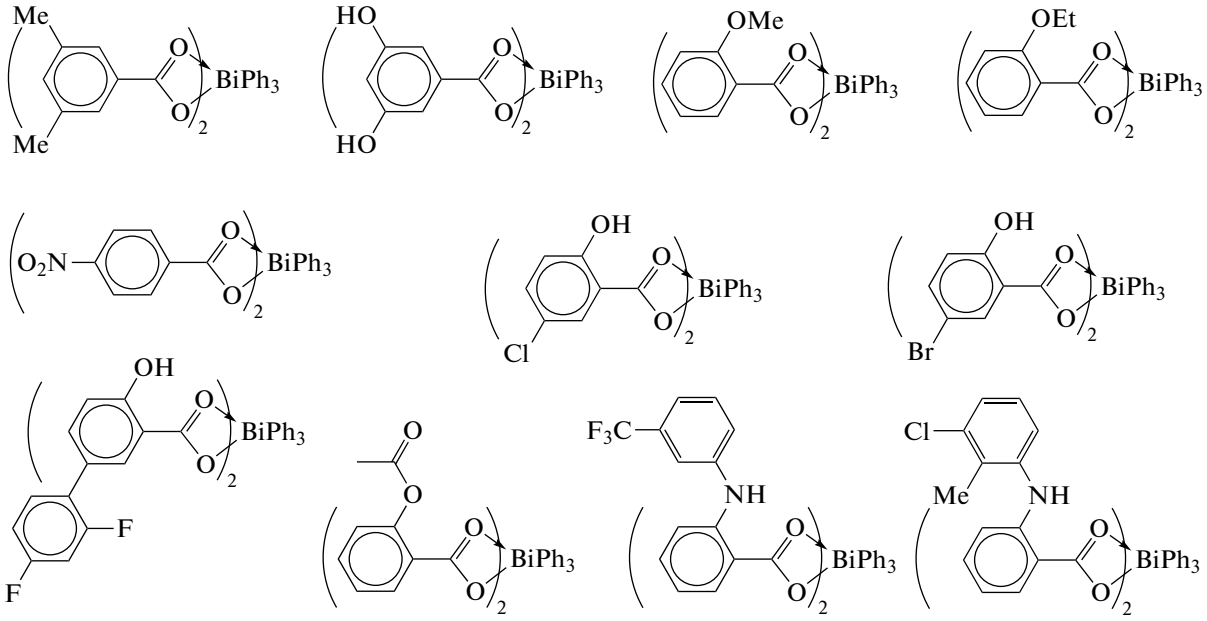

Scheme 148.

An analogous large series of tritolylbismuth dicarboxylates $(RCOO)_2BiTol_3$ based on the functionalized derivatives of benzoic or salicylic acid with *ortho*-, *meta*-, or *para*-tolyl ligands was synthesized similarly

[160]. Among them, 15 compounds were estimated for the toxicity toward promastigotes of leishmaniasis and human fibroblast cells, and the subsequent estimation of the toxicity against parasitic amastigotes was performed for ten compounds. The highest activity and selectivity are observed for the bismuth compounds containing the *o*- and *m*-tolyl ligands.

The replacement of diethyl ether by isopropyl alcohol does not change the reaction scheme. In this case, triphenylbismuth dicarboxylates $(RCOO)_2BiPh_3$ (where R = 5-Br-2-OH$-C_6H_3$, 2-OH$-C_6H_4$, 2,6-$(OH)_2$-C_6H_3, 3-Me-2-$NH_2-C_6H_3$, Ph, and Me) were obtained from triphenylbismuth, carboxylic acid, and hydrogen peroxide in an isopropanol solution in higher yields than those in the known methods for the synthesis of the target products [161].

Another method for the synthesis of triarylbismuth dicarboxylates is based on the substitution of halogen atoms in triarylbismuth dihalides. Triphenylbismuth dicarboxylates $Ph_3Bi[OC(O)R]_2$ (R = $C_6H_3F_2$-3,5, $C_6H_4CF_3$-4, and C_4H_3S) were synthesized via this scheme by mixing solutions of triphenylbismuth dichloride and sodium salt of the acid in methanol [162].

The corresponding triphenylbismuth dicarboxylates were synthesized from sodium or potassium salts of *para*- and *meta*-pyridinecarboxylic acids and triphenylbismuth dichloride (Scheme 149) in an alcoholic solution [163].

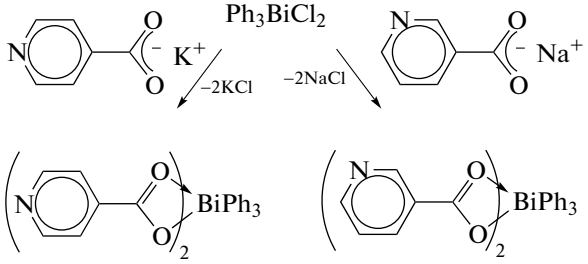

Scheme 149.

The reactions of the synthesized triphenylbismuth dicarboxylates afforded coordination polymers in which the silver atoms crosslink the dicarboxylate molecules into a chain due to the coordination of the transition metal atom with the nitrogen atoms of the pyridinecarboxylate ligands.

Triphenylbismuth dicarboxylate (4-$FC_6H_4COO)_2$-$BiPh_3$ was chosen as the object for studying the photochemical activity due to its chemical stability, low toxicity, and simple synthesis in the photodegradation reactions of three abundant dyes [164]: methylene blue, rhodamine B, and methyl violet. A solution of triphenylbismuth dichloride in toluene was added to a solution of the acid and sodium methoxide in methanol, and the reaction mixture was stirred at 25°C for 2 h. The yield was 66%. The complex was shown to possess a high photocatalytic ability in the degradation of the organic dyes under the UV or visible light irradiation. The result of this study would help to develop new photocatalytic materials.

In some cases, the efficient synthesis of triarylbismuth dicarboxylates can be carried out from triarylbismuth and carboxylic acid in the presence of trimethylamine (Scheme 150) [165].

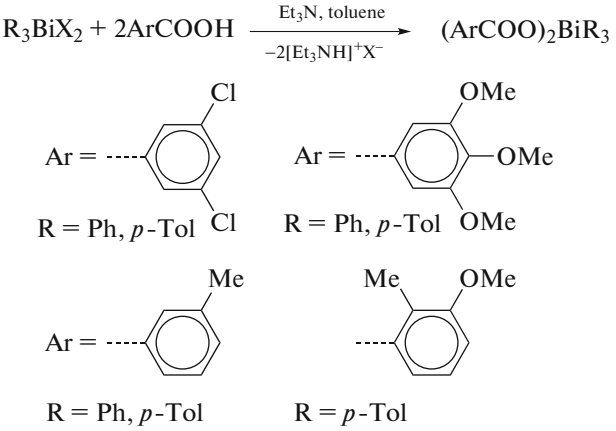

Scheme 150.

Compound [(2-Me)(3-OMe)$C_6H_3C(O)O]_2Bi(p$-Tol$)_3$ turned out to be very efficient against leishmaniasis.

The reaction of triphenylbismuth dichloride with lapachol (Lp) in the presence of trimethylamine afforded the binuclear bismuth compound $(LpPh_3Bi)_2O$, which was characterized by XRD [166]. The binuclear complex contains two hexacoordinate bismuth atom linked through the oxygen atom: $(Lp)_2(Ph_3Bi)_2O$. The compound inhibits the growth of the cell line of chronical myelogenous leukemia, and the complex is more active by approximately 5 times than free lapachol.

The case is known where triphenylbismuth dichloride reacts with carboxylic acid to form triphenylbismuth dicarboxylate, for example, with salicylic acid (Scheme 151) [167].

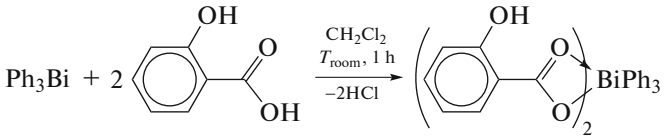

Scheme 151.

It is known that the intramolecular interaction of the bismuth atom with the carbonyl oxygen atoms (potent coordinating centers of carboxylate ligands) takes place in triarylbismuth dicarboxylates, which makes it possible to assign these derivatives to complexes of highly coordinated bismuth [152–172]. The strength of the intramolecular Bi···O(=C) contacts, which is based on donor–acceptor interactions, is determined, to a high extent, by the nature of the substituents in the aryl rings at the metal atom (affect the acceptor abilities of the metal) and in the organic radical of the carboxylic acid residue (enhance or weaken the donor properties of the carbonyl oxygen atom). The intramolecular Bi···O(=C) distances were shown to differ between each other to a higher extent: the longer Bi–O bond corresponds to the shorter Bi···O(=C) distance, which indicates the electron density redistribution upon the appearance of a strong donor–acceptor interaction. The longer Bi–O bond corresponds to the shorter Bi···O(=C) distances in the $(RCOO)_2BiAr_3$ compounds, indicating the electron density redistribution upon the appearance of a strong donor–acceptor interaction. The weakest intramolecular interactions are observed in molecules of triarylbismuth dicarboxylates in which the donor abilities of the carbonyl oxygen atom are weakened because of the electron density shift caused by the presence of the electronegative substituents in the organic radical of the acid ($-I$ effect). In the molecules of triarylbismuth dicarboxylates with the same aryl substituents at the bismuth atoms, the nonvalent interactions are enhanced with an increase in the donor properties of the carbonyl oxygen atom due to the $+M$ effect of the radical. In the dicarboxylate molecules, the shortening of the Bi···O(=C) distances correlates with an increase in one of the equatorial CBiC angles (to 152.9°) from the side of intramolecular contacts.

Triarylbismuth dicarboxylates can be used for the production of compounds of other classes, for example, in the synthesis of triarylbismuth disulfonates when triphenylbismuth diacetate under the action of trifluoromethanesulfonic acid was transformed into the corresponding disulfonate (Scheme 152), which is fairly efficient in glycosylation reactions at room temperature. This promoting agent demonstrated advantages over the most part of the modern thioglycoside activators, namely, high solubility and resistance to air and light [173].

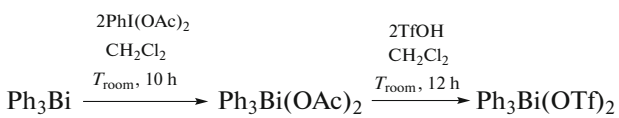

Scheme 152.

A number of triarylbismuth bis(arenesulfonates) was synthesized from triphenyl-, tris(*meta*-tolyl)-, and tris(2-methoxy-5-bromophenyl)bismuth and arenesulfonic acid in ether. Hydrogen peroxide was used as an oxidant, since no formation of the target product was observed in the presence of *tert*-butyl hydroperoxide. Triarylbismuth disulfonates $Ph_3Bi(OSO_2C_6H_3Me_2\text{-}3,4)_2$ [172], $(m\text{-Tol})_3Bi(OSO_2C_6H_3Me_2\text{-}3,4)_2$ [171], and $[(2\text{-MeO})(5\text{-Br})C_6H_3]_3Bi(OSO_2Ph)_2$ were isolated from the reaction mixture [174] in the yield up to 85% at the ratio of the starting reagents 1 : 2 : 1 (mol). It follows from the XRD data that the bismuth atoms in the triarylbismuth disulfonate molecules have a trigonal bipyramidal coordination with the arenesulfonate substituents in the axial positions. The arenesulfonate groups in the former two disulfonates are *cis*-oriented relative to the C_3Bi equatorial fragment. Intramolecular contacts between the central Bi atom and O atoms of the arenesulfonate groups (3.189(4), 3.122(3), and 3.244(6), 3.406(6) Å, respectively) are observed from the side of the maximum equatorial CBiC angle (140.77(11)° and 133.69(17)°). The third compound also exhibits intramolecular contacts between the metal atom and oxygen atoms of the sulfonate groups. However, the Bi···O distances in two crystallographically independent molecules (3.265(4)–3.296(4) Å) are somewhat longer than those in the former two compounds. Note that a similar tendency of the ligands for manifesting the bidentate properties is characteristic of triarylbismuth dicarboxylates [78]. In addition, the molecules of the third disulfonate contains the intramolecular coordination of the oxygen atoms of the methoxy groups to the bismuth atom (Bi···OMe 3.062(9)–3.215(9) Å).

The reaction of tris(2-methoxy-5-bromophenyl)bismuth with benzenesulfonic acid (1 : 2 mol/mol) in a diethyl ether solution in the presence of air oxygen was accompanied by the formation of tris(5-bromo-2-methoxyphenyl)bismuth bis(benzenesulfonate) [174], which was isolated in 48 h from the reaction mixture in a yield of 7%. Evidently, air oxygen played the role of the oxidant of triarylbismuth in the absence of peroxide.

Triphenylbismuth bis(trifluoromethanesulfonate) can be synthesized from triphenylbismuth dichloride and silver triflate, and its reactions with donor ligands, such as triphenylphosphine oxide, aminopyridine, and bipyridyl, afford ionic complexes with pentacoordinate bismuth cations (Scheme 153) [175].

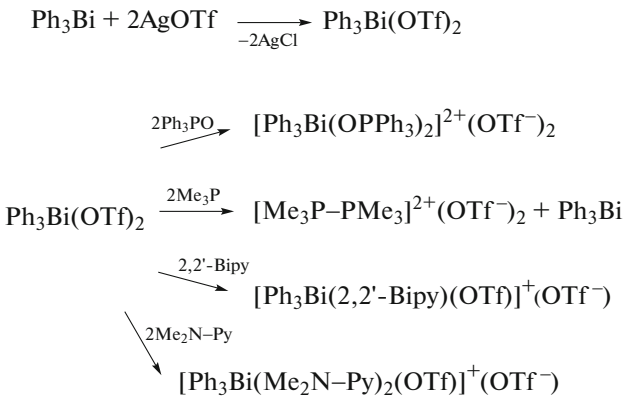

Scheme 153.

This synthetic method is promising for a wide development of the chemistry of coordination bismuth compounds.

The reactions of tri-*p*-tolylbismuth dibromide with silver perchlorate and silver hydrate gave tri-*p*-tolylbismuth diperchlorate and μ-oxobis((perchlorate)tri-*p*-tolylbismuth), respectively [176]. In the molecular structure of the former compound, the bismuth atoms have a distorted trigonal bipyramidal coordination with the apically arranged oxygen atoms of the perchlorate groups (Bi–C bonds 2.180(5)–2.201(5), Bi–O 2.324(4)–2.355(4) Å, OBiO axial angles 170.1(1)°, 174.5(1)°). The structure of the second compound contains the binuclear $[p\text{-Tol}_3Bi(ClO_4)]_2O$ molecules (Bi–O bonds 2.371(15), 1.9107(7) Å, OBiO axial angle 180.0°).

The first triphenylbismuth perfluoroalkyl phosphinate, $[(C_2F_5)_2PO_2]_2BiPh_3$, was synthesized from Ph_3BiCl_2 and $[(C_2F_5)_2PO_2]Ag$ (Scheme 154). This phosphinate was successfully used as a catalyst in the Diels–Alder reaction [91].

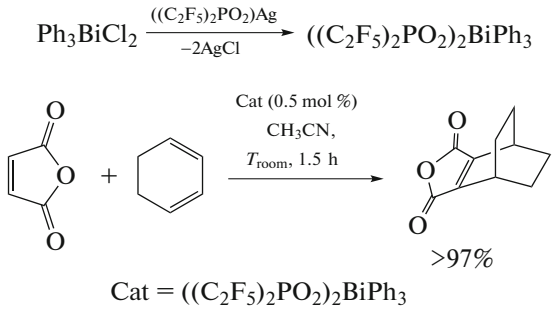

Scheme 154.

The authors [148] developed an efficient method for the generation of triphenylfluorobismuthonium $[Ph_3BiF]^+$ and triphenyl(diacetonitrilo)bismuthonium $[Ph_3Bi(NCMe)_2]^{2+}$ cations from easily accessible Ph_3BiF_2 (Scheme 155).

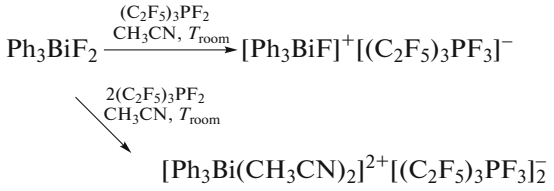

Scheme 155.

Tetraphenylbismuthonium salts are formed under the action of acids on pentaphenylbismuth. For instance, the titration of pentaphenylbismuth with an ethereal solution of hydrogen chloride is accompanied by the disappearance of the violet color characteristic of pentaphenylbismuth and by the formation of labile colorless crystals of tetraphenylbismuth chloride that decomposes at room temperature to triphenylbismuth and chlorobenzene [177]. Its structure was determined [178] by the XRD method. It is found that chlorine occupies the axial position in the trigonal bipyramidal environment of the central atom. The bismuth atom shifts from the equatorial plane toward the axially arranged carbon atom. The Bi–Cl bond length (2.9116(19) Å) exceeds the sum of covalent radii of bismuth and chlorine atoms (2.50 Å) but is substantially less than the sum of their van der Waals radii (3.82 Å) [20].

Kinetically unstable tetraphenylbismuth bromide, which was obtained from pentaphenylbismuth and a solution of hydrogen bromide in acetone, had a similar structure [179].

The reactions of pentaphenylbismuth with equimolar amounts of sulfuric, 2,4-dinitrobenzenesulfonic, and nitric acids afforded tetraphenylbismuth hydrosulfate $(HOSO_3)BiPh_4$, tetraphenylbismuth 2,4-dinitrobenzenesulfonate $(2,4\text{-}(NO_2)_2C_6H_3SO_2O)BiPh_4$, and tetraphenylbismuth nitrate hydrate $Ph_4BiNO_3 \cdot 1/3H_2O$, respectively [180]. The crystal structures of the bismuth compounds were determined by XRD. The bismuth atoms are pentacoordinate in the former two compounds (environment C_4BiO), whereas the latter contains the nitratotetraphenylbismuth molecule and tetraphenylbismuthonium cations of two types, one of which is coordinated to the nitrate anion and water molecule.

A number of the indicated derivatives was synthesized by the reactions of pentaphenylbismuth (toluene, 0.5–5 min, 20°C) with phenols containing the electron-withdrawing substituents (Scheme 156) in order to establish the effect of the nature of the substituents in the aroxyl group on the values of bond angles and bond lengths at the bismuth atom in tetraphenylantimony aroxides [181].

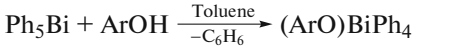

Scheme 156.

The color of the solution changed to yellow or yellow-brown due to the interaction of the reactants, and the target products were isolated by crystallization from a benzene–octane mixture. Tetraphenylbismuth aroxides are yellow or yellow-brown crystalline substances stable in air and soluble in aliphatic and aromatic hydrocarbons. The yields of the synthesized tetraphenylbismuth aroxides reached 86%.

The reaction of ligand redistribution for the phenyl compounds of pentavalent bismuth was discovered in 1999 using as examples the reactions of pentaphenylbismuth with triphenylbismuth bis(2,5-dimethylbenzenesulfonate) and triphenylbismuth bis(2,4-dimethylbenzenesulfonate) [182]. Tetraphenylbismuth aroxides were also synthesized by an analogous method from pentaphenylbismuth and triphenylbismuth diaroxide in benzene (Scheme 157) [181].

$$Ph_5Bi + Ph_3Bi(OAr)_2 \xrightarrow{C_6H_6} 2(ArO)BiPh_4$$

Ar = 4-*t*Bu-2,6-Br_2-C_6H_2, 2,6-$Cl_2C_6H_3$, 4-NO_2-2,6-Br_2-C_6H_2, 2,4-$(NO_2)_2C_6H_3$, 2,4,6-$(NO_2)_3C_6H_2$

Scheme 157.

The tetraphenylbismuth aroxide molecules have the trigonal bipyramidal configuration characteristic of the most part of the pentacoordinate bismuth derivatives, and the most electronegative substituent (aroxyl ligand) occupies one of the axial positions. The axial CBiO angles are close to the ideal value, and the bismuth atom shifts from the equatorial plane toward the carbon atom of the axially arranged phenyl ligand, which induces a distortion of the bond angles between the axial and equatorial substituents. The Bi–O distances (2.451–2.925 Å) are longer than the sum of covalent radii of the atoms (2.31 Å [20]), and the longest Bi–O bond was observed in tetraphenylbismuth picrate [183].

The general regularity in the arrangement of the equatorial phenyl groups was revealed in all studied structures. For example, two phenyl rings in each structure turn around the equatorial Bi–C bonds by significant torsion angles, whereas the plane of the third ring is nearly perpendicular to the axial Bi–O bond. The aroxy group is arranged above this equatorial phenyl, which causes the interaction of their π systems (so-called π–π-stacking effect). In tetraphenylbismuth aroxides, the geometry characteristic of the π–π-stacking interaction is distorted: the intercenter distances are 3.666–4.021 Å and the interplanar angles are 14.2°–32.4°, which are close to the ideal values for interactions of this type [184, 185].

A series of the platinum and gold derivatives are synthesized by the substitution reactions in the preparative chemistry of organic compounds of pentavalent bismuth. For instance, the reaction product of tetraphenylbismuth chloride Ph_4BiCl with potassium hexabromoplatinate (2 : 1 mol/mol) in water after recrystallization from DMSO is *S*-dimrthylsulfoxidotribromoplatinate of *O*-dimethylsulfoxidotetraphenylbismuth $[Ph_4Bi{\cdot}DMSO\text{-}O]^+[PtBr_3{\cdot}DMSO\text{-}S]^-$. The recrystallization from acetonitrile of the complex derived from tetraphenylbismuth chloride and potassium hexachloroplatinate gives tetraphenylbismuth hexachloroplatinate $[Ph_4Bi]_2^+[PtCl_6]^{2-}$ [178].

The gold complexes $[Ph_4Bi]^+[Au(CN)_2Cl_2]^-$ and $[Ph_4Bi]^+[Au(CN)_2Br_2]^-$ were synthesized by the reactions of tetraphenylbismuth bromide with potassium dichloro- and dibromodicyanoaurate in water followed by water removal and recrystallization of the solid residue from acetonitrile and were structurally characterized [186].

Equimolar amounts of tetraphenylbismuth sulfosalicylate and bismuth iodide in acetone react to form red-orange crystals of the ionic complex $[Ph_4Bi]_4^+[Bi_4I_{16}]^{4-}{\cdot}2(Me_2C{=}O)$ [187]. The XRD data show that in the complex two independent tetraphenylbismuthonium cations have somewhat different geometries. In one of them, the coordination of the bismuth atom is distorted tetrahedral (Bi–C bond lengths lie in a range of 2.184–2.207 Å, and the range of the CBiC bond angles is 106.0°–113.7°). The coordination sphere of another cation contains the acetone molecule (Bi···O distance is 3.094 Å), which results in the appearance of the contribution of the trigonal bipyramidal component in the tetrahedral structure: a noticeable deviation of the CBiC bond angles from the value ideal for tetrahedron is observed (102.1°–120.8°). The tetranuclear centrosymmetric $[Bi_4I_{16}]^{4-}$ anion (Scheme 158) in the complex consists of two pairs of BiI_6 octahedra joined along the common edges. The environments of the Bi(2) and Bi(2') atoms consist of three terminal and three bridging iodine atoms each (Bi–I distances are 2.909–2.947 and 3.284–3.337 Å, respectively). The Bi(1) and Bi(1') atoms have two terminal and four bridging iodine atoms in the environment (corresponding bond lengths are 2.898, 2.904, and 3.027–3.312 Å).

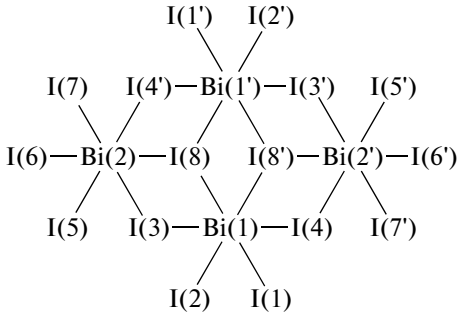

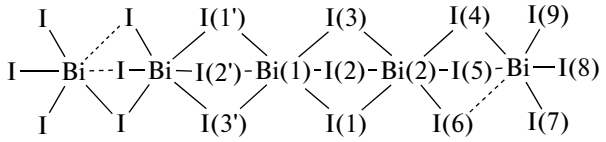

Scheme 158.

The complex with the linear pentanuclear three-charge anion $[Ph_4Bi]_3^+[Bi_5I_{18}]^{3-}$ is formed with an increase in the amount of bismuth iodide (molar ratio of tetraphenylbismuth arenesulfonate to bismuth iodide is 1 : 2) [188]. In the centrosymmetric $[Bi_5I_{18}]^{3-}$ anion (Scheme 158), the octahedrally coordinated Bi atoms are joined pairwise by the triple iodine bridges. The terminal Bi(3) atom is linked to the adjacent Bi(2) atom by the Bi(3)—I(4–6) bonds that are less strong than Bi(2)—I(4–6) (3.423–3.582 and 2.940–2.954 Å, respectively). The terminal Bi(3)—I(7,8,9) bonds (2.842–2.860 Å) are the shortest contacts in the $[Bi_5I_{18}]^{3-}$ anion.

Note an efficient method for the synthesis of tetraphenylarylbismuth fluorides, which consists of the treatment of triphenylbismuth difluoride with phenylboric acid in the presence of boron trifluoride etherate in dichloromethane followed by the treatment of the reaction mixture with a cesium fluoride excess. The method was first described by the Japanese authors in 2003 [189] and continued by the authors [190] who obtained triphenylarylbismuthonium fluorides via a similar scheme and studied the transport properties of cations of the general formula $[Ph_3BiAr]^+$, where Ar is phenyl, naphthyl, anthryl, or pyrenyl. These cations were shown to efficiently transfer hydroxide, fluoride, and chloride anions through the phospholipid bilayer.

CONCLUSIONS

Organic bismuth compounds attract increasing attention of researchers all over the world. This is caused by the recently found catalytic activity of a number of the organic bismuth compounds in various groups of reactions significant in organic and organoelement chemistry and by their high potential of application as reagents in fine organic synthesis. From the viewpoint of biochemistry and medicine, this class of bismuth compounds also has a high application potential as anticancer, antifungal, and antibacterial drugs. In addition, the organic compounds of bismuth(III,V) can form mono-, bi-, and polynuclear compounds with diverse structures of both molecular and ionic types, which is unambiguously important for the development of fundamental research of organobismuth compounds. The catalysis by the organobismuth compounds and the areas of their biochemical and medical use should be expected to develop more actively in the nearest future.

REFERENCES

1. Razuvaev, G.A., Osanova, N.A., and Sharutin V.V., *Dokl. Akad. Nauk SSSR*, 1975, vol. 225, no. 3, p. 581.
2. Sharutin, V.V. and Mosunova, T.V., *Vest. Yuzhno-Ural. Gos. Un-ta. Ser. Khim.*, 2020, vol. 12, no. 3, p. 7. https://doi.org/10.14529/chem200301
3. Kindra, D.R., Peterson, J.K., Ziller, J.W., and Evans, W.J., *Organometallics*, 2015, vol. 34, p. 395. https://doi.org/10.1021/om5010786
4. Schulz, S., Kuczkowski, A., Blaser, D., et al., *Organometallics*, 2013, vol. 32, p. 5445. https://doi.org/10.1021/om400730r
5. Lichtenberg, C., Pan, F., Spaniol, T.P., et al., *Angew. Chem., Int. Ed.*, 2012, vol. 51, p. 13011. https://doi.org/10.1002/anie.201206782
6. Casely, I.J., Ziller, J.W., Mincher, B.J., and Evans, W.J., *Inorg. Chem.*, 2011, vol. 50, p. 1513. https://doi.org/10.1021/ic102119y
7. Auer, A.A., Mansfeld, D., Nolde, C., et al., *Organometallics*, 2009, vol. 28, p. 5405. https://doi.org/10.1021/om900536r
8. Solyntjes, S., Bader, J., Neumann, B., et al., *Chem.-Eur. J.*, 2017, vol. 23, p. 1557. https://doi.org/10.1002/chem.201604910
9. Ishii, T., Suzuki, K., Nakamura, T., and Yamashita, M., *J. Am. Chem. Soc.*, 2016, vol. 138, p. 12787. https://doi.10.1021/jacs.6b08714
10. Tomaschautzky, J., Neumann, B., Stammler, H.-G., et al., *Dalton Trans.*, 2017, vol. 46, p. 1645. https://doi.org/10.1039/C6DT04293G
11. Urbanova, I., Jambor, R., Ruzicka, A., et al., *Dalton Trans.*, 2014, vol. 43, p. 505. https://doi.org/10.1039/c3dt51733k
12. Olaru, M., Nema, M.G., Soran, A., et al., *Dalton Trans.*, 2016, vol. 45, p. 9419. https://doi.org/10.1039/c5dt05074j
13. Soran, A., Breunig, H.J., Lippolis, V., et al., *J. Organomet. Chem.*, 2010, vol. 695, p. 850. https://doi:10.1016/j.jorganchem.2010.01.004
14. Schulz, A. and Villinger, A., *Organometallics*, 2011, vol. 30, p. 284. https://doi.org/10.1021/om1009796
15. Chalmers, B.A., Meigh, C.B.E., Nejman, P.S., et al., *Inorg. Chem.*, 2016, vol. 55, p. 7117. https://doi.org/10.1021/acs.inorgchem.6b01079
16. Plajer, A.J., Colebatch, A.L., Rizzuto, F.J., et al., *Angew. Chem., Int. Ed.*, 2018, vol. 57, p. 6648. https://doi.org/10.1002/anie.2018023501

17. Wade, C.R., Saber, M.R., and Gabbai, F.P., *Heteroat. Chem.*, 2011, vol. 22, p. 500. https://doi.org/10.1002/hc.20713

18. Tschersich, C., Hoof, S., Frank, N., et al., *Inorg. Chem.*, 2016, vol. 55, p. 1837. https://doi.org/10.1021/acs.inorgchem.5b02740

19. Materne, K., Braun-Cula, B., Herwig, C., et al., *Chem.-Eur. J.*, 2017, vol. 23, p. 11797. https://doi.org/10.1002/chem.201703489

20. Batsanov, S.S., *Zh. Neorg. Khim.*, 1991, vol. 36, no. 12, p. 3015.

21. Obata, T., Matsumura, M., Kawahata, M., et al., *J. Organomet. Chem.*, 2016, vol. 807, p. 17. http://dx.doi.org/10.1016/j.jorganchem.2016.02.008

22. Kawahata, M., Yasuike, S., Kinebuchi, I., et al., *Acta Crystallogr., Sect. E: Struct. Rep. Online*, 2011, vol. 67, p. m25. https://doi.org/10.1107/S1600536810043655

23. Breunig, H.J., Nema, M.G., Silvestru, C., et al., *Z. Anorg. Allg. Chem.*, 2010, vol. 636, p. 2378. https://doi.org/10.1002/zaac.201000233

24. Alcantara, E., Sharma, P., Perez, D., et al., *Synth. React. Inorg., Met.-Org., Nano-Met. Chem.*, 2012, vol. 42, p. 1139. https://doi.org/10.1080/15533174.2012.680162

25. Vranova, I., Jambor, R., Ruzicka, A., et al., *Organometallics*, 2015, vol. 34, p. 534. https://doi.org/10.1021/om5011879

26. Rao, M.L.N. and Dhanorkar, R.J., *RSC Advances*, 2016, vol. 6, p. 1012. https://doi.org/10.1039/c5ra23311a

27. Hebert, M., Petiot, P., Benoit, E., et al., *Org. Chem.*, 2016, vol. 81, p. 5401. https://doi.org/10.1021/acs.joc.6b00767

28. Petiot, P. and Gagnon, A., *Eur. J. Org. Chem.*, 2013, p. 5282. https://doi.org/10.1002/ejoc.201300850

29. Ahmad, T., Dansereau, J., Hebert, M., et al., *Tetrahedron Lett.*, 2016, vol. 57, p. 4284. https://doi.org/10.1016/j.tetlet.2016.08.021

30. Sharutin, V.V., Senchurin, V.S., Sharutina, O.K., and Chagarova, O.V., *Russ. J. Gen. Chem.*, 2011, vol. 81, no. 10, p. 2102. https://doi.org/10.1134/S1070363211100100

31. Sharutin, V.V., Sharutina, O.K., Ermakova, V.A., and Smagina, Ya.R., *Russ. J. Inorg. Chem.*, 2017, vol. 62, no. 8, p. 1043.

32. Benjamin, S.L., Karagiannidis, L., Levason, W., et al., *Organometallics*, 2011, vol. 30, p. 895. https://doi.org/10.1021/om1010148

33. Hirayama, T., Mukaimine, A., Nishigaki, K., et al., *Dalton Trans.*, 2017, vol. 46, p. 15991. https://doi.org/10.1039/c7dt03194g

34. Ohshita, J., Matsui, S., Yamamoto, R., et al., *Organometallics*, 2010, vol. 29, p. 3239. https://doi.org/10.1021/om100560n

35. Onishi, K., Douke, M., Nakamura, T., et al., *J. Inorg. Biochem.*, 2012, vol. 117, p. 77. https://doi.org/10.1016/j.jinorgbio.2012.09.009

36. Preda, A.M., Schneider, W.B., Rainer, M., et al., *Dalton Trans.*, 2017, vol. 46, p. 8269. https://doi.org/10.1039/C7DT01437F

37. Preda, A.M., Schneider, W.B., Schaarschmidt, D., et al., *Dalton Trans.*, 2017, vol. 46, p. 13492. https://doi.org/10.1039/C7DT02567J

38. Chen, J., Murafuji, T., and Tsunashima, R., *Organometallics*, 2011, vol. 30, p. 4532. https://dx.doi.org/10.1021/om200228x

39. Parke, S.M., Narreto, M.A.B., Hupf, E., et al., *Inorg. Chem.*, 2018, vol. 57, p. 7536. https://doi.org/10.1021/acs.inorgchem.8b00149

40. Worrell, B.T., Ellery, S.P., and Fokin, V.V., *Angew. Chem., Int. Ed.*, 2013, vol. 52, p. 13037. https://doi.org/10.1002/anie.201306192

41. Parke, S.M., Hupf, E., Matharu, G.K., et al., *Angew. Chem., Int.* Ed., 2018, vol. 57, p. 14841. https://doi.org/10.1002/anie.201809357

42. Ohshita, J., Yamaji, K., Ooyama, Y., et al., *Organometallics*, 2019, vol. 38, p. 1516. https://doi.org/10.1021/acs.organomet.8b00945

43. Bregadze, V.I., Glazun, S.A., Efremov, A.N., and Sharutin, V.V., *Vest. Yuzhno-Ural. Gos. Un-ta. Ser. Khim.*, 2020, vol. 12, no. 1, p. 5. https://doi.org/10.14529/chem200101

44. Egorova, I.V., Zhidkov, V.V., and Grinishak, I.P., *Russ. J. Gen. Chem.*, 2015, vol. 85, no. 7, p. 1692. https://doi.org/10.1134/S107036321507021X

45. Kumar, I., Bhattacharya, P., and Whitmire, K.H., *J. Organomet. Chem.*, 2015, vol. 794, p. 153. http://dx.doi org/10.1016/j.jorganchem.2015.06.023

46. Andrews, P.C., Frank, R., Junk, P.C., et al., *J. Inorg. Biochem.*, 2011, vol. 105, p. 454. https://doi:10.1016/j.jinorgbio.2010.08.007

47. Anjaneyulu, O., Maddileti, D., and Swamy, K.C.K., *Dalton Trans.*, 2012, vol. 41, p. 1004. https://doi.org/10.1039/c1dt11207d

48. Egorova, I.V., Sharutin, V.V., Ivanenko, T.K., et al., *Russ. J. Coord. Chem.*, 2006, vol. 32, no. 5, p. 321. https://doi.org/10.1134/S1070328406050022

49. Pathak, A., Blair, V.L., Ferrero, R.L., et al., *J. Inorg. Biochem.*, 2017, vol. 177, p. 266. http://dx.doi.org/10.1016/j.jinorgbio.2017.05.014

50. Stavila, V. and Whitmire, K.H., *Acta Crystallogr., Sect. E: Struct. Rep. Online*, 2010, vol. 66, m1547. https://doi.org/10.1107/S1600536810044235

51. Andrews, P.C., Deacon, G.B., Junk, P.C., et al., *Organometallics*, 2009, vol. 28, p. 3999. https://doi.org/10.1021/om9002158

52. Jambor, R., Ružicková, Z., Erben, M., and Dostál, L., *Inorg. Chem. Commun.*, 2017, vol. 76, p. 36. http://dx.doi.org/10.1016/j.inoche.2016.12.008

53. Sun, Y.-Q., Zhong, J.-C., Liu, L.-H., et al., *J. Mol. Struct.*, 2016, vol. 1124, p. 138. http://dx.doi.org/10.1016/j.molstruc.2016.02.085

54. Andrews, P.C., Junk, P.C., Kedzierski, L., Peiris, R.M., et al., *Aust. J. Chem.*, 2013, vol. 66, p. 1297. http://dx.doi.org/10.1071/CH13374

55. Andrews, P.C., Ferrero, R.L., Junk, P.C., et al., *Aust. J. Chem.*, 2012, vol. 65, p. 883. http://dx.doi.org/10.1071/CH12042

56. Chaudhari, K.R., Yadav, N., Wadawale, A., et al., *Inorg. Chim. Acta*, 2010, vol. 363, p. 375. https://doi.org/10.1016/j.ica.2009.11.002

57. Luqman, A., Blair, V.L., Bond, A.M., and Andrews, P.C., *Angew. Chem., Int. Ed.*, 2013, vol. 52, p. 7247. https://doi.org/10.1002/anie.201301200

58. Luqman, A., Blair, V.L., Brammananth, R., et al., *Chem.-Eur. J.*, 2014, vol. 20, p. 14362. https://doi.org/10.1002/chem.201404109

59. Luqman, A., Blair, V.L., Brammananth, R., et al., *Eur. J. Inorg. Chem.*, 2016, p. 2738. https://doi.org/10.1002/ejic.201600076

60. Luqman, A., Blair, V.L., Brammananth, R., et al., *Eur. J. Inorg. Chem.*, 2015, p. 725. https://doi.org/10.1002/ejic.201402958

61. Luqman, A., Blair, V.L., Brammananth, R., et al., *Eur. J. Inorg. Chem.*, 2015, p. 4935. https://doi.org/10.1002/ejic.201500795

62. Andrews, P.C., Ferrero, R.L., Forsyth, C.M., et al., *Organometallics*, 2011, vol. 30, p. 6283. http://dx.doi.org/10.1021/om2008869

63. Sharutin, V.V. and Sharutina, O.K., *Russ. J. Inorg. Chem.*, 2014, vol. 59, no. 10, p. 1119. https://doi.org/10.1134/S0036023614100179

64. Wrobel, L., Ruffer, T., Korb, M., et al., *Chem.-Eur. J.*, 2018, vol. 24, p. 16630. https://doi.org/10.1002/chem.201803664

65. Andrews, P.C., Busse, M., Deacon, G.B., et al., *Dalton Trans.*, 2010, vol. 39, p. 9633. https://doi.org/10.1039/c0dt00629g

66. Andrews, P.C., Deacon, G.B., Ferrero, R.L., et al., *Dalton Trans.*, 2009, p. 6377. https://doi.org/10.1039/b900774a

67. Beckmann, J., Bolsinger, J., Duthie, A., et al., *Inorg. Chem.*, 2012, vol. 51, p. 12395. https://dx.doi.org/10.1021/ic3017722

68. Metre, R.K., Kundu, S., Narayanan, R.S., and Chandrasekhar, V., *Phosphorus, Sulfur, Silicon Relat. Elem.*, 2015, vol. 190, p. 2134. https://doi.org/10.1080/10426507.2015.1072192

69. Chandrasekhar, V., Metre, R.K., and Narayanan, R.S., *Dalton Trans.*, 2013, vol. 42, p. 8709. https://doi.org/10.1039/c3dt50537e

70. Cui, L.-S., Meng, J.-R., Gan, Y.-L., et al., *Inorg. Nano-Metal Chem.*, 2017, vol. 47, p. 1537. http://dx.doi.org/10.1080/24701556.2017.1357606

71. Ritter, C., Ringler, B., Dankert, F., et al., *Dalton Trans.*, 2019, vol. 48, p. 5253. https://doi.org/10.1039/c9dt00408d

72. Armstrong, D., Taullaj, F., Singh, K., et al., *Dalton Trans.*, 2017, vol. 46, p. 6212. https://doi.org/10.1039/c7dt00428a

73. Breunig, H.J., Haddad, N., Lork, E., et al., *Organometallics*, 2009, vol. 28, p. 1202. https://doi.org/10.1021/om800934c

74. Schwamm, R.J., Fitchett, C.M., and Coles, M.P., *Chem. Asian J.*, 2019, vol. 14, p. 1204. https://doi.org/10.1002/asia.201801729

75. Sharutin, V.V., Egorova, I.V., Sharutina, O.K., et al., *Russ. J. Coord. Chem.*, 2003, vol. 29, no. 12, p. 838. https://doi.org/10.1023/B:RUCO.0000008395. 98029.6c

76. Briand, G.G., Decken, A., Hunter, N.M., et al., *Polyhedron*, 2012, vol. 31, p. 796. https://doi:10.1016/j.poly.2011.11

77. Breunig, H.J., Lork, E., and Nema, M.-G., *Z. Naturforsch., A: Phys. Sci.*, 2009, vol. 64, p. 1213.

78. Cambridge Crystallographic Data Centre, 2019. http://www.ccdc.cam.ac.uk/data_request/cif

79. Ramler, J., Poater, J., Hirsch, F., et al., *Chem. Sci.*, 2019, vol. 10, p. 4169. https://doi.org/10.1039/c9sc00278b

80. Nekoueishahraki, B., Sarish, S.P., Roesky, H.W., et al., *Angew. Chem., Int. Ed.*, 2009, vol. 48, p. 4517. https://doi.org/10.1002/anie.200901215

81. Nekoueishahraki, B., Samuel, P.P., Roesky, H.W., et al., *Organometallics*, 2012, vol. 31, p. 6697. https://doi.org/10.1021/jacs.6b03432

82. Lu, W., Hu, H., Li, Y., et al., *J. Am. Chem. Soc.*, 2016, vol. 138, p. 6650. https://doi.org/10.1021/jacs.6b03432

83. Waters, J.B., Chen, Q., Everitt, T.A., and Goicoechea, J.M., *Dalton Trans.*, 2017, vol. 46, p. 12053. https://doi.org/10.1039/c7dt02431b

84. Aprile, A., Corbo, R., Tan, K.V., et al., *Dalton Trans.*, 2014, vol. 43, p. 764. https://doi.org/10.1039/c3dt52715h

85. Wang, G., Freeman, L.A., Dickie, D.A., et al., *Inorg. Chem.*, 2018, vol. 57, p. 11687. https://doi.org/10.1021/acs.inorgchem.8b01813

86. Wang, G., Freeman, L.A., Dickie, D.A., et al., *Chem.-Eur. J.*, 2019, vol. 21, p. 4335. https://doi.org/10.1002/chem.201900458

87. Munzer, J.E., Kneusels, N.-J.H., Weinert, B., et al., *Dalton Trans.*, 2019, vol. 48, p. 11076. https://doi.org/10.1039/c9dt01784d

88. Olaru, M., Duvinage, D., Lork, E., et al., *Angew. Chem., Int. Ed.*, 2018, vol. 57, p. 10080. https://doi.org/10.1002/anie.201803160

89. Bresien, J., Hinz, A., Schulz, A., and Villinger, A., *Dalton Trans.*, 2018, vol. 47, p. 4433. https://doi.org/10.1039/c8dt00487k

90. Bresien, J., Schulz, A., Thomas, M., and Villinger, A., *Eur. J. Inorg. Chem.*, 2019, p. 1279. https://doi.org/10.1002/ejic.201900003

91. Solyntjes, S., Neumann, B., Stammler, H.-G., et al., *Chem.-Eur. J.*, 2017, vol. 23, p. 1568. https://doi.org/10.1002/chem.201604914

92. Nishimoto, Y., Takeuchi, M., Yasuda, M., and Baba, A., *Chem.-Eur. J.*, 2013, vol. 19, p. 14411. https://doi.org/10.1002/chem.201302194

93. Nishimoto, Y., Takeuchi, M., Yasuda, M., and Baba, A., *Angew. Chem., Int. Ed.*, 2012, vol. 51, p. 1051. https://doi.org/10.1002/anie.201107127

94. Ritschel, B., Poater, J., Dengel, H., et al., *Angew. Chem., Int. Ed.*, 2018, vol. 57, p. 3825. https://doi.org/10.1002/anie.201712725

95. Stavila, V. and Dikarev, E.V., *J. Organomet. Chem.*, 2009, vol. 694, p. 2956. https://doi.org/10.1016/j.jorganchem.2009.04.036

96. Chirca, I., Silvestru, C., Breunig, H.J., and Rat, C.I., *Inorg. Chim. Acta*, 2018, vol. 475, p. 155. https://doi.org/10.1016/j.ica.2017.11.021

97. Tan, N., Chen, Y., Zhou, Y., et al., *ChemPlusChem*, 2013, vol. 78, p. 1363. https://doi.org/10.1002/cplu.201300288

98. Toma, A., Rat, C.I., Silvestru, A., et al., *J. Organomet. Chem.*, 2013, vol. 745, p. 71. https://dx.doi.org/10.1016/j.jorganchem.2013.06.044

99. Nema, M.G., Breunig, H.J., Soran, A., and Silvestru, C., *J. Organomet. Chem.*, 2012, vol. 705, p. 23. https://doi.org/10.1016/j.jorganchem.2012.01.011

100. Kannan, R., Kumar, S., Andrews, A.P., et al., *Inorg. Chem.*, 2017, vol. 56, p. 9391. https://doi.org/10.1021/acs.inorgchem.7b01243

101. Li, Y., Zhu, H., Tan, G., et al., *Eur. J. Inorg. Chem.*, 2011, p. 5265. https://doi.org/10.1002/ejic.201100821

102. Simon, P., Jambor, R., Ruzicka, A., and Dostal, L., *Organometallics*, 2013, vol. 32, p. 239. https://dx.doi.org/10.1021/om3010383

103. Soran, A., Breunig, H.J., Lippolis, V., et al., *Dalton Trans.*, 2009, vol. 7, p. 77. https://doi.org/10.1039/b811713f

104. Simon, P., Proft, F., Jambor, R., et al., *Angew. Chem., Int. Ed.*, 2010, vol. 49, p. 5468. https://doi.org/10.1002/anie.201002209

105. Peveling, K., Schurmann, M., Herres-Pawlis, S., et al., *Organometallics*, 2011, vol. 30, p. 5181. https://dx.doi.org/10.1021/om200544r

106. Vrana, J., Jambor, R., Ruzicka, A., et al., *Collect. Czech. Chem. Commun.*, 2010, vol. 75, p. 1041. https://doi.org/10.1135/cccc2010051

107. Zhang, X.-W., Xia, J., Yan, H.-W., et al., *J. Organomet. Chem.*, 2009, vol. 694, p. 3019. https://doi.org/10.1016/j.jorganchem.2009.05.003

108. Toma, A., Rat, C.I., Silvestru, A., et al., *J. Organomet. Chem.*, 2016, vol. 806, p. 5. https://dx.doi.org/10.1016/j.jorganchem.2016.01.019

109. Toma, A.M., Pop, A., Silvestru, A., et al., *Dalton Trans.*, 2017, vol. 46, p. 3953. https://doi.org/10.1039/c7dt00188f

110. Tan, N., Chen, Y., Yin, S.-F., et al., *Dalton Trans.*, 2013, vol. 42, p. 9476. https://doi.org/10.1039/c3dt50922b

111. Tan, N., Yin, S., Li, Y., et al., *J. Organomet. Chem.*, 2011, vol. 696, p. 1579. https://doi.org/10.1016/j.jorganchem.2010.12.035

112. Qiu, R., Meng, Z., Yin, S., et al., *ChemPlusChem*, 2012, vol. 77, p. 404. https://doi.org/10.1002/cplu.201200030

113. Qiu, R., Yin, S., Song, X., et al., *Dalton Trans.*, 2011, vol. 40, p. 9482. https://doi.org/10.1039/c0dt01419b

114. Sindlinger, C.P., Stasch, A., and Wesemann, L., *Organometallics*, 2014, vol. 33, p. 322. https://dx.doi.org/10.1021/om401059x

115. Strimb, G., Pollnitz, A., Rat, C.I., and Silvestru, C., *Dalton Trans.*, 2015, vol. 44, p. 9927. https://doi.org/10.1039/c5dt00603a

116. Mairychova, B., Svoboda, T., Stepnicka, P., et al., *Inorg. Chem.*, 2013, vol. 52, p. 1424. https://dx.doi.org/10.1021/ic302153s

117. Korenkova, M., Mairychova, B., Ruzicka, A., et al., *Dalton Trans.*, 2014, vol. 43, p. 7096. https://doi.org/10.1039/c3dt53012d

118. Fridrichova, A., Mairychova, B., Padelkova, Z., et al., *Dalton Trans.*, 2013, vol. 42, p. 16403. https://doi.org/10.1039/c3dt52230j

119. Fanfrlik, J., Sedlak, R., Pecina, A., et al., *Dalton Trans.*, 2016, vol. 45, p. 462. https://doi.org/10.1021/acs.inorgchem.5b00893

120. Dostal, L., Jambor, R., Ruzicka, A., et al., *Inorg. Chem.*, 2015, vol. 54, p. 6010. https://doi.org/10.1021/acs.inorgchem.5b00893

121. Fridrichova, A., Svoboda, T., Jambor, R., et al., *Organometallics*, 2009, vol. 28, p. 5522. https://doi.org/10.1021/om900607n

122. Svoboda, T., Jambor, R., Ruzicka, A., et al., *Eur. J. Inorg. Chem.*, 2010, p. 1663. https://doi.org/10.1002/ejic.200901194

123. Svoboda, T., Jambor, R., Ruzicka, A., et al., *Organometallics*, 2012, vol. 31, p. 1725. https://dx.doi.org/10.1021/om201025d

124. Mairychova, B., Svoboda, T., Erben, M., et al., *Organometallics*, 2013, vol. 32, p. 157. https://dx.doi.org/10.1021/om3009553

125. Chovancova, M., Jambor, R., Ruzicka, A., et al., *Organometallics*, 2009, vol. 28, p. 1934. https://doi.org/10.1021/om801194h

126. Dostal, L., Jambor, R., Ruzicka, A., et al., *Organometallics*, 2010, vol. 29, p. 4486. https://doi.org/10.1021/om100613x

127. Dostal, L., Jambor, R., Erben, M., and Ruzicka, A., *Z. Anorg. Allg. Chem.*, 2012, vol. 638, p. 614. https://doi.org/10.1002/zaac.201100515

128. Tan, N. and Zhang, X., *Acta Crystallogr. Sect. E: Struct. Rep. Online*, 2011, vol. 67, p. m252. https://doi.org/10.1107/S1600536811002510

129. Zhang, X., Qiu, R., Tan, N., et al., *Tetrahedron Lett.*, 2010, vol. 51, p. 153. https://doi.org/10.1016/j.tetlet.2009.10.104

130. Qiu, R., Qiu, Y., Yin, S., et al., *Adv. Synth. Catal.*, 2010, vol. 352, p. 153. https://doi.org/10.1002/adsc.200900679

131. Qiu, R., Yin, S., Zhang, X., et al., *Chem. Commun.*, 2009, p. 4759. https://doi.org/10.1039/b908234d

132. Liu, Y.-P., Lei, J., Tang, L.-W., et al., *Eur. J. Med. Chem.*, 2017, vol. 139, p. 826. http://dx.doi.org/10.1016/j.ejmech.2017.08.043

133. Toma, A.M., Rat, C.I., Pavel, O.D., et al., *Cat. Sci. Tech.*, 2017, vol. 7, p. 5343. https://doi.org/10.1039/c7cy00521k

134. Zhang, X., Yin, S., Qiu, R., et al., *J. Organomet. Chem.*, 2009, vol. 694, p. 3559. https://doi.org/10.1016/j.jorganchem.2009.07.018

135. Zhang, X.-W. and Fan, T., *Acta Crystallogr., Sect. E: Struct. Rep. Online*, 2011, vol. 67 p. m875. https://doi.org/10.1107/S1600536811021039

136. Murafuji, T., Kitagawa, K., Yoshimatsu, D., et al., *Eur. J. Med. Chem.*, 2013, vol. 63, p. 531. http://dx.doi.org/10.1016/j.ejmech.2013.02.036

137. Breunig, H.J., Nema, M.G., Silvestru, C., et al., *Dalton Trans.*, 2010, vol. 39, p. 11277. https://doi.org/10.1039/c0dt00927j

138. Dostal, L., Jambor, R., Ruzicka, A., et al., *Dalton Trans.*, 2011, vol. 40, p. 8922. https://doi.org/10.1039/c1dt10234f

139. Tan, N., Wu, S., Huiqiong, Y., et al., *Z. Kristallogr. New Cryst. Struct.*, 2019, vol. 234, p. 509. https://doi.org/10.1515/ncrs-2018-0507

140. Vranova, I., Erben, M., Jambor, R., et al., *Z. Anorg. Allg. Chem.*, 2016, vol. 642, p. 1212. https://doi.org/10.1002/zaac.201600305

141. Tan, N., Dang, L., Lan, D., et al., *Z. Kristallogr.-New Cryst. Struct.*, 2018, vol. 233, p. 875. https://doi.org/10.1002/zaac.201600305

142. Soran, A.P., Nema, M.G., Breunig, H.J., and Silvestru, C., *Acta Crystallogr., Sect. E: Struct. Rep. Online*, 2011, vol. 67, p. m153. https://doi.org/10.1107/S160053681005453X

143. Simon, P., Jambor, R., Ruzicka, A., and Dostal, L., *J. Organomet. Chem.*, 2013, vol. 740, p. 98. http://dx.doi.org/10.1016/j.jorganchem.2013.05.005

144. Casely, I.J., Ziller, J.W., Fang, M., et al., *J. Am. Chem. Soc.*, 2011, vol. 133, p. 5244. https://dx.doi.org/10.1021/ja201128d

145. Kindra, D.R., Casely, I.J., Fieser, M.E., et al., *J. Am. Chem. Soc.*, 2013, vol. 135, p. 7777. https://dx.doi.org/10.1021/ja403133f

146. Kindra, D.R., Casely, I.J., Ziller, J.W., and Evans, W.J., *Chem.-Eur. J.*, 2014, vol. 20, p. 15242. http://dx.doi.org/10.1002/chem.201404910

147. Egorova, I.V., Zhidkov, V.V., Grinishak, I.P., and Rezvanova, A.A., *Russ. J. Gen. Chem.*, 2014, vol. 84, no. 7, p. 1374. https://doi.org/10.1134/S1070363214070226

148. Solyntjes, S., Neumann, B., Stammler, H.-G., et al., *Eur. J. Inorg. Chem.*, 2016, p. 3999. https://doi.org/10.1002/ejic.201600539

149. Verkhovykh, V.A., Kalistratova, O.S., Grishina, A.I., et al., *Vest. Yuzhno-Ural. Gos. Un-ta. Ser. Khim.*, 2015, vol. 7, no. 3, p. 61.

150. Gushchin, F.V., Kalistratova, O.S., Maleeva, A.I., et al., *Vest. Yuzhno-Ural. Gos. Un-ta. Ser. Khim.*, 2016, vol. 8, no. 1, p. 51. https://doi.org/10.14529/chem160108

151. Gushchin, A.V., Shashkin, D.V., Prytkova, L.K., et al., *Russ. J. Gen. Chem.,* 2011, vol. 81, no. 3, p. 493. https://doi.org/10.1134/S107036321103008X

152. Sharutin, V.V., Senchurin, V.S., and Sharutina, O.K., *Russ. J. Inorg. Chem.*, 2011, vol. 56, no. 10, p. 1565. https://doi.org/10.1134/S0036023611100202

153. Sharutin, V.V., Sharutina, O.K., and Senchurin, V.S., *Zh. Inorg. Chem.*, 2014, vol. 59, no. 1, p. 42. https://doi.org/10.1134/S003602361401015X

154. Sharutin, V.V. and Sharutina, O.K., *Russ. J. Inorg. Chem.*, 2014, vol. 59, no. 6, p. 558. https://doi.org/10.1134/S0036023614060199

155. Gusakovskaya, A.A., Kalistratova, O.S., Andreev, P.V., et al., *Cryst. Rep.*, 2018, vol. 63, no. 2, p. 186. https://doi.org/10.7868/S0023476118020066

156. Sharutin, V.V., Sharutina, O.K., and Efremov, A.N., *Russ. J. Inorg. Chem.*, 2019, vol. 64, no. 2, p. 196. https://doi.org/10.1134/S0036023619020189

157. Duffin, R.N., Blair, V.L., Kedzierski, L., and Andrews, P.C., *Dalton Trans.*, 2018, vol. 47, p. 971. https://doi.org/10.1039/c7dt04171c

158. Duffin, R.N., Blair, V.L., Kedzierski, L., and Andrews, P.C., *J. Inorg. Biochem.*, 2018, vol. 189, p. 151. https://doi.org/10.1016/j.jinorgbio.2018.08.015

159. Ong, Y.C., Blair, V.L., Kedzierski, L., and Andrews, P.C., *Dalton Trans.*, 2014, vol. 43, p. 12904. https://doi.org/10.1039/c4dt00957f

160. Ong, Y.C., Blair, V.L., Kedzierski, L., et al., *Dalton Trans.*, 2015, vol. 44, p. 18215. https://doi.org/10.1039/c5dt03335g

161. Kumar, I., Bhattacharya, P., and Whitmire, K.H., *Organometallics*, 2014, vol. 33, p. 2906. https://doi.org/10.1021/om500337z

162. Cui, L., Bi, C., Fan, Y., et al., *Inorg. Chim. Acta*, 2015, vol. 437, p. 41. https://doi.org/10.1016/j.ica.2015.07.008

163. Kiran, A.B., Mocanu, T., Pollnitz, A., et al., *Dalton Trans.*, 2018, vol. 47, p. 2531. https://doi.org/10.1039/C7DT04516F

164. Zhang, X.-Y., Wu, R.-X., Bi, C.-F., et al., *Inorg. Chim. Acta*, 2018, vol. 483, p. 129. https://doi.org/10.1016/j.ica.2018.07.027

165. Feham, K., Benkadari, A., Chouaih, A., et al., *Cryst. Struct. Theor. Appl.*, 2013, vol. 2, p. 28. http://dx.doi.org/10.4236/csta.2013.21004

166. Andreev, P.V., Somov, N.V., Kalistratova, O.S., et al., *Cryst. Rep.*, 2015, vol. 60, no. 4, p. 517. https://doi.org/10.1134/S1063774515040057

167. Sharutin, V.V., Egorova, I.V., Kazakov, M.A., and Sharutina, O.K., *Russ. J. Inorg. Chem.*, 2009, vol. 54, no. 7, p. 1095. https://doi.org/10.1134/S0036023609070171

168. Andreev, P.V., Somov, N.V., Kalistratova, O.S., et al., *Acta Crystallogr., Sect. E: Struct. Rep. Online*, 2013, vol. 69, p. m333. https://doi.org/10.1107/S1600536813013317

169. Sharutin, V.V., Senchurin, V.S., Sharutina, O.K., et al., *Russ. J. Gen. Chem.,* 2010, vol. 80, no. 10, p. 1941. https://doi.org/10.1134/S1070363210100117

170. Sharutin, V.V., Sharutina, O.K., Senchurin, V.S., et al., *Butlerovskie Soobshcheniya*, 2012, vol. 29, p. 51.

171. Sharutin, V.V. and Sharutina, O.K., *Russ. J. Gen. Chem.,* 2016, vol. 86, no. 5, p. 1073. https://doi.org/10.1134/S1070363216050157

172. Sharutin, V.V., Sharutina, O.K., and Senchurin, V.S., *Russ. J. Inorg. Chem.*, 2016, vol. 61, no. 3, p. 317. https://doi.org/10.1134/S0036023616030207

173. Goswami, M., Ellern, A., and Pohl, N.L.B., *Angew. Chem., Int. Ed*., 2013, vol. 52, p. 8441. https://doi.org/10.1002/anie.201304099

174. Sharutin, V.V. and Sharutina, O.K., *Russ. J. Inorg. Chem.*, 2016, vol. 61, no. 8, p. 975. https://doi.org/10.1134/S0036023616080155

175. Robertson, A.P.M., Burford, N., McDonald, R., and Ferguson, M.J., *Angew. Chem., Int. Ed.*, 2014, vol. 53, p. 3480. https://doi.org/10.1002/anie.201310613

176. Egorova, I.V., Zhidkov, V.V., Grinishak, I.P., et al., *Russ. J. Inorg. Chem.*, 2018, vol. 63, no. 7, p. 861. https://doi.org/10.1134/S0036023618070069

177. Wittig, G. and Clauss, K., *Lieb. Ann.*, 1952, vol. 578, no. 1, p. 136.

178. Sharutin, V.V., Sharutina, O.K., and Senchurin V.S., *Russ. J. Inorg. Chem.*, 2020, vol. 65, no. 11, p. 1712. https://doi.org/10.1134/S0036023620110170

179. Senchurin, V.S., Sharutin, V.V., and Sharutina, O.K., *Russ. J. Inorg. Chem*. 2020, vol. 65, no. 3, p. 323. https://doi.org/10.1134/S0036023620030122

180. Sharutin, V.V., Sharutina, O.K., and Senchurin, V.S., *J. Struct. Chem*., 2020, vol. 61, p. 5, p. 734. https://doi.org/10.1134/S0022476620050091

181. Sharutin, V.V., Egorova, I.V., Sharutina, O.K., et al., *Russ. J. Coord. Chem*., 2008, vol. 34, no. 2, p. 85. https://doi.org/10.1134/S1070328408020024

182. Sharutin, V.V., Sharutina, O.K., Egorova, I.V., et al., *Russ. Chem. Bull*., 1999, no. 12, p. 2325. https://doi.org/10.1007/BF02498282

183. Egorova, I.V., *Doctoral Sci. (Chem.) Disseration*, Nizhny Novgorod, 2008.

184. Glowka, M.L., Martynowski, D., and Kozlowska, K., *J. Mol. Struct.*, 1999, vol. 474, p. 81. https://doi.org/10.1016/S0022-2860(98)00562-6

185. Tsuzuki, S., Honda, K., Uchimaru, T., et al., *J. Am. Chem. Soc.*, 2002, vol. 124, no. 1, p. 104. https://doi.10.1021/ja0105212

186. Senchurin, V.S., *Vest. Yuzhno-Ural. Gos. Un-ta. Ser. Khim.*, 2019, vol. 11, no. 3, p. 50. https://doi.org/10.14529/chem190306

187. Sharutin, V.V., Egorova, I.V., Klepikov, N.N., et al., *Russ. J. Inorg. Chem*. 2009, vol. 54, no. 1, p. 53. https://doi.org/10.1134/S0036023609010124

188. Sharutin, V.V., Egorova, I.V., Klepikov, N.N., et al., *Russ. J. Inorg. Chem*. 2009, vol. 54, no. 11, p. 1847. https://doi.org/10.1134/S0036023609110126

189. Ooi, T., Goto, R., and Maruoka, K., *J. Am. Chem. Soc.*, 2003, vol. 125, p. 10494. https://doi.10.1021/ja030150k

190. Park, G., Brock, D.J., Pellois, J.-P., and Gabbai, F.P., *Chem. Cell Press*, 2019, vol. 5, p. 2215. https://doi.org/10.1016/j.chempr.2019.06.013

Translated by E. Yablonskaya